THESIS FOR THE DEGREE OF DOCTOR OF PHILOSOPHY (PHD)

In vitro antioxidant activity, cytotoxicity and oxidative transformation of flavonoid derivatives

by Péter Szabados-Fürjesi

UNIVERSITY OF DEBRECEN

DOCTORAL SCHOOL OF PHARMACEUTICAL SCIENCES

DEBRECEN, 2019

THESIS FOR THE DEGREE OF DOCTOR OF PHILOSOPHY (PHD)

In vitro antioxidant activity, cytotoxicity and oxidative transformation of flavonoid derivatives

by Péter Szabados-Fürjesi

supervisor: Dr. István Bak

UNIVERSITY OF DEBRECEN

DOCTORAL SCHOOL OF PHARMACEUTICAL SCIENCES

DEBRECEN, 2019

Oscar Wilde once said: "the old believe everything; the middle-aged suspect everything; the young know everything"; and the scientist question everything.

TABLE OF CONTENTS

1. ABBREVIATIONS

AAPH	2,2'-Azobis(2-amidinopropane) dihydrochloride
ABTS	2,2'-Azino-bis(3-ethylbenzothiazoline-6-sulphonic acid)
ACN	Acetonitrile
ADME	Absorption, distribution, metabolism, excretion
API	Active pharmaceutical ingredient
ATP	Adenosine triphosphate
AUC	Area under the curve
CAT	Catalase
CPR	NADPH-dependent cytochrome P450 reductase
CVD	Cardiovascular disease
CYP	Cytochrome P450
DMEM	Dulbecco's modified eagle's medium
DNA	Deoxyribonucleic acid
DPPH	2,2-Diphenyl-1-picrylhydrazyl
EC	Electrochemisty/ electrochemical
ESI	Electrospray ionization
EU	European Union
EWG	Electron-withdrawing group
FDA	Food and Drug Administration
FE	Ferrous equivalent
FRAP	Ferric reducing antioxidant power
GC	Gas chromatography/ gas chromatograph
GPx	Glutathione peroxidase
GSH	Glutathione
HAT	Hydrogen atom transfer
Hlg	Halogen
HTN	Hypertension
IHD	Ischaemic heart disease
LC	Liquid chromatography/ liquid chromatograph
LDL	Low-density lipoprotein
MPTP	Mitochondrial permeability transitions pore

MS	Mass spectrometry/ mass spectrometer
MTT	3-(4,5-Dimethylthiazol-2-yl)-2,5-diphenyltetrazolium bromide
NADPH	Nicotinamide-adenine dinucleotide phosphate
NCE	New chemical entity
NMR	Nuclear magnetic resonance
ORAC	Oxygen radical absorbance capacity
PBS	Phosphate buffered saline
PK	Pharmacokinetics
PMCA	Plasma membrane Ca^{2+}-ATPase
RNS	Reactive nitrogen species
ROS	Reactive oxygen species
SAR	Structure–activity relationship
SERCA	Sarcoplasmic reticulum Ca^{2+}-ATPase
SET	Single electron transfer
SOD	Superoxide dismutase
TEAC	Trolox equivalent antioxidant capacity
TPTZ	2,4,6-Tris(2-pyridyl)-s-triazine

2. INTRODUCTION

2.1. CARDIOVASCULAR DISEASE

Cardiovascular disease (CVD), the group of disorders of the heart and circulatory system is the leading cause of death by being responsible for the 45% of all deaths, killing 3.95 million people a year just in Europe. By contrast, the cancer as the second most common cause of mortality kills 2.0 million people. The two most common types of the CVDs are ischaemic heart disease (IHD) and stroke. Figure 1 shows that in the European Union (EU), IHD as the leading single cause of mortality is accountable for 630000 deaths (13%) a year, while stroke being the second most common single cause of death is responsible for 430000 (9%) deaths each year.

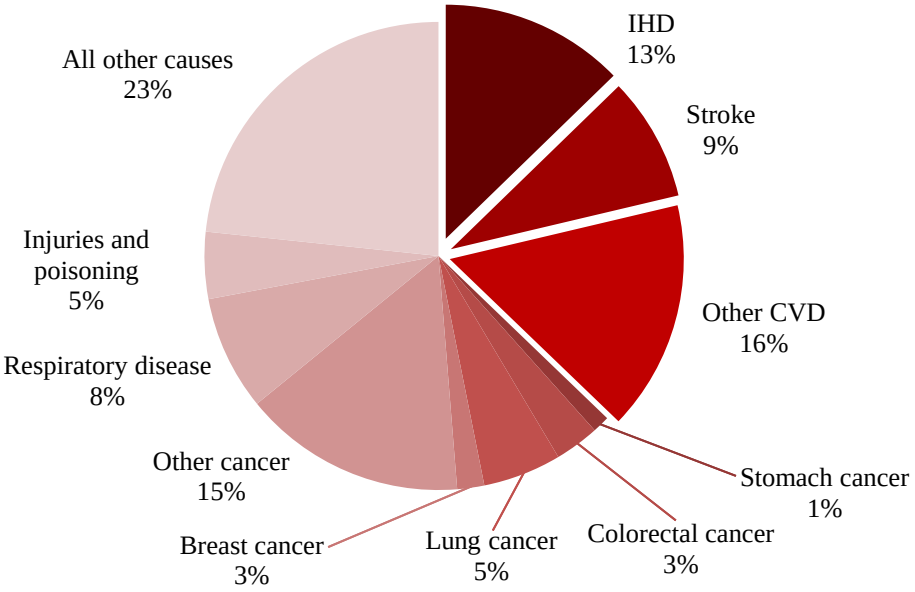

Figure 1. Deaths by cause in the EU, in 2014 (WHO Mortality Database).

Hungary has the 4th highest mortality caused by IHD in the EU; in 2014, 32000 people died by IHD and 31000 more by other CVDs including stroke (Figure 2). There is an overall decrease in the prevalence of CVDs in the EU; this decline is smaller in Central and Eastern Europe. The economic burden of CVDs is about €210 billion a year; €111 billion (53%) is spent on health care costs, €54 billion (26%) is lost due to productivity reduction and €45 billion (21%) to the care outside the framework of organized, paid and professional work. As the aging population grows, the incidence rate of CVDs is expected to be higher and higher. Therefore, the development of more effective preventive measures and therapeutic

possibilities becomes increasingly important. The natural products stand in the focus of these efforts.

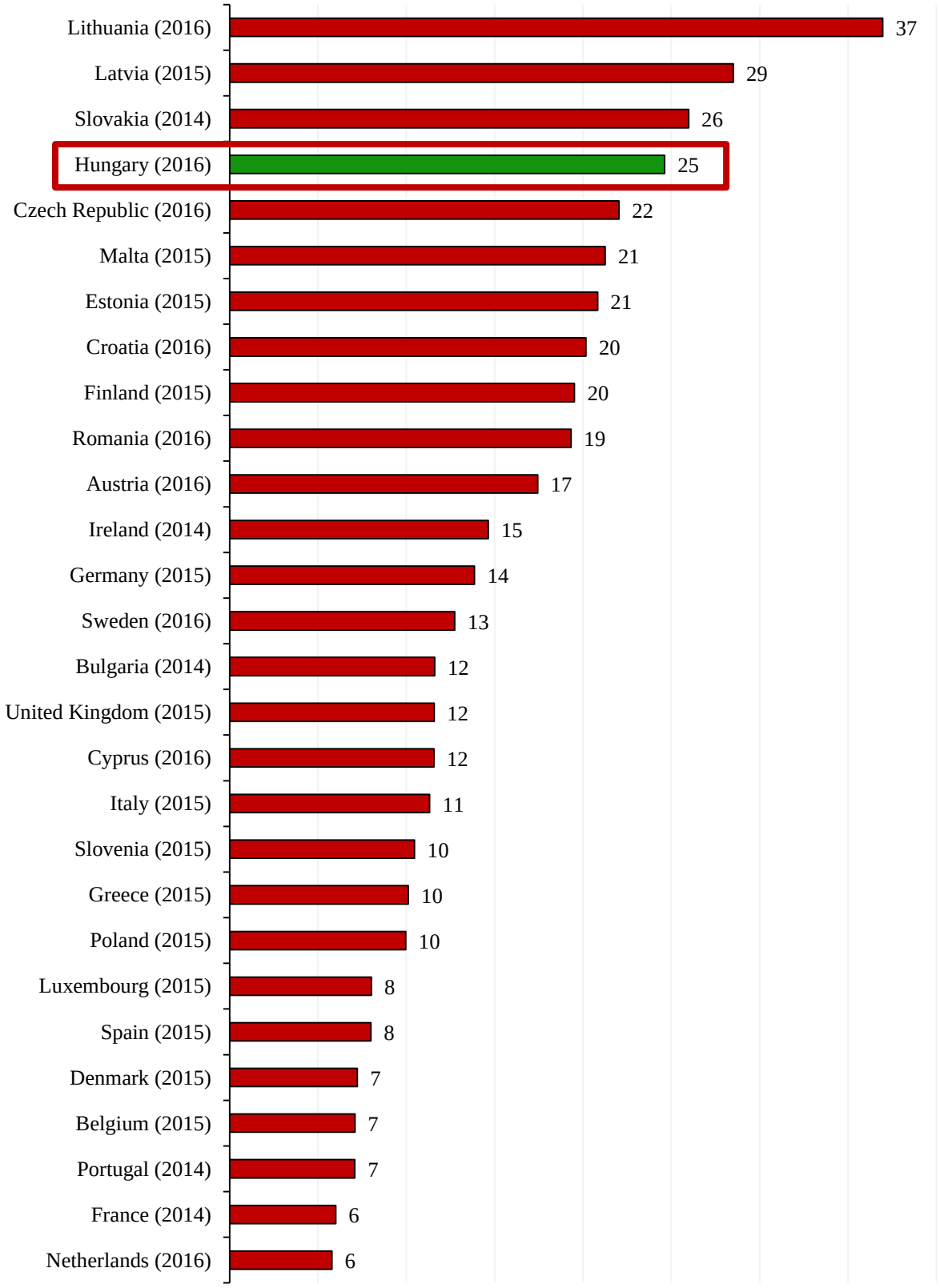

Figure 2. Deaths from IHD in percentage (age-standardised, all ages, all sex) in the EU, the latest available year (WHO Mortality Database).

Ischemic heart disease and hypertension are the two main factors for the incidence and progression of heart failure. Atherosclerosis caused partial or complete blockage of the coronary artery and coronary artery vasospasm are the two causes of cardiac ischemia. These conditions decrease the perfusion of the myocardium or in case of a total coronary occlusion the perfusion stops, consequently blocking the supply of oxygen and nutrients of the heart muscle. This ischemia induced confusion of the substrate and oxygen flow leads to the incomplete removal of metabolic end products, which result in cell dysfunction and afterwards cell death due to apoptosis or necrosis. The consequences of oxygen deprivation includes the change from aerobic glycolysis to anaerobic glycolysis of glucose, the decrease of adenosine triphosphate (ATP) production, however by increasing the amount of creatine phosphate the body can sustain the ATP level; however, later it decreases rapidly and ATP demand of the cells cannot be met. The anaerobic glycolysis of glucose increases the level of lactic acid leading to the elevation of intracellular H^+ concentration. The pH-decrease causes the increase of the intracellular Na^+ level via the Na^+/H^+ change. As the result of the reduced coronary perfusion, the Ca^{2+} has already piled up in the cardiomyocytes and because the intracellular Na^+ amount will be lowered through the Na^+/Ca^{2+} exchanger; the intracellular Ca^{2+} level further will increase [1]. The low ATP level stops the Na^+/K^+-ATPase causing the increase of intracellular Na^+ and Ca^{2+} levels [2].

To ensure the survival of the remaining myocardial cells, reperfusion is essential, but also injurious; sudden reperfusion results in rapid increase of reactive oxygen species (ROS) production [3]. During reperfusion, the H^+ and ATP levels are close to normal, but the intracellular Ca^{2+} still elevated. The excessive ROS formation by the mitochondrial electron transport chain and the re-established oxygen flow remains unbalanced due to the weakened antioxidant defence system leading to oxidative stress. The mitochondria provide the vast majority of cellular ROS [4]. Most of the ions and small molecules cannot pass though the inner membrane of the mitochondria, which is crucial to maintaining the pH gradient that drives oxidative phosphorylation step in ATP synthesis. However, during reperfusion the mitochondrial permeability transition pore (MPTP) opens as a result of the elevated Ca^{2+}, the close-to-normal pH and the increased ROS production [5]. The MPTP opening induces the depolarization of mitochondria, matrix swelling and the disruption of outer mitochondrial membrane leading to the necrosis and apoptosis of cardiomyocytes.

2.2. OXIDATIVE STRESS

The condition, when the weakened antioxidant defence system cannot counteract the enhanced ROS and reactive nitrogen species (RNS) production is defined as oxidative stress, and was first characterized as an imbalance in the equilibrium between the pro-oxidants and antioxidants in favour of the former, which leads to potential damage [6]. All type of cells in the vasculature, including adventitial cells, vascular smooth muscle and endothelial cells produce ROS [7]. The free heme, nicotinamide-adenine dinucleotide phosphate (NADPH) oxidase, xanthine oxidase, mitochondrial respiration chain, and uncoupled nitric oxide synthase (NOS) enzyme systems are the major sources of cardiovascular disease-related ROS generation. These reactive species are molecules with unpaired valence electrons making them extremely reactive with very short half-life, and thus they are highly toxic to the cells and tissues. Oxidative stress is one of the major factors contributing in the development of several cardiovascular diseases such as atherosclerosis [8, 9], high blood pressure [10, 11], heart failure [12, 13], cardiac ischemic reperfusion injury. The superoxide dismutase (SOD) enzyme plays an important role in the endogenous antioxidant defence system by catalysing the transformation of the superoxide anion ($O_2^{-\bullet}$), a product of the partial reduction of oxygen, into hydrogen peroxide (H_2O_2). The decrease of SOD enzyme activity in patients suffering from coronary artery disease (CAD) supports the aforementioned fact regarding its importance [14]. In biological systems, the conversion of $O_2^{-\bullet}$ into H_2O_2 and O_2 can happen by non-enzymatic reactions as well [15]. However, the formed H_2O_2 is also very reactive, and during the Fenton reaction with transition metals (Figure 3), for example in biological systems with Fe^{2+} it produces hydroxyl radical ($^{\bullet}OH$) [16].

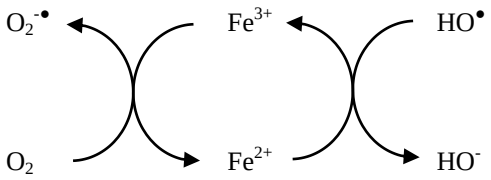

Figure 3. Schematic overview of $^{\bullet}OH$ production in Fenton reaction adapted from Jang et al [17].

During the oxidative stress, the free-radicals can damage bio-macromolecules. These modify the structure of the phospholipids, the major components of cell membranes. During the process called lipid peroxidation these “take” electrons from lipids resulting in the formation of fatty acid radicals, and thus initiating a chain reaction; these fatty acid radicals are very

unstable, therefore producing peroxyl-fatty acid radicals with O_2. The peroxyl-fatty acid radicals, being very reactive molecule, reacts with another free fatty acid molecule generating a different fatty acid radical and a lipid peroxide and the cycle repeats itself until the amount of radicals is high enough to increasing the likelihood of two radicals reacting with each other resulting in the production of a non-radical molecule. The lipid peroxidation causes a change in the permeability and structure of the membrane of the cytoplasm and different cell organelles [18]. The lipid peroxidation can also oxidize the low-density lipoprotein (LDL) contributing in the development of the coronary artery disease [19]; the free radical-oxidised LDL cholesterol advances the generation of foam cells from macrophages and helps monocyte accumulation in the arterial wall and therefore, as the early event of atherogenesis leading to atherosclerotic plaque formation [20], increasing vasoconstriction and apoptosis of endothelial cells [21]. The oxidative damage of DNA is attributed to the $^{\bullet}OH$ [22]; via different mechanisms it produces base lesions and sugar lesions in the DNA and causes single-strand breaks, double-strand breaks DNA-protein cross-links eventually leading to cell death, mutagenesis, and carcinogenesis [23, 24]. The ROS-caused protein damage can result in structural changes and degradation of plasma membrane Ca^{2+}-ATPase (PMCA) causing induced Ca^{2+} influx and reduced Ca^{2+} efflux [25]. The free-radicals inhibit the pumping activity of the sarcoplasmic reticulum Ca^{2+}-ATPase (SERCA) [26]. As the result of the aforementioned dysfunction of Ca^{2+}-ATPase proteins, the death of cardiomyocyte cells increases due to the high intracellular Ca^{2+} level [27].

2.3. ANTIOXIDANTS AND ANTIOXIDANT ASSAYS

Antioxidant compounds, when they are present at lower concentration than the oxidizable substrate, prevent or delay its oxidation, and thus counterbalance the oxidative stress and its damaging effect on biomolecules. The antioxidants found in aqueous and membrane cell compartments can be enzymatic and non-enzymatic, and based on their role in the defence system there are two subclasses; antioxidants whose prevent the generation of ROS and those that block, intercept or scavenge the produced radicals. Enzymatic antioxidant systems are for example glutathione peroxidase (GPx), SOD, and catalase (CAT), while the non-enzymatic systems are cyclooxygenase or lipooxygenase inhibitors, enzyme cofactors like selenium, coenzyme Q_{10}, and ROS scavengers such as polyphenols, vitamin E and vitamin C. Furthermore, apart from the ROS generation prevention, interception and scavenging, the antioxidants play major part in repair processes by removing the damaged biomolecules prior to their accumulation which would lead to altered cell metabolism or viability; the oxidized nucleic acids are repaired by specific enzymes, proteolytic systems remove damaged proteins, and the impairment of membrane lipids can be restored by enzymes like phospholipases, peroxidases and acyl transferases [28]. The balance between the antioxidants and prooxidants under normal physiological conditions slightly favours the latter, and therefore inducing moderate oxidative stress, which requires the counteraction of the antioxidant systems [29], however, the effectiveness of some these defence and repair systems to act upon this pro-oxidative shift decreases by the age [30], while the ROS generation increases [31]. These systems include enzymatic and non-enzymatic endogenous and exogenous antioxidants, which act interactively to sustain or restore the balance, and thus preventing or treating the oxidative stress caused cell damages and diseases. If sufficient amount of exogenous antioxidants is available for maintaining the redox homeostasis, the use of endogenous antioxidants remains unchanged [32]. There are numerous sources of these exogenous antioxidants; the intake of vitamins and phytochemicals can be achieved by consume naturally-occurring antioxidant rich fruits and vegetables, another providers of the necessary nutrients are the synthetic dietary supplements. Thus, there has been a growing interest in finding and synthetizing drugs, which can be used as exogenous antioxidants.

There are numerous *in vitro* and *in vivo* methods for measuring the antioxidant activity of a molecule, however only those relevant to the present studies will be discussed below. The *in vitro* methods can be divided into two subgroups based on the underlying mechanism of action; assays based on hydrogen atom transfer (HAT) and single electron transfer (SET)

based tests. There are several assays, which can be used for the evaluation of the antioxidant activity, The schematic overview of the two mechanisms is depicted in Figure 4.

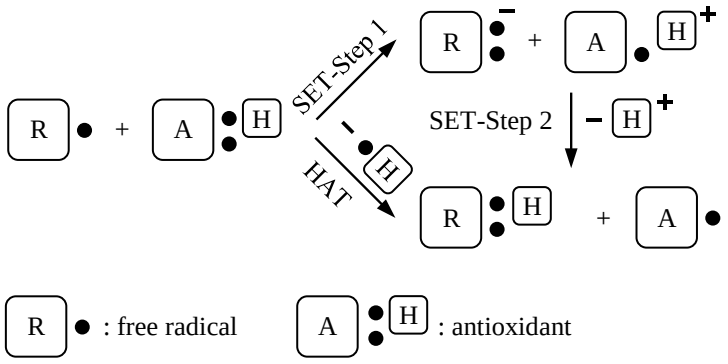

Figure 4. The schematic representation of the SET and HAT mechanisms of antioxidant reacting with a free radical.

The HAT-based methods measure the free radical, mostly the biologically important peroxyl radical scavenging activity by a hydrogen atom donation. The reaction between a phenol (ArOH) and a peroxyl radical ($ROO^{\bullet}$) results in resonance-stabilized aryloxy radical ($ArO^{\bullet}$) via an H-atom transfer. The mechanism of action can be summarized with the following reaction:

$$ROO^{\bullet} + AH/ArOH \rightarrow ROOH + A^{\bullet}/ArO^{\bullet} \qquad (1)$$

The protection of the biomolecules from oxidative damage by the phenolic antioxidant can only be achieved, if the peroxyl radical reacts faster with the antioxidant than with the biomolecule. The oxygen radical absorbance capacity (ORAC) assay is HAT-based antioxidant assay in which not just the presumed antioxidant, but a fluorescent probe react with the $ROO^{\bullet}$; the antioxidant potency is determined by the measuring of the fluorescence decay curve of the probe followed by the calculation of the area under the curve (AUC). The radicals are produced by the thermal decomposition of the 2,2'-azobis(2-amidinopropane) dihydrochloride (AAPH), a free radical-generating azo compound [33] (Figure 5).

In case of most of the SET-based antioxidant test, the antioxidant reacts with a coloured oxidising agent, which is generally a stable radical. The antioxidant compound reduces the coloured probe molecule, and therefore a change in the absorbance of the solution, which is detectable at a given wavelength by a spectrophotometer. The 2,2-diphenyl-1-picrylhydrazyl (DPPH) is a stable nitrogen-centred free radical (Figure 5), in which the

unpaired electron is delocalised over the whole molecule, and thus preventing it from dimerization as it would happen with the majority of the radicals.

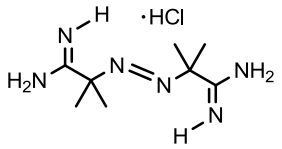

AAPH

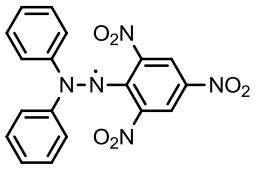

DPPH

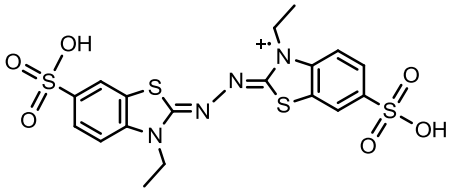

$ABTS^{\bullet+}$

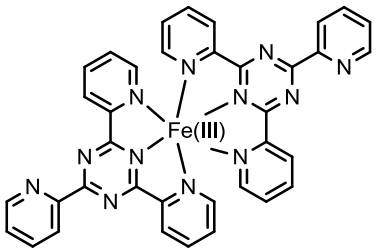

Fe^{3+}-TPTZ

Figure 5. The structures of the AAPH, the DPPH free radical, the ABTS radical cation and the Fe^{3+}-TPTZ complex.

The method was described first by Brand-Williams et al., is based on the fact that DPPH solution has a colour of deep violet, but when it is mixed with a hydrogen atom-donating antioxidant, the reduced DPPH loses its colour [34]. This change can be detected at about 517 nm depending on the used solvent. The DPPH shows very little resemblance to the peroxyl radicals, and thus antioxidants which are good DPPH scavengers may be inactive against peroxyl radicals.

The method of 2,2'-azino-bis(3-ethylbenzothiazoline-6-sulphonic acid) (ABTS) assay was reported first by Miller et al. [35], and it is based on the same principle as the DPPH assay, however, the metastable blue-green ABTS radical cation (Figure 5) must be generated from its neutral salt form prior to the measurement by H_2O_2, $K_2S_2O_8$ or manganese dioxide. The decolourization of this blue-green coloured solution is the result of the $ABTS^{\bullet+}$ reduction by the antioxidant and it can be measured at approximately 730 nm depending on the solvent. This assay is also called as trolox equivalent antioxidant capacity (TEAC) assay, when the trolox, the water-soluble antioxidant vitamin E analog is used as standard. The ABTS radical is neither exists naturally in biological systems nor similar to any radical present in those.

A very fast and useful assay the ferric reducing antioxidant power (FRAP) is based on the antioxidants ability to reduce the yellow-coloured ferric tripyridyltriazine complex (Fe^{3+}-TPTZ) (Figure 5)to blue ferrous complex (Fe^{2+}-TPTZ) via electron-donation [36]. This change can be detected with a spectrophotometer at 593 nm and it is linearly related to the reducing power of antioxidants. The results can be expressed as Ferrous Equivalent (FE) when the data are given by the antioxidants are compared to a $FeSO_4$ standard curve; the concentration of the investigated compound which has the same absorbance as 1 mmol Fe^{2+}. However, any compound with redox potential lower than Fe^{3+}/Fe^{2+} can donate electron, and thus it can exhibit false FRAP values even without antioxidant activity [37].

It is important to note, that a single antioxidant assay does not give an accurate overview about the mechanism of action of the antioxidants and the ROS sources in a complex *in vivo* system [38], an antioxidant molecule can react differently with numerous types of free-radicals; carotenoids, for example, have been known as very efficient singlet-oxygen quenchers [39], and yet their ability of peroxyl radicals scavenging is different. Hence, in order to classify the compound of interest as antioxidant, several assays must be performed, however the comparison and the correct interpretation of these assay results pose a serious challenge, but efforts have been made recently to investigate the correlations and make comparisons between different antioxidant tests [40-42].

2.4. DRUG METABOLISM AND ITS ROLE IN THE DRUG DEVELOPMENT

The drug research and development makes the pharmaceutical industry one of the most costly industrial sectors of the modern world; the estimated post-approval capitalized cost of bringing a new drug to the market in 2014 was almost $2.9 billion (2013 dollars) [43]. It is important to note, that not every chemical compound will finish this process as a candidate to treat a disease. Therefore, this high cost involves the compound failures, new chemical entities (NCEs), which will never attain regulatory success due to failure during their development. Hence, one of the major goals is to optimize the development process via rational drug designs and early evaluation of absorption, distribution, metabolism, and excretion (ADME). To identify better drug candidates more efficiently the fate of the drug must be investigated after administration. The ADME studies the complex processes of transporters and enzymes which determine the pharmacological and toxicological effect of a NCE. The evaluation of the metabolism of the compounds plays a major part in the identification of lead candidates.

Chemical substances such as drug molecules, which are foreign to the biochemistry of the organism, are called xenobiotics and they are mostly nonpolar lipid-soluble compounds. During the process of the drug metabolism the living organism modifies these xenobiotics in order to eliminate them from its system. Based on their polarity, some drugs must undergo structural modifications to increase their water solubility, and thus they can be excreted with in the urine or bile. The hydrophilic compounds can be eliminated without any structural change. The drug metabolism generally renders a drug into its inactive form resulting in the termination of the intended action. Furthermore, following the administration the effect will be abolished if the absorption of the active form is minimal or it has rapid first-pass elimination. In some cases the metabolite will be the pharmacologically active form of the compound; the prodrugs can overcome these obstacles by having enhanced absorption or protecting the active moiety from the fast first-pass effect. There are two phases of the drug metabolism; during the first phase the nonpolar compounds are modified to increase their polarity via oxidation reduction or hydrolysis. Based on their polarity, the produced metabolites can be excreted by the kidneys or they can undergo phase II reactions, in which they are conjugated with endogenous substrates, and therefore the second phase is often called conjugation phase. It is noteworthy, that not every molecule goes through the two phases and not necessarily in this order; some compounds are eliminated without transformation, while others are excreted immediately after conjugation. These reactions are mostly enzyme

catalysed; the most important and most widely studied enzyme system in the metabolic processes is the cytochrome P450 (CYP). The CYPs contain a single heme molecule and they are present in all the five kingdoms of life [44]. They can be found in almost all types of mammalian tissue, but predominantly in the membrane of the endoplasmic reticulum of the liver [45]. Liver is the main site of the drug metabolism, but the intestines, lungs, kidneys and even the skin take part in the biotransformation of xenobiotics. The first studies about the CYPs were published in the late 1950s [46, 47], and it was soon realized that there are several types of this enzymes. Families noted by unique Arabic number, subfamilies are given a letter and the individual enzymes are differentiated also by a unique Arabic number. CYP1, CYP2 and CYP3 play the key roles in the drug metabolism, while the other families catalyse endogenous processes [48]. Figure 6 depicts the catalytic cycle of the CYPs, which must be discussed in order to understand their importance in the biotransformation.

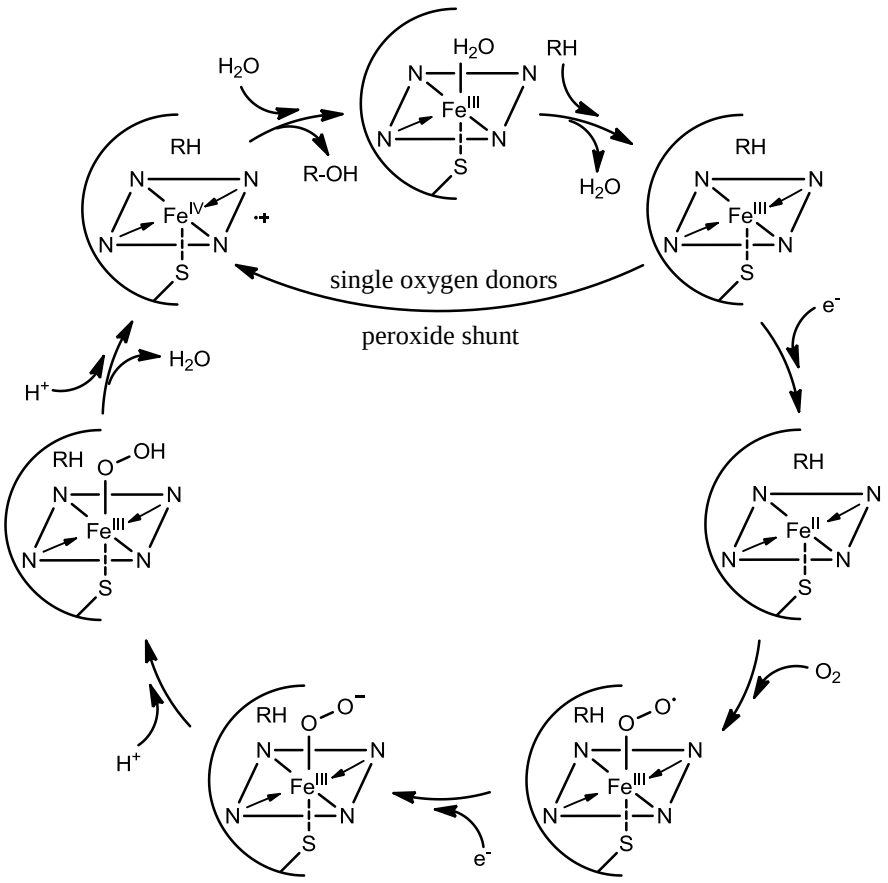

Figure 6. The schematic overview of the CYP catalytic cycle. The electrons and H^+ are provided by the NADPH with the aid of NADPH-dependent cytochrome P450 reductase (CPR).

In the beginning of the cycle the iron(III) located in the centre binds the substrate, and following the gain of an electron its oxidation state is reduced to 2+. During the next steps an

O_2, an e^- and an H^+ bind to the heme. The oxidation of the substrate happens in the state when the extremely reactive oxoiron complex is formed, in which the iron is in 4+ oxidation state. Then, the oxidized substrate leaves the enzyme, which returns its original form after a gain of water. It is notable that there is an alternate pathway called “peroxide-shunt”; in this case the necessary oxygen and e^- are provided by different peroxides instead of O_2 and NADPH. The pathway is used by biomimetic model systems such as the synthetic porphyrin.

As it was mentioned before; to avoid compound failures during the API development process, one of the most important objectives is to evaluate the metabolic fate of the compound in the body; the metabolism and pharmacokinetics of the drug candidate must be investigated as early as possible. The compound can be rapidly excreted causing the loss of the wanted effect, or in case of slow elimination it can accumulate leading to undesirable or even toxic effect. The active metabolites of a drug can exhibit toxic effects, and therefore their identification and characterization are also essential for their further progress in the development phases. These investigations related to the drug metabolites can be achieved with different *in vivo* and *in vitro* metabolism modelling techniques or biomimetic systems [49].

2.5. PHASE I DRUG METABOLISM MODELLING

The aforementioned importance of the early metabolic evaluation of drug candidates and the increasing number of novel chemical compounds created a great demand for fast and reliable screening techniques. Numerous *in vivo* and *in vitro* models have been used for elucidate metabolic stability. Johansson et al. [50] used three non-enzymatic *in vitro* biomimetic systems in order to model the phase I metabolism of metoprolol; Fenton reaction, EC/ESI/MS and synthetic metalloporphine. These biomimetic strategies have lower complexity than CYP containing tissue based *in vitro* methods or *in vivo* animal models, consequently their practicability is higher, but they have the smallest resemblance with the *in vivo* transformation pathways (Figure 7) [51].

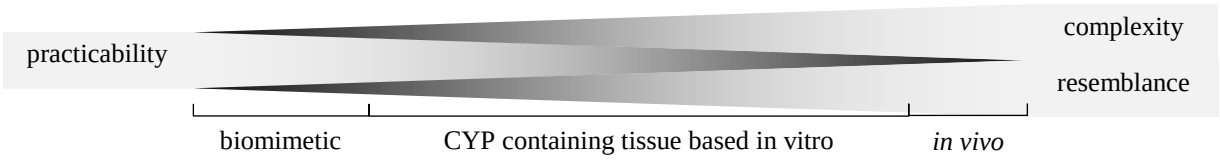

Figure 7. Advantages and disadvantages of the methods of drug metabolism modelling.

H.J.H. Fenton published his paper more than a century ago about the oxidation of tartaric acid to dihydroxymalenic acid by H_2O_2 in the presence of iron [16]. However, the complete mechanism of the Fenton reaction is still undiscovered; the simplified reaction mechanism is the following [52]:

$$Fe^{2+} + H_2O_2 \rightarrow Fe^{3+} + OH^- + {}^{\bullet}OH \qquad (2)$$

After an electron transfer from the Fe^{2+} to H_2O_2, the Fe^{2+} is oxidized to Fe^{3+} followed by the formation of the highly reactive hydroxyl radical, which oxidizes most organic compounds. Publications about the Fenton chemistry are mostly related to its application in wastewater treatment and in degradation processes. In the late 1980s, Zbaida et al. [53, 54] and Masumoto et al. [55] used the Fenton reaction for mimicking drug metabolism. The hydroxyl radical was prepared by mixing $FeCl_2$ with H_2O_2. During recent studies, the Fe^{2+} is electrochemically or chemically *in situ* generated from Fe^{3+} [50, 56], and thus only catalytic amount of iron is needed. The formed metabolites can be characterized using various analytical instruments, such as NMR, GC/MS and LC/MS(/MS). Its simplicity and ability to mimic *N*-dealkylation, *S*-oxidation, and hydroxylation make the Fenton reaction a useful tool for drug metabolism

modelling in the early stages of the research and development, especially for gathering initial information about the behaviour of the investigated compound.

The synthetic metalloporphines currently used in metabolism modelling studies are the results from decades of research, which was mainly focused on creating an artificial catalyst mimicking the heme-iron centre containing active site of CYP450 enzymes. Figure 8 represents the three generations of the metalloporphines.

M: Fe, Mn, Cr, Ru
First generation: R: H; X: H
Second generation: R: H; X: Hlg, alkyl, SO_3H
Third generation: R: Hlg; X: Hlg, alkyl, SO_3H

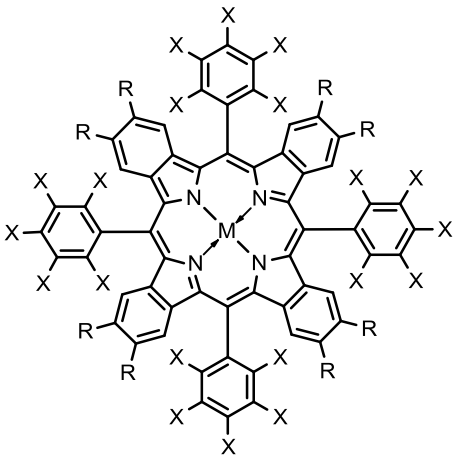

Figure 8. The structures of the generations of synthetic metalloporphines; the central metal atom can be manganese, chromium or ruthenium. In the structure of the second generation the phenyl groups are substituted with different substituents, such as halogen atoms, different alkyl groups or with sulfonic acids. The third generation metalloporphines bear halogen substituents on their pyrrole rings.

The first generation of these compounds were simple structured porphine complexes; they undergo oxidative degradation quite easily and form dimers resulting in the loss of catalytic activity. Furthermore, because their hydrophobic properties their water solubility is poor. In the molecules of the second generation the phenyl groups are substituted, hence increasing the steric hindrance in order to prevent dimerization [57, 58]. The electron withdrawing groups (EWGs) on the phenyl groups enhance the catalytic activity by causing electron deficiency of the central metal atom [59]. The sulfonic acid groups increase the water solubility, therefore helping to mimic the physiological conditions. The third generation compounds were developed by the modification of the previous generation: they have halogen substituents on their pyrrole rings, thus the electron deficiency of the central metal atom and consequently the catalytic activity have been increased further [60]. Mimicking of the whole catalytic cycle of CYP450 enzymes with molecular oxygen and reducing agent has been found to be

problematic as the reducing cofactor and a substrate can compete for the active oxidant. This competition can be avoided by using H_2O_2, sodium hypochlorite, iodosylbenzene or *tert*-butylhydroperoxide as single oxygen donor [61]; the difficult reductive activation of molecular oxygen is by-passed by creating a shorter, alternative mono-oxygenation pathway, which called the "peroxide shunt" (Figure 3). Using metalloporphines as a biomimetic system several reactions can be modelled; oxidation of heteroatoms, epoxidation or aliphatic and aromatic hydroxylation [62].

Electrochemical oxidation can also be used to generate phase I drug metabolites; Shono et al. used a homemade batch electrolysis cell to model the *N*-dealkylation of *N*-acyl- and *N*-sulfonylamines [63]. In 1986 Hambitzer and Heitbaum used the *on-line* combination of electrochemical cell and thermospray mass spectrometry for the generation and detection of the oxidation products of *N,N*-dimethylaniline, thus establishing an *on-line* model system for oxidative drug metabolism [64]. The type of the electrochemical cells used in the production of phase I metabolites plays an important role. Nowadays, there are numerous types of electrochemical cells are available to choose from, but generally two types are preferred for phase I drug metabolism studies; coulometric flow-through cells and amperometric thin-layer cells (Figure 9). These electrochemical cells have three electrodes; the working electrode (WE), the counter (CE) or auxiliary (AUX) electrode and the reference electrode (REF).

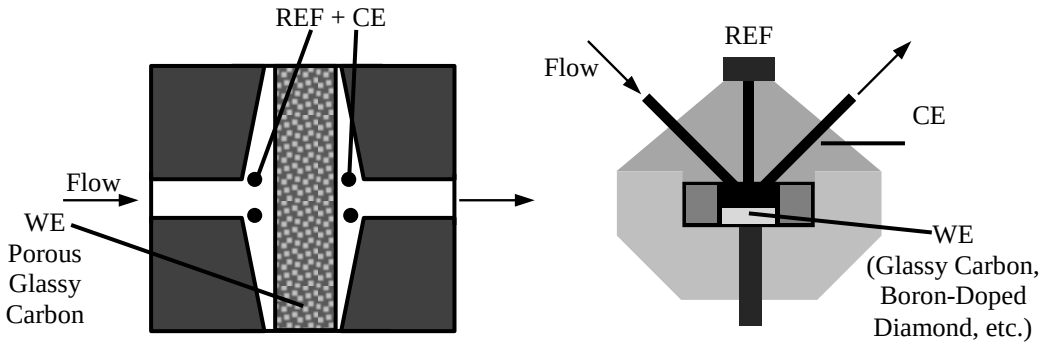

Figure 9. The coulometric flow-through (left) and the amperometric thin-layer cell (right) are the two most common EC cells used for phase I metabolism modelling.

Depending on the potential, the oxidation of the electroactive molecules happens at the WE. Typical WE materials are the glassy carbon, boron-doped diamond and platinum. The counter electrode together with the working electrode provides circuit over which current is applied. The current flowing between these two electrodes may affect the potential, and thus making

difficult to fix and measure the applied potential. With the REF, this problem can be overcome; it determines the potential between the working and reference electrodes. The flow-through cells generally have glassy carbon WEs [65], which is embedded into the electrode block, and therefore the maintenance is very circuitous. However, because the porous design, the surface area is large enough to reach almost quantitative conversion. This cell can be used with higher flow rates up to several 100 μL/min, which allows its integration into a LC or a LC/MS system (Figure 10).

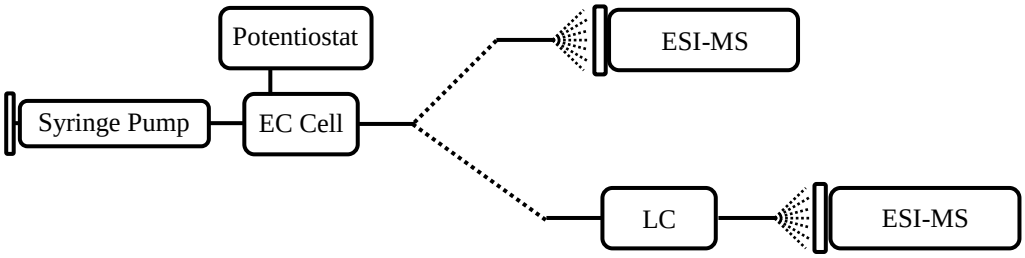

Figure 10. The schematic overview of the EC/(LC)/ESI-MS instrumentation used for phase I drug metabolism modelling. The syringe pump injects the solution of the investigated compound at a given flow rate into the EC cell, where the compound is oxidized on the WE. The potential is controlled by a potentiostat. The effluent is then introduced to the ESI-MS (EC/ESI-MS system) or to the LC and after the separation step, the detection is performed by ESI-MS.

The electrodes of the thin-layer cells are simply accessible, and thus in case of performance decrease, their cleaning and the exchange of the electrodes can be carried out more easily. The amperometric cells require lower flow rate than the flow-through cells, otherwise the conversion rate decreases dramatically. The lower flow rate makes the integration more difficult; the performance of the coupled instruments will decrease. The results obtained with the EC/LC/ESI-MS system correlate well with the results gained by the incubation with rat, mouse and human liver microsomes. EC cell as a biomimetic model system can model electron-transfer initiated CYP450 reactions, such as *S*- and *P*-oxidation, *N*-dealkylation, dehydrogenation and alcohol oxidation [66].

3. OBJECTIVES

There is a growing need for exogenous antioxidants to prevent or treat oxidative stress and reset the balance in the redox state to avoid further functional damage of biological macromolecules. To be a successful drug candidate during the research and development, the stability and toxicity must also be evaluated in the early stages of the process to prevent cost-increasing compound failures. Metabolism is one of the most important factors affecting the toxicity of a compound. The main objective of Study I was to evaluate the *in vitro* antioxidant activity, the cytotoxicity and the oxidative transformation of nine flavonoid derivatives (Table 1), which were chosen from the molecule bank of the University of Debrecen. The structures of the investigated in Study I can also be found in the Annex, section 13.1.1.

Table 1. The structure of the nine flavonoid derivatives investigated in Study I.

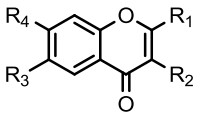

ID	R_1	R_2	R_3	R_4
865	4-(dimethylamino)phenyl	H	H	H
870	4-bromophenyl	H	H	H
874	4-[(4-methylpiperazin-1-yl)carbonyl]phenyl	H	H	H
876	2H-1,3-benzodioxol-5-yl	H	H	H
890	phenyl	H	NAc	H
893	3,4-dihydro-2H-1,5-benzodioxepin-7-yl	H	H	OH
987/3	3,4-dihydro-2H-1,5-benzodioxepin-7-yl	H	Me	Me
991	4-methoxyphenyl	H	Me	Me
1019/2	phenyl	OAc	H	H

The antioxidant activity was measured using different assays (ABTS, FRAP and ORAC), the cytotoxicity and the effects of against H_2O_2-induced cell death on H9c2 cardiomyoblasts were determined by MTT assay. The oxidative transformation of the selected flavonoids based on their biological activity was investigated with biomimetic model systems, such as chemical Fenton reaction, synthetic metalloporphyrin system and on-line EC/LC/MS.

The aim of Study II was to design, synthetize and evaluate the biological activity of new flavonol derivatives (Table 2). The structures of the investigated in Study II can also be found in the Annex, section 13.2.1.

Table 2. The structures of the six flavonol derivatives synthetized and investigated in Study II.

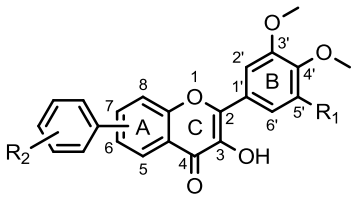

ID	R_1	R_2	Position of R_2-Ph
6a	H	3-$N(CH_3)_2$	6
6b	H	4-$CH_2(O)CH_3$	6
6c	H	3-$N(CH_3)_2$	7
6d	H	4-$CH_2(O)CH_3$	7
6e	OMe	3-$N(CH_3)_2$	7
6f	OMe	4-$CH_2(O)CH_3$	7

Furthermore, the additional objective was to investigate the possible involvement of the phenyl-*N*,*N*-dimethlyamino group in the biological activity of compounds with 2-phenyl-1,4-benzopyrone skeleton. The *in vitro* antioxidant activity was measured by different assays (DPPH, ABTS, FRAP and ORAC), the cytotoxicity on H9c2 cardiomyocyte cell line was determined using MTT assay. The oxidative transformation of the selected flavonols based on their biological activity was investigated with chemical Fenton reaction as biomimetic model system.

4. MATERIALS AND METHODS

4.1. MATERIALS AND METHODS FOR STUDY I

4.1.1. Materials

Ultra-pure water was prepared by using the Poll Lab (Bielsko-Biala, Poland) SolPure 78 water purification system. $FeCl_3$, H_2O_2, KH_2PO_4, K_2HPO_4, $CH_3COONa•3H_2O$, NH_4HCO_2, sodium citrate, citric acid, isopropanol, fluorescein, DPPH, ABTS-salt, 3-(4,5-dimethylthiazol-2-yl)-2,5-diphenyltetrazolium bromide (MTT), 2,2'-azobis(2-amidinopropane) dihydrochloride (AAPH), 2,4,6-tris(2-pyridyl)-s-triazine (TPTZ) and Dulbecco's Modified Eagle's medium (DMEM) were purchased from Sigma-Aldrich Kft. (Budapest, Hungary). L(+)-Ascorbic acid, ethylenediaminetetraacetic acid disodium salt dihydrate (EDTA-Na_2), EtOH, ACN, CH_3COOH and HCOOH were obtained from Scharlab Magyarország Kft. (Debrecen, Hungary). Fe(III) meso-tetra(4-sulfonatophenyl) porphine chloride was delivered by Frontier Scientific (Logan, UT, USA). The H9c2 cells (ATCC, CRL-1446) were obtained from LGC Standards GmbH (Wesel, Germany). The compounds of interest were selected from the molecule bank of the University of Debrecen.

4.1.2. ABTS Assay

The ABTS radical cation (100 μM) was generated via the ABTS/H_2O_2/metmyoglobin system using dissolved ABTS-salt in citric acid-sodium citrate buffer (pH 6.0, 50 mM) with 2% ethanol, and then it was mixed with the compounds of interest (25 μM). The absorbance of the reaction mixture was recorded at 730 nm for 2 hours at room temperature with a Helios-α-spectrophotometer (Thermo Fisher Scientific, Waltham, MA, USA) at 0, 5, 15, 30, 60, 90 and 120 min. Each experiment was performed three times.

4.1.3. ORAC Assay

The oxygen radical absorption capacity was evaluated using a modified method of Glazer et al. [67]. AAPH (37.5 mM) and fluorescein (0.6 μM) stock solutions in phosphate buffer (pH 7.0, 75 mM) were prepared freshly. The investigated compounds was tested in 0.05 mg/mL concentration. Each well contained 65 μL buffer, 20 μL fluorescein, 15 μL sample solution and 100 μL of AAPH solution. The plates were kept at 37 °C. The fluorescence was monitored every 2 min for 1 hour by the FLUOstar OPTIMA (BMG Labtech, Ortenberg, Germany) plate reader at 485 nm excitation and 520 nm emission wavelength. The AUC was calculated using this formula:

$$AUC = 0.5 + (R_2/R_1) + (R_3/R_1) + (R_4/R_1) + \ldots + (R_n/R_1), \quad (3)$$

where R_1 is the initial fluorescence at 0 min and R_n is the fluorescence at n min. The net AUC was obtained by subtracting the AUC_{blank} from AUC_{sample}. Each measurement was performed in duplicate and repeated four times.

4.1.4. FRAP Assay

For the FRAP assay, the following solutions were prepared; acetate buffer (pH 3.6, 300 mM), TPTZ (10 mM) in 40 mM HCl and $FeCl_3$ (20 mM). The FRAP reagent was freshly prepared and consisted of 25 mL of acetate buffer, 2.5 mL of TPTZ and 2.5 mL $FeCl_3$ solution. The reagent was activated by incubation on 37 °C for 15 min. The reaction mixture was prepared by mixing 950 µL FRAP reagent with 50 µL solution of the tested compound (0.05 mg/mL). Following a 15 min incubation period at 37 °C, the absorbance was measured at 593 nm using a Helios-α-spectrophotometer (Thermo Fisher Scientific, Waltham, MA, USA). Trolox standard calibration curve was recorded by measuring the absorbance of samples containing trolox in various concentrations from 0.015 mM to 0.21 mM. Based on this standard curve, the FRAP values were expressed as trolox equivalents (µM/mL). The experiments were run in duplicate and repeated four times.

4.1.5. MTT Assay

The cytotoxic effect of the compounds was investigated on H9c2 cells by MTT assay. The cells were dissociated by trituration in DMEM containing 10% FBS, 1% penicillin-streptomycin, and then they were seeded into 96-well plates and cultured for 1 day. The following day, the cells were treated with the compounds of interest (150 µM) in medium. After a 30 min incubation period, 0, 125 or 250 µM H_2O_2 was added to the wells. Four hours later, 20 µL MTT solution (5 mg/mL) in PBS was pipetted into the wells and the plates were further incubated for 3 hours at 37 °C in order to allow the mitochondrial uptake. After the removal of the medium, the cells were lysed with 150 µL isopropanol and incubated for 15 min. The absorbance was measured at 570 and 690 nm by a FLUOstar OPTIMA (BMG Labtech, Ortenberg, Germany) plate reader. The experiments were run in four replicate and repeated three times.

4.1.6. Chemical Fenton System

The oxidation of the compounds by Fenton reaction was carried out with modified method of Jurva et al. [56]. 400 µL solution of the investigated compound (2.5 mM) was

mixed with 50 μL solution of $FeCl_3$ (20 mM), 50 μL EDTA-Na_2 (20 mM), 500 μL ascorbic acid (10 mM). The reaction was started by the addition of 1 μL H_2O_2 (30%), and the mixture was stirred at room temperature. Samples were drawn at 30 min, 140 min, 18 hours, 71 hours and 261 hours were immediately injected off-line into an API 2000 Triple Quadrupole mass spectrometer equipped with an ESI source (Applied Biosystems, Waltham, MA, USA) using a syringe pump. The mass spectra were recorded in the range of *m/z* 100–500 in positive-ion mode and were analysed using Analyst 1.5.1. Software (AB SCIEX, Concord, ON, Canada).

4.1.7. Synthetic Porphyrin System

For experiments using synthetic porphyrin, the work of Johansson et al. [50] was followed closely, applying minor changes. 50 μL compound of interest (10 mM), 35 μL ACN, 315 μL formic acid (100 mM), 50 μL Fe(III) meso-tetra(4-sulfonatophenyl)porphine chloride (10 mM) and 50 μL H_2O_2 (30%) were mixed together and shaken at 37 °C for 30 min at 700 rpm in a ThermoMixer (Eppendorf AG, Hamburg, Germany). Off-line LC-MS analysis (on Kinetex XB-C18 2.6 μm column, using 0.1% formic acid and ACN with 0.1% formic acid as eluents with gradient elution) was performed using a LTQ XL (Thermo Fisher Scientific, Waltham, MA, USA) linear ion trap mass spectrometer equipped with ESI ion source in positive mode.

4.1.8. Electrochemical System

A thin-layer electrochemical cell (FlexCell, Antec, Zoeterwoude, The Netherlands) with a boron-doped diamond working electrode, a graphite doped teflon counter electrode and a Pd/H_2 reference electrode with a homemade potentiostat was used for oxidation. The potential ramp from 0-2500 mV was applied with 10 mV/s scan rate. The solution of the investigated compound in the mixture of ammonium formate (pH 7.4, 10 mM) and ACN was infused through the cell at 10 μL/min flow rate, and then this effluent was immediately analysed with an Exactive mass spectrometer (Thermo Fisher Scientific, Waltham, MA, USA) equipped with an ESI ion source. The full scan spectra were recorded in positive mode in the range of *m/z* 100–800 with XCalibur 2.1 (Thermo Fisher Scientific, Waltham, MA, USA) software. The three-dimensional mass voltammogram was achieved by plotting mass spectra in against the applied potential using Origin 9.1 (OriginLab, Northhampton, MA, USA) software.

4.2. MATERIALS AND METHODS FOR STUDY II

4.2.1. Materials

Aluminium backed TLC plates of silica gel 60 F254 (Merck, 0.2 mm) were used for reaction monitoring under UV light. Separation was performed using column chromatography on silica gel (Merck 60, 70−230 mesh). The melting points were measured using Büchi B-540 (BÜCHI Labortechnik AG, Flawil, Switzerland) apparatus and they are uncorrected. LTQ XL (Thermo Fisher Scientific, Waltham, MA, USA) linear ion trap mass spectrometer with ESI ion source in positive mode was used for evaluating the products purity. The ^{1}H and ^{13}C NMR spectra were acquired by Bruker Avance 300 III (300 MHz for ^{1}H), Bruker 360 AM Avance (360 MHz for ^{1}H and 91 MHz for ^{13}C) and Bruker DRX 400 (400 MHz for ^{1}H and 101 MHz for ^{13}C) spectrometers (Bruker, Billerica, MA, USA). Chemical shifts (δ) are reported in parts per million (ppm, d) and are given for ^{1}H NMR from internal signals using $CHCl_3$ (δ = 7.26 ppm) or TMS (δ =0.00 ppm), and for ^{13}C NMR from $CHCl_3$ (δ = 77.00 ppm) or DMSO (δ = 39.52 ppm). Coupling constants (J) reported in hertz (Hz). Elementar vario MICRO cube (Elementar Analysensysteme GmbH, Langenselbold, Germany) instrument was used for Elemental analyses (C, H). The IR spectra were recorded by a JASCO FT-IR 4100A (Jasco Inc., Easton, MD, USA) Fourier-transform infrared spectrometer in KBr discs.

Iron(II) sulfate heptahydrate, KBr and $K_2S_2O_8$ were purchased from Sigma-Aldrich Kft. (Budapest, Hungary). ABTS salt was provided by Fluorochem Ltd. (Hadfield, United Kingdom).

4.2.2. General Procedure for the Synthesis of **3a-c**

Benzaldehyde (**2a,b**, 6.3 mmol) suspension in MeOH (5 mL) was added to the mixture of acetophenone (**1a,b,** 1.29 g, 6 mmol) solution (10 mL MeOH) and 50% aq. NaOH (1.26 mL, 24 mmol). After stirring the solution for 1 hour, the reaction mixture was kept at room temperature for 1 day. In order to reach pH 1, 10% HCl solution was added to the flask and the precipitate was filtered off and washed with H_2O (3 × 30 mL) to give **3a-c** with 88-97% yields.

(*E*)-1-(5-Bromo-2-hydroxyphenyl)-3-(3,4-dimethoxyphenyl)prop-2-en-1-one (**3a**)

^{1}H NMR (300 MHz, 298 K, $CDCl_3$): δ (ppm)= 3.95-3.98 (m, 6H, OMe), 6.89-6.93 (m, 2H, 5-H, 3'-H), 7.17 (s, 1H, 2-H), 7.27-7.29 (d, *J*= 7.35 Hz, 1H, 6-H), 7.37-7.41 (d, *J*= 15.25

Hz, 1H, α-H), 7.53-7.56 (dd, 1H, 4'-H), 7.87-7.92 (d, *J*= 15.34 Hz, 1H, β-H), 8.00-8.00 (d, *J*= 1.62 Hz, 6'-H), 12.89 (s, 1H, OH).

(*E*)-1-(4-Bromo-2-hydroxyphenyl)-3-(3,4-dimethoxyphenyl)prop-2-en-1-one (**3b**)

^{1}H NMR (360 MHz, 298 K, $CDCl_3$): δ (ppm)= 3.94-3.96 (m, 6H, OMe), 6.89-6.91 (d, *J*= 8.36 Hz, 1H, 5-H), 7.03-7.06 (dd, 1H, 6-H), 7.14-7.19 (m, 2H, 2-H, 3'-H), 7.23-7.26 (dd, 1H, 5'-H), 7.38-7.42 (d, *J*= 15.51 Hz, 1H, α-H), 7.73-7.76 (d, *J*=8.36 Hz, 1H, 6'-H), 7.85-7.89 (d, *J*= 15.63 Hz, 1H, β-H), 13.09 (s, 1H, OH).

(*E*)-1-(4-Bromo-2-hydroxyphenyl)-3-(3,4,5-trimethoxyphenyl)prop-2-en-1-one (**3c**)

^{1}H NMR (400 MHz, 298 K, $CDCl_3$): δ (ppm)= 3.92-3.93 (m, 9H, OMe), 6.87 (s, 2H, 2-H, 6-H), 7.05-7.07 (d, *J*= 7.70 Hz, 1H, 5'-H), 7.20 (s, 1H, 3'-H), 7.41-7.45 (d, *J*= 15.40 Hz, 1H, α-H), 7.74-7.77 (d, *J*= 7.70 Hz, 1H, 6'-H), 7.82-7.86 (d, *J*= 15.40 Hz, 1H, β-H), 12.99 (s, 1H, OH).

4.2.3. General Procedure for the Synthesis of **4a-c**

The chalcone (**3a-c**, 2.7 mmol) was suspended in EtOH (15 mL) and cooled with water-bath, while 8% aq. NaOH (3.9 mL, 8.41 mmol) in order to produce a solution, followed by a dropwise addition of 30% H_2O_2 (3.9 mL, 38.2 mmol). The reaction mixture was stirred at room temperature for 2 hours, and then it was poured into ice-water mixture (250 mL). The pH of the solution was set to pH 1 by adding 10% HCl, and it was kept for 1 day to allow sedimentation. The precipitate was filtered off and washed with cc. $NaHCO_3$ solution (2 × 50 mL) and with water (4 × 50 mL) to give **4a-c** with 57-76% yields.

6-Bromo-2-(3,4-dimethoxyphenyl)-3-hydroxy-4H-chromen-4-one (**4a**)

^{1}H NMR (360 MHz, 298 K, DMSO-D_6): δ (ppm)= 3.85 (s, 6H, OMe), 7.14-7.16 (d, *J*= 7.85 Hz, 1H, 5'-H), 7.80-7.82 (m, 3H, 2'-H, 6'-H), 7.87-7.90 (d, J= 8.16 Hz, 1H, 8-H), 7.93-7.96 (dd, 7-H), 8.16-8.16 (d, *J*= 1.92 Hz, 1H, 5-H), 9.72 (s, 1H, OH).

7-Bromo-2-(3,4-dimethoxyphenyl)-3-hydroxy-4H-chromen-4-one (**4b**)

^{1}H NMR (400 MHz, 298 K, DMSO-D_6): δ (ppm)= 3.85-3.86 (m, 6H, OMe), 7.14-7.16 (d, *J*= 8.02 Hz, 1H, 5'-H), 7.61-7.64 (dd, 1H, 6'-H) 7.81-7.81 (d, *J*= 1.67 Hz, 1H, 2'-H), 7.90-7.93 (dd, 1H, 6-H), 8.00-8.02 (d, *J*= 8.55 Hz, 5-H), 8.20-8.20 (d, *J*= 1.44 Hz, 1H, 8-H), 9.63 (s, 1H, OH).

7-Bromo-3-hydroxy-2-(3,4,5-trimethoxyphenyl)-4H-chromen-4-one (**4c**)

^{1}H NMR (400 MHz, 298 K, DMSO-D_6): δ (ppm)= 3.75 (s, 3H, 4'-MeO), 3.86 (s, 6H, 3'-MeO, 5'-MeO), 7.56 (s, 2H, 2'-H, 6'-H), 7.59-7.62 (d, *J*= 8.46 Hz, 1H, 6-H), 7.98-8.00 (d, *J*= 8.46 Hz, 5-H), 8.21 (s, 1H, 8-H), 9.74 (s, 1H, OH).

4.2.4. General Procedure for the Synthesis of **6a-f**

In a pressure tube the mixture of 3-hydroxyflavone (**4a-c**, 0.265 mmol), KF (46.3 mg, 0.795 mmol), $Pd(OAc)_2$ (3 mg, 0.0133 mmol), XPhos (12.6 mg, 0.0265 mmol) and boronic acid (**5a,b**, 0.53 mmol) in toluene/t-BuOH (6:1, 3.5 mL) were stirred under argon for 4 hours at 100 °C. The solvent was removed using rotary evaporator under reduce pressure, the residue was purified with adsorptive filtration using toluene/EtOAc (2:1) as eluent. Diisopropyl ether was used to wash the crude product, which was then filtered to result the pure product **6a-f** with 63-74% yields.

2-(3,4-Dimethoxyphenyl)-6-[3-(dimethylamino)phenyl]-3-hydroxy-4H-chromen-4-one (**6a**)

Yellow solid; yield 69.1 mg (63%). Mp. 187.7-188.8 °C. Rf: 0.35 (toluene/EtOAc, 2:1). ^{1}H NMR (360 MHz, 298 K, $CDCl_3$): δ (ppm)= 3.02 (s, 6H, $N(Me)_2$), 3.95-3.99 (m, 6H, OMe), 6.75-6.77 (d, *J*= 7.35 Hz, 1H, 6"-H), 6.97-6.99 (m, 3H, 8-H, 5'-H, 2"-H), 7.13-7.17 (m, 1H, 2'-H), 7.30-7.34 (m, 1H, 5"-H), 7.60 (s, 1H, OH), 7.85-7.90 (m, 3H, 7-H, 6'-H, 4"-H), 8.42 (s, 1H, 5-H). ^{13}C NMR (91 MHz, 298 K, $CDCl_3$): δ (ppm)= 40.8 (C-$N(Me)_2$), 56.0, 56.1 (C-3'-MeO, 4'-MeO), 110.8 (C-2'), 111.1 (C-5'), 111.3 (C-2"), 112.2 (C-4"), 115.7 (C-6"), 118.5 (C-8), 120.8 (C-1'), 121.6 (C-6'), 123.1 (C-5), 123.8 (C-4a), 129.7 (C-5"), 132.8 (C-7), 137.9 (C-3), 138.7 (C-6), 140.3 (C-1"), 145.2 (C-4'), 148.9 (C-3'), 150.8(C-3"), 151.1 (C-2), 154.6 (C-8a),173.3 (C-4). LC-MS: *m/z*= 418.42 [$M+H^+$]. IR (KBr, cm^{-1}): ν= 3292, 2934, 2839, 1605, 1561, 1516, 1489, 1463.71, 1430, 1381, 1338, 1271, 1247, 1216, 1195, 1149, 1118, 1042, 1024, 991, 964, 933, 901, 869, 814, 770, 724, 694, 665, 634. Anal. Calcd for $C_{25}H_{23}NO_5$: C, 71.93; H, 5.55; Found: C 71.79; H 5.52.

2-(3,4-Dimethoxyphenyl)-3-hydroxy-6-[4-(methoxymethyl)phenyl]-4H-chromen-4-one (**6b**)

Yellow solid; yield 80.3 mg (72%). Mp. 192.8-194.3 °C. Rf: 0.30 (toluene/EtOAc, 2:1). ^{1}H NMR (360 MHz, 298 K, $CDCl_3$): δ (ppm)= 3.43 (s, 3H, Bn-MeO), 3.96-4.00 (m, 6H, 3'-MeO, 4'-MeO), 4.52 (s, 2H, Bn-H_2), 7.00-7.02 (d, *J*= 7.37 Hz, 1H, 5'-H), 7.08 (s, 1H, 2'-H), 7.43-7.45 (d, *J*= 7.55 Hz, 2H, 2"-H, 6"-H), 7.62-7.69 (m, 3H, OH, 3"-H, 5"-H), 7.86-7.93 (m, 3H, 7-H, 8-H, 6"-H), 8.43 (s, 1H. 5-H). ^{13}C NMR (91 MHz, 298 K, $CDCl_3$): δ (ppm)=

56.1, 56.1 (C-3'-MeO, 4'-MeO), 58.4 (C-Bn-MeO), 74.4 (C-Bn-CH_2), 110.9 (C-2'), 111.1 (C-5'), 118.8 (C-8), 120.9 (C-1'), 121.6 (C-6'), 123.1 (C-5), 123.8 (C-4a), 127.3 (C-2", C-6"), 128.4 (C-3", C-5"), 132.4 (C-7), 137.4 (C-4"),138.0 (C-3), 138.1 (C-6), 138.7 (C-1"), 145.2 (C-4'), 149.0 (C-3'), 150.9 (C-2), 154.7 (C-8a), 173.2 (C-4). LC-MS: *m/z*= 419.33 [$M+H^+$]. IR (KBr, cm^{-1}): ν= 3265, 3030, 2993, 2939, 2833, 2737, 2603, 2039, 1922, 1843, 1801, 1714, 1601, 1561, 1516, 1483, 1459, 1411, 1388, 1336, 1298, 1269, 1218, 1197, 1174, 1148, 1112, 1025, 967, 944, 932, 904, 875, 857, 815, 806, 784, 770, 727, 699, 661, 629. Anal. Calcd for $C_{25}H_{22}O_6$: C, 71.76; H, 5.30; Found: C 71.95; H 5.29.

2-(3,4-Dimethoxyphenyl)-7-[3-(dimethylamino)phenyl]-3-hydroxy-4H-chromen-4-one (**6c**)

Pale-brown solid; yield 79.0 mg (71%). Mp. 191.6-192.7 °C. Rf: 0.39 (toluene/EtOAc, 2:1). ^{1}H NMR (400 MHz, 298 K, $CDCl_3$): δ (ppm)= 3.04 (s, 6H, $N(Me)_2$), 3.96-3.99 (m, 6H, OMe), 6.79-6.81 (d, *J*= 7.84 Hz, 1H, 6"-H), 6.97-7.02 (m, 3H, 8-H, 5'-H, 2"-H), 7.10 (s, 1H, 2'-H), 7.33-7.37 (m, 1H, 5"-H), 7.63-7.65 (d, *J*= 7.84 Hz, 1H, 6-H), 7.75 (s, 1H, OH), 7.87-7.91 (m, 2H, 6'-H, 4"-H), 8.24-8.26 (d, *J*= 7.83 Hz, 1H, 5-H). ^{13}C NMR (101 MHz, 298 K, $CDCl_3$): δ (ppm)= 40.8 (C-$N(Me)_2$), 56.1, 56.2 (C-3'-MeO, 4'-MeO), 110.9 (C-2'), 111.0 (C-5'), 111.4 (C-2"), 112.9 (C-4"), 115.9 (C-6"), 116.2 (C-8), 119.4 (C-1'), 121.5 (C-6'), 123.9 (C-4a), 124.1 (C-6), 125.7 (C-5), 129.8 (C-5"), 138.0 (C-3), 140.3 (C-1"), 145.3 (C-4'), 147.8 (C-7), 149.0 (C-3'), 150.8 (C-3"), 151.1 (C-2), 155.6 (C-8a), 173.0 (C-4). LC-MS: *m/z*= 418.42 [$M+H^+$]. IR (KBr, cm^{-1}): ν= 3228, 3028, 2992, 2919, 2847, 2800, 2592, 2034, 1940, 1885, 1713, 1617, 1576, 1555, 1514, 1489, 1453, 1428, 1397, 1346, 1265, 1236, 1213, 1171, 1147, 1111, 1039, 1024, 994, 969, 921, 883, 861, 847, 835, 821, 771, 717, 699, 648, 639. Anal. Calcd for $C_{25}H_{23}NO_5$: C, 71.93; H, 5.55; Found: C 71.97; H 5.52.

2-(3,4-Dimethoxyphenyl)-3-hydroxy-7-[4-(methoxymethyl)phenyl]-4H-chromen-4-one (**6d**)

Yellow solid; yield 79.3 mg (72%). Mp. 212.1-214.2 °C. Rf: 0.31 (toluene/EtOAc, 2:1). ^{1}H NMR (400 MHz, 298 K, $CDCl_3$): δ (ppm)= 3.44 (s, 3H, Bn-MeO), 3.96-4.00 (m, 6H, 3'-MeO, 4'-MeO), 4.53 (s, 2H, Bn-H_2), 6.99-7.01 (d, *J*= 7.46 Hz, 1H, 5'-H), 7.10 (s, 1H, 2'-H), 7.46-7.48 (m, 2H, 2"-H, 6"-H), 7.62-7.69 (m, 3H, 6-H, 3"-H, 5"-H), 7.75 (s, 1H, OH), 7.85-7.91 (m, 2H, 8-H, 6'-H), 8.25-8.27 (d, *J*= 7.46 Hz, 1H, 5-H). ^{13}C NMR (101 MHz, 298 K, $CDCl_3$): δ (ppm)= 56.1, 56.1 (C-3'-MeO, 4'-MeO), 58.4 (C-Bn-MeO), 74.3 (C-Bn-CH_2), 110.8 (C-2'), 111.0 (C-5'), 116.0 (C-8), 119.5 (C-1'), 121.6 (C-6'), 123.7 (C-6), 123.8 (C-4a), 125.9 (C-5), 127.5 (C-2", C-6"), 128.4 (C-3", C-5"), 138.0 (C-3), 138.5 (C-4"), 139.1 (C-1"), 145.3 (C-4'), 146.3 (C-7), 149.0 (C-3'), 150.8 (C-2), 155.6 (C-8a), 172.9 (C-4). LC-MS: *m/z*=

419.42 [M+H^+]. IR (KBr, cm^{-1}): ν= 3234, 3022, 2977, 2920, 2839, 2597, 2030, 1923, 1848, 1797, 1714, 1611, 1574, 1555, 1515, 1488, 1467, 1450, 1417, 1397, 1354, 1333, 1271, 1243, 1212, 1173, 1147, 1103, 1039, 1020, 914, 858, 843, 818, 807, 774, 706, 635. Anal. Calcd for $C_{25}H_{22}O_6$: C, 71.76; H, 5.30; Found: C 71.70; H 5.32.

7-[3-(Dimethylamino)phenyl]-3-hydroxy-2-(3,4,5-trimethoxyphenyl)-4H-chromen-4-one (**6e**)

Pale-brown solid; yield 88.2 mg (74%). Mp. 179.5-181.8 °C. Rf: 0.47 (toluene/EtOAc, 2:1). ^{1}H NMR (360 MHz, 298 K, $CDCl_3$): δ (ppm)= 3.04 (s, 6H, $N(Me)_2$), 3.95 (s, 3H, 4'-MeO), 3.97 (s, 6H, 3'-MeO, 5'-MeO), 6.80-6.82 (d, *J*= 7.17 Hz, 1H, 6"-H), 6.97-7.03 (m, 2H, 8-H, 2"-H), 7.15-7.17 (d, *J*= 7.17 Hz, 1H, 4"-H), 7.34-7.37 (m, 1H, 5"-H), 7.56 (s, 2H, 2'-H, 6'-H), 7.64-7.66 (d, *J*= 7.96 Hz, 1H, 6-H), 7.76 (s, 1H, OH), 8.25-8.27 (d, *J*= 8.22 Hz, 1H, 5-H). ^{13}C NMR (91 MHz, 298 K, $CDCl_3$): δ (ppm)= 40.8 (C-$N(Me)_2$), 56.4 (C-3'-MeO, 5'-MeO), 61.1 (C-4'), 105.6 (C-2' C-6'), 111.5 (C-2"), 113.0 (C-4"), 115.9 (C-6"), 116.3 (C-8), 119.3 (C-1'), 126.4 (C-4a), 124.3 (C-6), 125.7 (C-5), 129.9 (C-5"), 138.4 (C-3), 140.2 (C-1"), 144.8 (C-4'), 148.1 (C-7), 151.1 (C-2), 151.2 (C-3"), 153.3 (C-3', C-5'), 155.7 (C-8a), 173.2 (C-4). LC-MS: *m/z*= 448.33 [M+H^+]. IR (KBr, cm^{-1}): ν= 3247, 3079, 2999, 2968, 2938, 2838, 1603, 1579, 1556, 1504, 1453, 1427, 1393, 1353, 1283, 1263, 1242, 1209, 1172, 1127, 1057, 1027, 1011, 994, 928, 841, 831, 821, 773, 734, 714, 697, 652. Anal. Calcd for $C_{26}H_{25}NO_6$: C, 69.79; H, 5.63; Found: C 69.86; H 5.59.

3-Hydroxy-7-[4-(methoxymethyl)phenyl]-2-(3,4,5-trimethoxyphenyl)-4H-chromen-4-one (**6f**)

Brown solid; yield 82.0 mg (69%). Mp. 208.1-209.2 °C. Rf: 0.48 (toluene/EtOAc, 2:1). ^{1}H NMR (400 MHz, 298 K, $CDCl_3$): δ (ppm)= 3.45 (s, 3H, Bn-MeO), 3.95 (s, 3H, 4'-MeO), 3.98 (s, 6H, 3'-MeO, 5'-MeO), 4.54 (s, 2H, Bn-H_2), 7.15 (s, 1H, 8-H), 7.48 (s, 2H, 2'-H, 6'-H), 7.56 (s, 2H, 2"-H, 6"-H), 7.63-7.69 (m, 3H, 6-H, 3"-H, 5"-H), 7.77 (s, 1H, OH), 8.26-8.28 (d, *J*=7.47 Hz, 1H, 5-H). ^{13}C NMR (101 MHz, 298 K, $CDCl_3$): δ (ppm)= 56.4 (C-3'-MeO, 5'-MeO), 58.4 (C-Bn-MeO), 61.1 (C-4'), 74.3 (C-Bn-CH_2), 105.5 (C-2'), 116.1 (C-8), 119.4 (C-1'), 123.9 (C-6), 126.4 (C-4a), 126.0 (C-5), 127.5 (C-2", C-6"), 128.4 (C-3", C-5"), 138.4 (C-3), 138.5 (C-4"), 139.2 (C-1"), 140.1 (C-2), 144.8 (C-4'), 146.6 (C-7), 153.3 (C-3', C-5'), 155.7 (C-8a), 173.1 (C-4). LC-MS: *m/z*= 449.33 [M+H^+]. IR (KBr, cm^{-1}): ν= 3278, 3010, 2983, 2969, 2939, 2899, 2837, 2154, 2064, 2010, 1928, 1602, 1583, 1574, 1551, 1508, 1491, 1451, 1409, 1394, 1379, 1338, 1296, 1244, 1211, 1194, 1172, 1130, 1114, 1056, 1026, 1011, 970, 936, 930, 913, 887, 844, 824, 779, 765, 712, 671, 624. Anal. Calcd for $C_{26}H_{24}O_7$: C, 69.63; H, 5.39; Found: C 69.57; H 5.43.

4.2.5. ABTS Assay

The ABTS radical scavenging activity of the investigated compounds was evaluated using an altered method of Sugahara et al. [68] and Re et al. [69] . The $ABTS^{\bullet+}$ was generated by mixing ABTS solution (7 mM) with $K_2S_2O_8$ solution (2.45 mM) and keeping it in the dark for 16 hours. The work solution was prepared freshly by mixing 150 µL of ABTS•+ stock solution with 2.9 mL MeOH. The reaction mixture consisted of 180 µL work solution and 20 µL of the investigated compound or quercetin standard in DMSO (10, 20, 50, 100 and 200 µM). The decrease in $ABTS^{\bullet+}$ concentration was monitored by measuring the absorbance at 737 nm for 2 hours after a short shaking period (10 sec) using a Multiskan GO microplate spectrophotometer (Thermo Fisher Scientific, Waltham, MA, USA). Each experiment was run in duplicate and repeated three times. The mean (SD) IC_{50} values were calculated based on the inhibition percentage measured at 120 min.

4.2.6. DPPH Assay

The DPPH free radical scavenging assay was performed using a modified method of Clarke et al. [70] . In each well, 180 µL freshly made DPPH solution (0.2 mM) in MeOH and 20 µL of the compound of interest or quercetin standard (10, 20, 50, 100 or 200 µM) in DMSO were mixed together. The decrease in DPPH free radical concentration was monitored by measuring the absorbance at 515 nm for 90 min after a short gentle shaking period (10 sec) using a Multiskan GO microplate spectrophotometer (Thermo Fisher Scientific, Waltham, MA, USA). Each measurement was performed in duplicate and repeated three times. The mean (SD) IC_{50} values were calculated based on the inhibition percentage measured at 90 min.

4.2.7. FRAP Assay

The compounds were tested for their FRAP using a previously reported method of Benzie and Strain [36] with a few changes. The FRAP working solution was prepared freshly by mixing 10 mL acetate buffer (pH 3.6, 300 mM), 1 mL TPTZ solution (10 mM) in HCl (40 mM) and 1 mL $FeCl_3$ (10 mM) together, followed by 15 min incubation at 37 °C. Solutions (20 µL) of the compound of interest or quercetin standard (10, 20, 50, 100 or 200 µM) were allowed to react with 180 µL FRAP working solution for 30 min in the dark. The absorbance of the coloured ferrous tripyridyltriazine complex was measured at 593 nm by a Multiskan GO microplate spectrophotometer (Thermo Fisher Scientific, Waltham, MA, USA). The solution of ferrous sulphate was used as standard and the calculated FRAP values are

expressed as mean (SD) μM Ferrous equivalents. Measurements were run in duplicate and repeated three times.

4.2.8. ORAC Assay

The oxygen radical absorbance capacity of the derivatives was measured using black 96-well plates. Solutions of fluorescein (50 nM) and AAPH (180 mM) in phosphate buffer (pH 7.0, 75 mM) were prepared freshly for each experiment. The mixture of 20 μL solution of the compound of interest or quercetin standard (2 and 10 μM) in ACN and 160 μL fluorescein (50 nM) was incubated for 15 min at 37 °C. The reaction was initiated by adding rapidly 20 μL AAPH solution (180 mM) to each well. The decrease in the fluorescence of the fluorescein was measured at 485 nm excitation and 520 nm emission wavelength for 2 hours in every 2 minutes using FLUOstar OPTIMA (BMG Labtech, Ortenberg, Germany) plate reader. The AUC was calculated using the following formula:

$$AUC = 0.5 + (A_1/A_0) + (A_2/A_0) + (A_3/A_0) + \ldots + (A_n/A_0), \quad (4)$$

where A_0 is the fluorescence at 0 min and A_n is the fluorescence at n min. The ORAC values were calculated by subtracting the blank AUC from the sample AUC and expressed as mean (SD) AUCnet. Experiments were performed in duplicate and repeated three times.

4.2.9. MTT Assay

The cytotoxic evaluation of the investigated compounds cell on cell survival was accomplished by utilizing the MTT assay using H9c2 rat cardiomyocyte cell line (ATCC, CRL-1446, LGC Standards GmbH, Wesel, Germany). The cells were seeded into 96-well plates in 200 μL DMEM media with 10% FBS and supplemented with penicillin and streptomycin, the density was 6000 cells/well. The cells were cultured overnight, followed by the addition of the flavonol derivatives (20 μM). Twelve hours later, 20 μL of MTT solution (5 mg/μL in PBS) was pipetted to the wells, followed by incubation at 37 °C for 4 hours to allow mitochondrial uptake. After the careful removal of the media, 100 μL DMSO was pipetted in order to dissolve the formed formazan crystals. The measurement of absorbance was performed at 540 and 630 nm using a Synergy HT (BioTek, Winoosky, VT, USA) plate reader. The results are given in mean (SD) cell viability percentage. The experiments were carried out in triplicate and repeated two times

4.2.10. Chemical Fenton System

The oxidation of the flavonol derivatives was accomplished using chemical Fenton reaction system, which was prepared as written in section 4.1.6.

5. RESULTS

5.1. RESULTS OF STUDY I

5.1.1. Biological Activity

5.1.1.1. ABTS Radical Cation Scavenging Assay

Figure 11 shows the results of the ABTS assay, which was used to evaluate the ABTS radical cation scavenging potency of the compounds of interest. Compound **865** demonstrated the highest scavenging rate followed by **893**. The compound **1019/2** showed results similar to the coumarin standard, while the other investigated compounds have significantly lower scavenging rate.

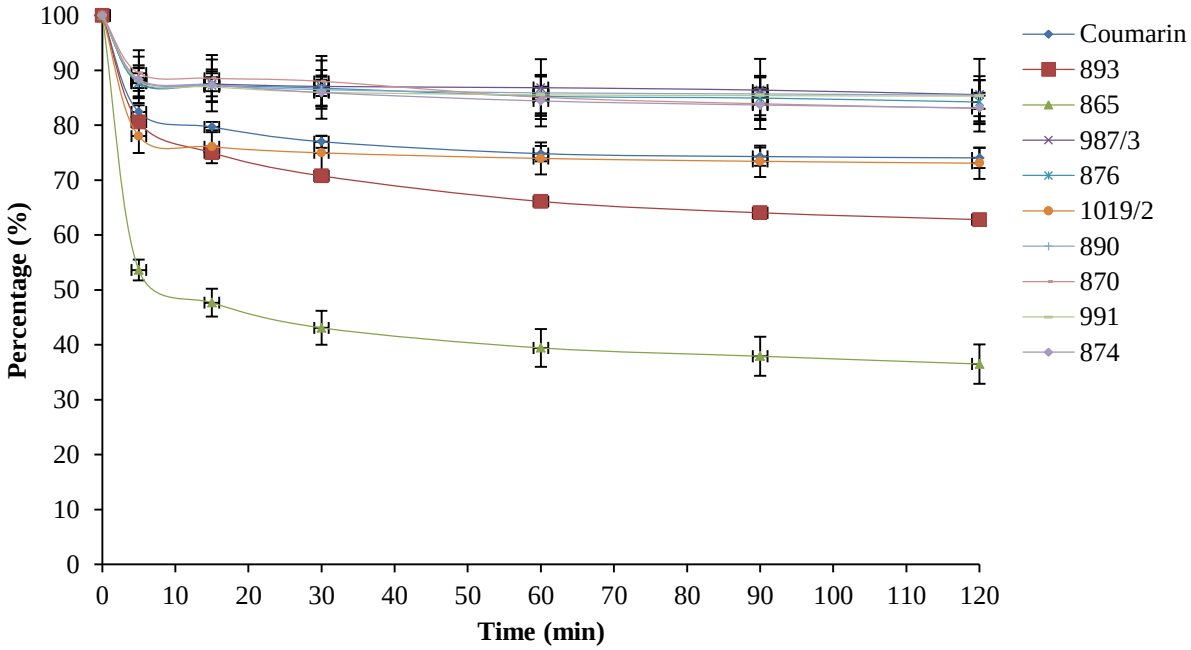

Figure 11. The results of the ABTS assay. The ABTS radical cation was generated using the ABTS/hydrogen peroxide/metmyoglobin system. The change in the absorbance due to the regeneration of the ABTS was monitored at 730 nm for 2 hours with a spectrophotometer. The experiments were performed three times.

5.1.1.2. Oxygen-Radical Absorption Capacity Assay

The oxygen radical absorbance capacity of the flavonoid derivatives was measured with ORAC assay and expressed mean ± SEM trolox equivalents (μM/mL) using coumarin as standard and trolox for calibration. The results are shown on Figure 12; compound **865** had the highest ORAC value, but it is noteworthy that all the tested compounds have shown significantly higher capacity than the coumarin standard. Compound **865** was followed by **874**, **890**, **893**, **987/3** and **1010/2**.

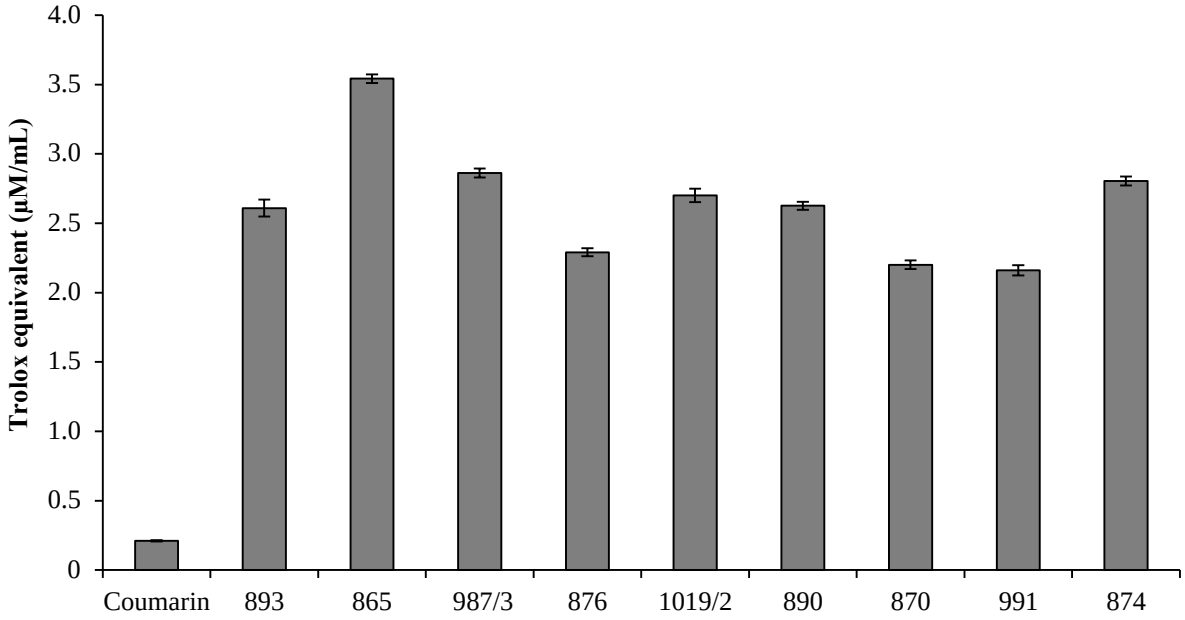

Figure 12. The results of the ORAC assay, the values are expressed as mean ± SEM trolox equivalents (μM/mL) calculated based on trolox calibration curve. Coumarin was used as standard compound. The reaction was initiated by the rapid addition of 2,2'-azobis(2-amidinopropane) dihydrochloride stock solution into the mixture of the tested compounds and fluorescein. The fluorescence was monitored at 485 nm excitation and 520 nm emission wavelength for 1 hour in every 2 min. Each measurement was performed in duplicate and repeated four times. The netAUC was calculated by subtracting the blankAUC from sampleAUC.

5.1.1.3. Ferric Reducing Antioxidant Power Assay

Figure 13 represents the FRAP assay results, which was used to measure the antioxidant potency of the investigated chromone derivatives directly through the reduction of ferric iron (Fe^{3+}) to ferrous iron (Fe^{2+}) using coumarin as standard and trolox for calibration. The FRAP values are expressed as mean ± SEM trolox equivalents (μM/mL). Compound **865** showed significantly increased FRAP activity, while the other tested compounds have slightly increased (**870**, **874**, **991** and **1019/2**) trolox equivalents compared to the coumarin standard or similar (**876**, **890**, **893** and **987/3**).

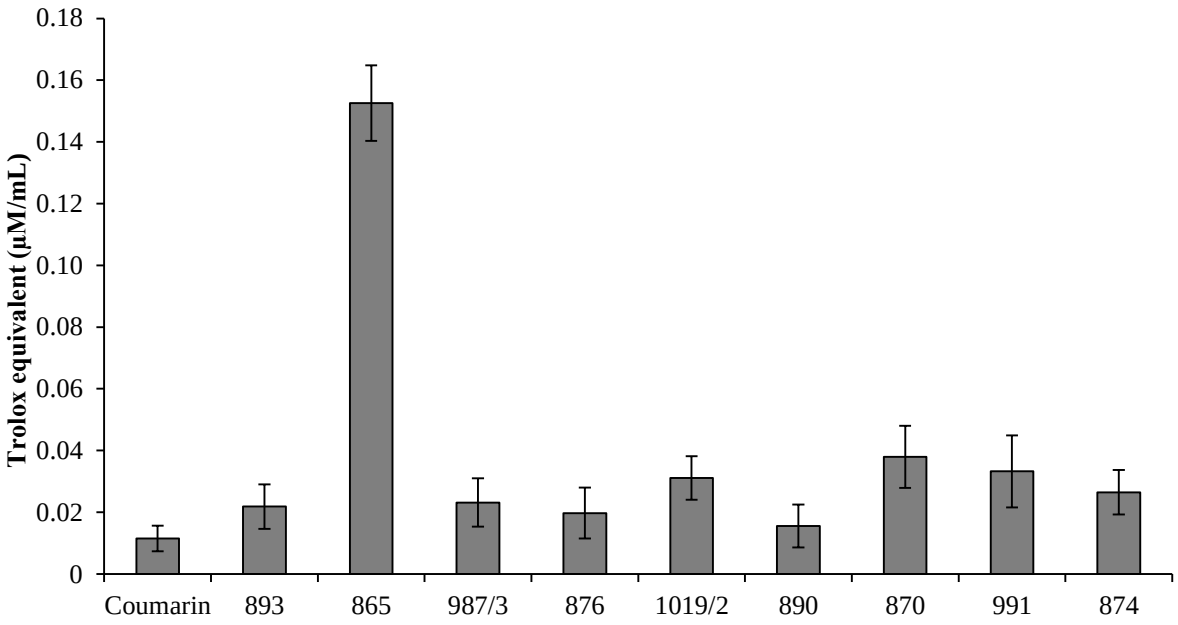

Figure 13. The results of the FRAP assay, the values are expressed as mean ± SEM trolox equivalents (μM/mL) calculated based on trolox calibration curve. Coumarin was used as standard compound. After the reaction between the tested compounds and the activated FRAP working reagent, the absorbance of the coloured solution was measured with spectrophotometer at 593 nm. The experiments were run in duplicate and repeated four times.

5.1.1.4. Cytotoxic Activity

Cytotoxicity of the compounds of interest and their effects on H_2O_2-induced cell death were evaluated on H9c2 cell line by MTT assay. The results are presented on Figure 14; none of the investigated compounds showed cytotoxic effect; compounds **893**, **865**, **987/3**, **876**, **1019/2** and **890** augmented the viability when the cells were treated with 125 μM H_2O_2. In case of the treatment with 250 μM H_2O_2, all investigated compounds except **874** significantly increased cell viability.

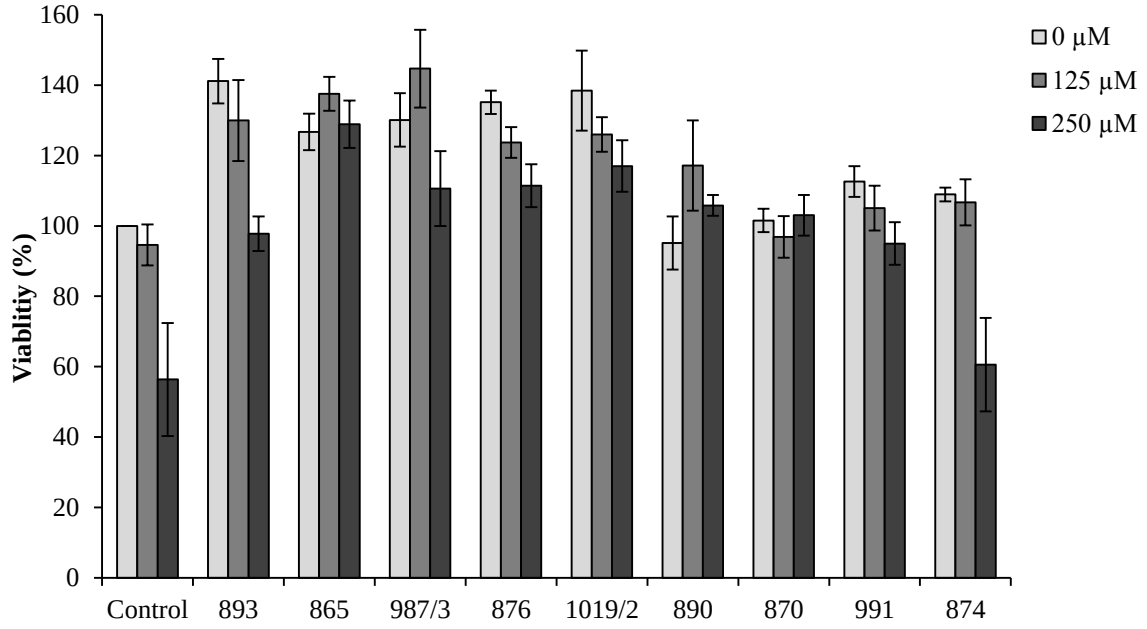

Figure 14. Cytotoxicity of the compounds of interest and their effects on H_2O_2-induced cell death at 125 and 250 μM hydrogen-peroxide concentrations were measured using MTT assay and H9c2 cells and expressed as viability percentage mean ± SEM. The experiments were run in four replicate and repeated three times.

5.1.2. Oxidative Transformation

Among the investigated molecules, compound **865** demonstrated very good antioxidant potency and positive effect on H9c2 cell viability, therefore it was selected for further studies in which its oxidative stability was investigated.

5.1.2.1. Chemical Fenton System

The chemical Fenton system was used to gather information about the oxidation of compound **865**. The sample was analysed by off-line ESI-MS technique. Based on the spectral data (Figure 15) obtained with this method, three oxidation products were identified as potential metabolites; **865-CH_3** (*m/z* 252.0) with the highest intensity, followed by **865+O** (*m/z* 282.3) and **865-2CH_3** (*m/z* 238.0).

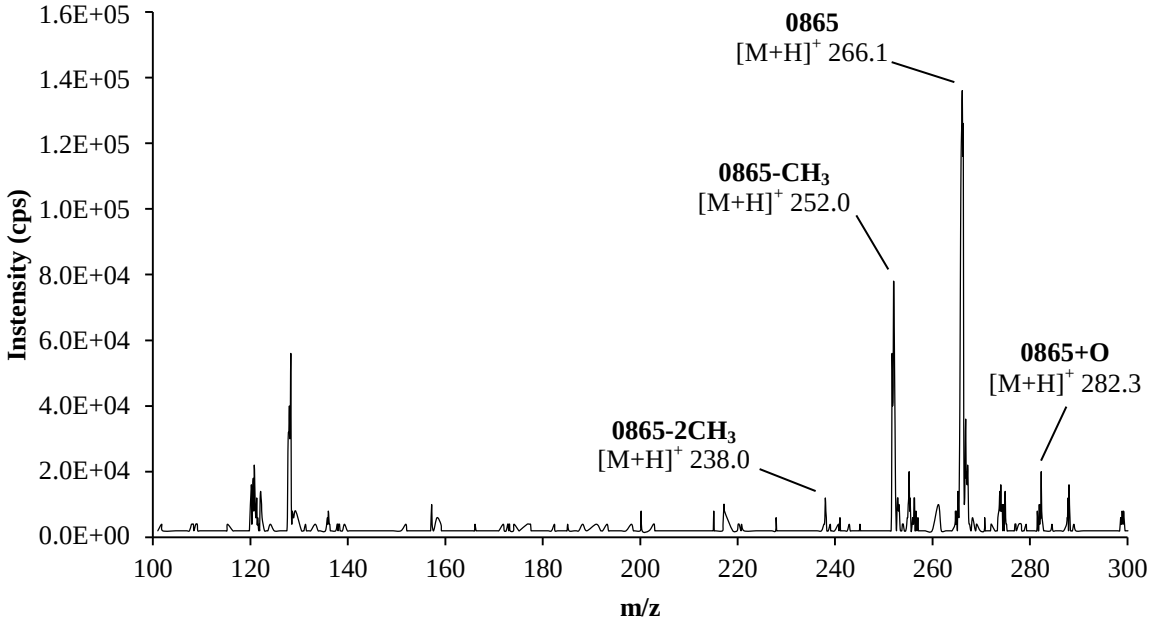

Figure 15. The ESI-MS spectra were obtained by the off-line analysis of the sample. The oxidation of the compound 865 was performed using chemical Fenton system.

5.1.2.2. Synthetic Porphine System

After gathering information about the oxidation of compound **865** achieved by the chemical Fenton system, we investigated the oxidative transformation of **865** using the Fe(III) meso-tetra (4-sulfonatophenyl) porphine chloride metalloorganic complex. The analysis of the sample was performed by LC-MS. Based on the recorded data (Figure 16), three oxidative products were detected: **865+O** (*m/z* 282.42), **865-2CH$_3$** (*m/z* 238.42) and **865+O-2H** (*m/z* 280.25). The peak with *m/z* 252.33 was also present in the control sample; in this case it is considered an impurity of **865**, as there was no evidence to prove otherwise.

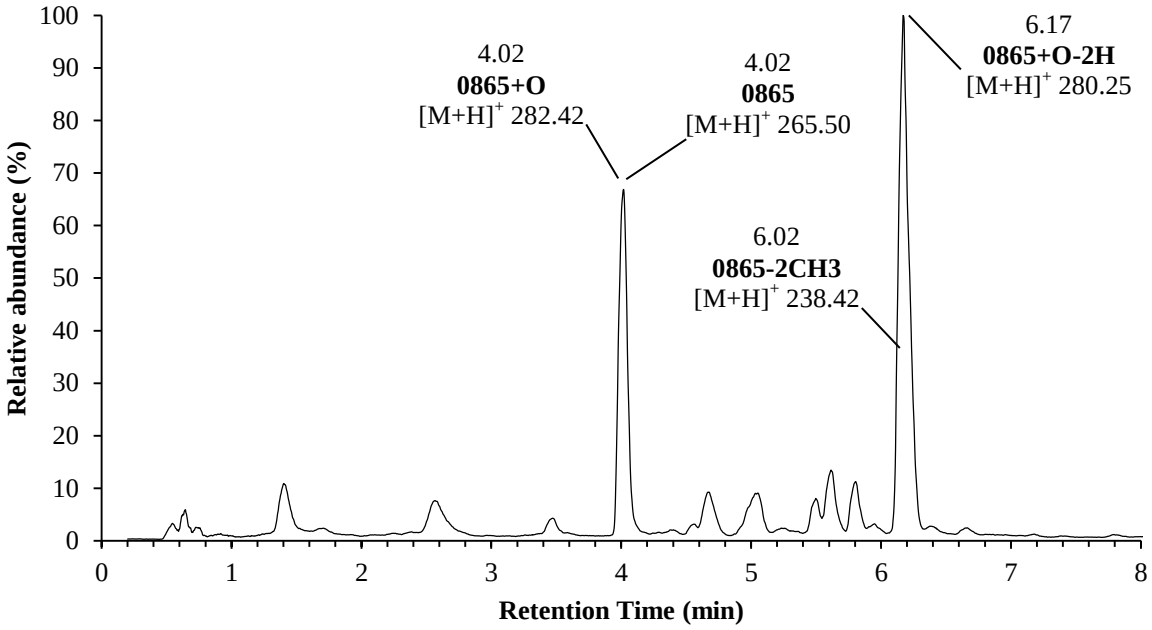

Figure 16. Chromatogram of the compound **865** oxidation by synthetic porphyrin. The data were recorded using LC-ESI-MS/MS technique.

5.1.2.3. Electrochemical System

The electrochemical oxidation of compound **865** was performed using EC-MS system. Figure 17 depicts the generated mass voltammogram by plotting the obtained mass spectra against the applied potential. The oxidation of **865** begins at approximately 1500 mV; its peak (*m/z* 266.1165) intensity has decreased, while the intensity of other peaks has increased. The **865-CH_3** (*m/z* 252.1014) was detected even at 0 mV; this is due to its oxidation in the ion source, although the intensity increase at 1500 mV confirms **865-CH_3** as oxidation product and at higher potential it is oxidized further to **865-2CH_3** (*m/z* 238.0858) primary amine. The aromatic hydroxylated product **865+O** (*m/z* 282.1133) was also observed along with its **865+O-2H** (*m/z* 280.0959) dehydrogenated derivative.

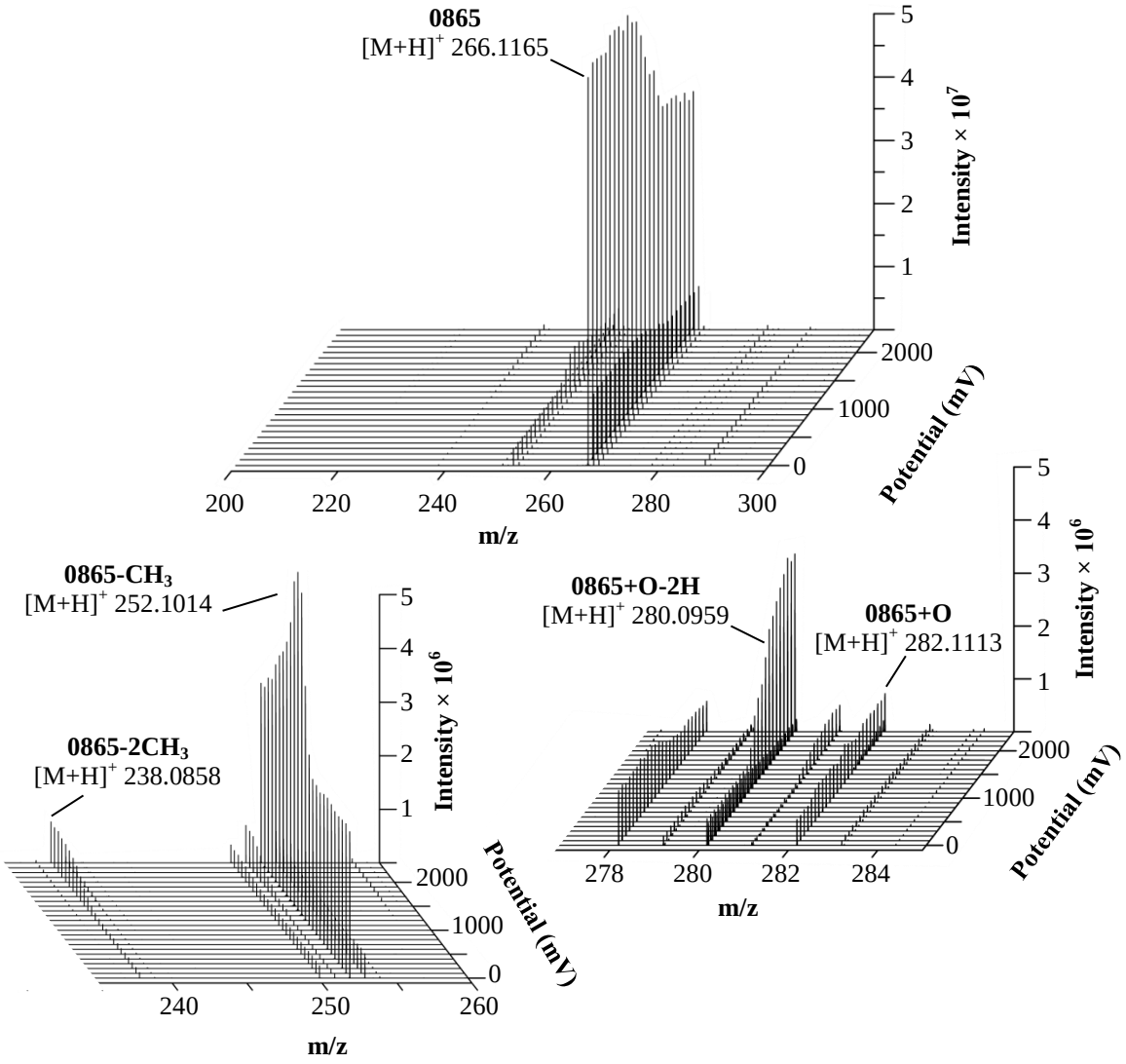

Figure 17. The generated mass voltammogram represents the electrochemical oxidation of compound **865**. The effluent from the thin-layer electrochemical cell was immediately introduced to a mass spectrometer equipped with ESI ion source.

*5.1.2.4. The Possible Routes of the Oxidative Transformation of Compound **865***

Scheme 1 shows the possible oxidative transformation pathway of compound **865** based on gathered information using three biomimetic systems and the detected metabolites. Reactions, such as aromatic hydroxylation, *N*-demethylation and dehydrogenation were observed. The exact location of the aromatic hydroxylation is unknown due to the limitations of the used techniques. However, we were able to determine that it happened on the B ring; as the result of the Retro-Diels-Alder reaction, which is a characteristic fragmentation of six membered ring systems containing double bonds, like flavonoids, fragment I and fragment II are formed. Fragment II of **865+O** (*m/z* 282.11) has higher *m/z* than the fragment II of **865** (*m/z* 266.11), confirming the aromatic hydroxylation of the B ring. The *N*-demethylation of **865** (*m/z* 266.11) leads to metabolite **865-CH$_3$** (*m/z* 252.09), which was *N*-demethylated further giving metabolite **865-2CH$_3$** (*m/z* 238.08). The product **865+O-2H** (*m/z* 280.09) is the result of the dehydrogenation followed by a possible ring closure between C3 and C6′ of the **865+O** (*m/z* 282.11).

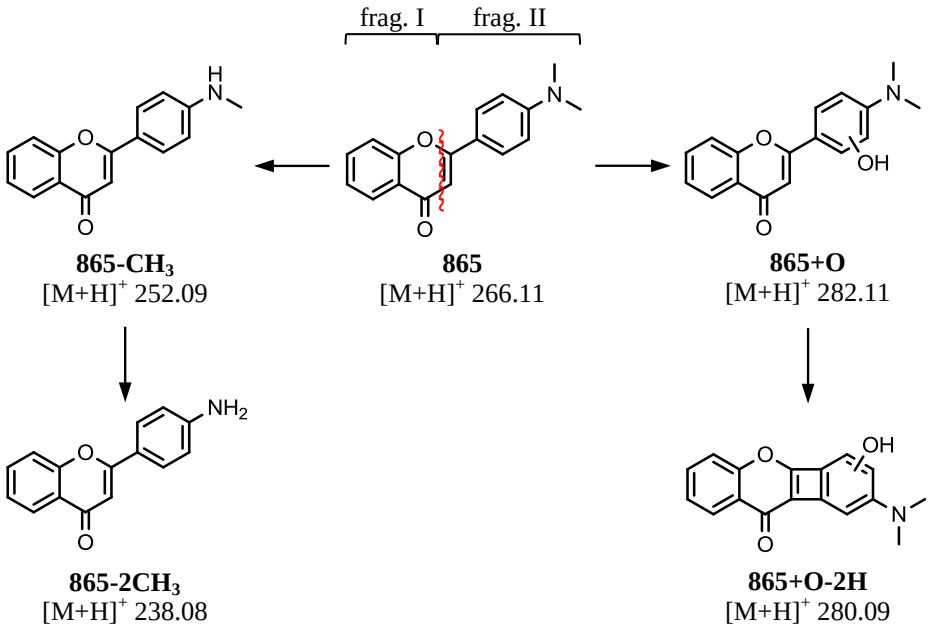

Scheme 1. The structure of compound **865** and its potential metabolites. The red line indicates formation of fragment I and II as results of the Retro-Diels-Alder reaction, which helped to identify the B ring as the location of the aromatic hydroxylation producing **865+O** (*m/z* 282.11). The dehydrogenation of **865+O** is followed by a likely cyclization between C3 and C6' resulting in **865+O-2H** (*m/z* 280.09). *N*-demethylation afforded metabolite **865-CH$_3$** (*m/z* 252.09), after the loss of the second methyl group, the formation of **865-2CH$_3$** (*m/z* 238.08) primary amine was observed.

5.2. RESULTS OF STUDY II

5.2.1. Chemistry

The synthesis of the flavonols (**6a-f**) is illustrated on Scheme 2. The first step was the Claisen-Schmidt condensation (i) of commercially available bromoacetophenones (**1a,b**) and benzaldehydes (**2a,b**) in MeOH using 4 equiv. NaOH, which gave the corresponding **3a-c** chalcones with excellent yields (88-97%). The cyclization (ii) into the flavonol backbone (**4a-c**) was carried out by adding 14.1 equiv. H_2O_2 to the solution of the chalcone (**3a-c**) in EtOH. The bromoflavon derivatives (**4a-c**) were coupled with the appropriate boronic acid (**5a,b**) under argon atmosphere (iii), in the presence of potassium-fluoride, $Pd(OAc)_2$ and XPhos in using toluene/*t*-BuOH (6:1) as solvent, thus providing the compounds of interest with the desired side chains on B ring (**6a-f**) with good yields (63-74%).

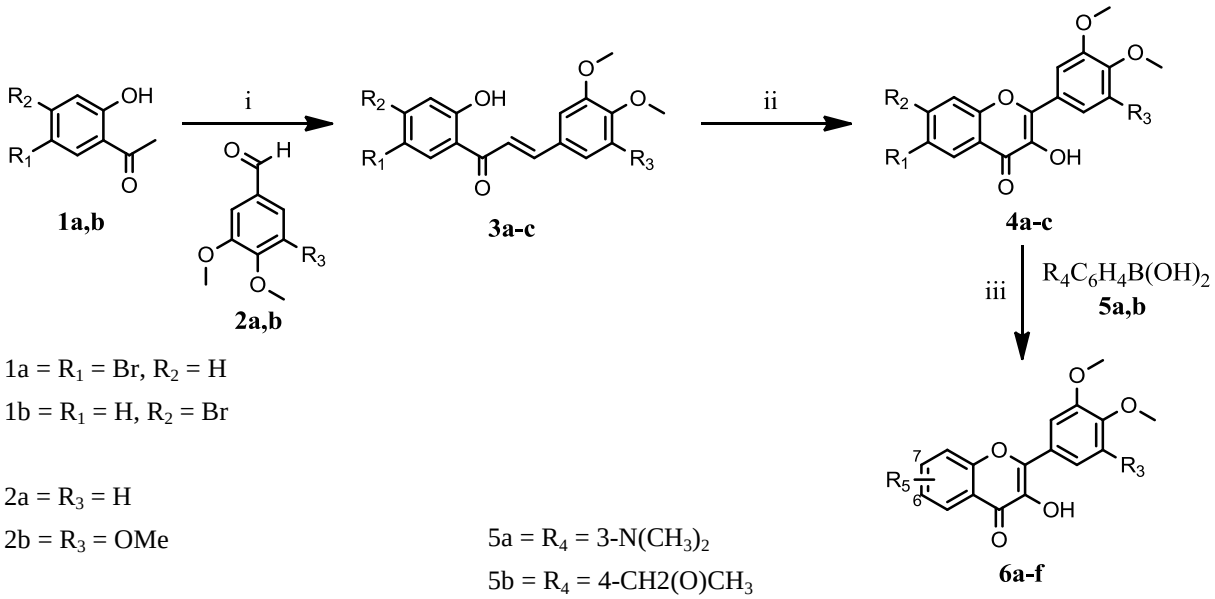

1a = R_1 = Br, R_2 = H
1b = R_1 = H, R_2 = Br

2a = R_3 = H
2b = R_3 = OMe

5a = R_4 = 3-$N(CH_3)_2$
5b = R_4 = 4-CH2(O)CH_3

3a = R_1 = Br, R_2 = H, R_3 = H (88%)
3b = R_1 = H, R_2 = Br, R_3 = H (97%)
3c = R_1 = H, R_2 = Br, R_3 = OMe (89%)

4a = R_1 = Br, R_2 = H, R_3 = H (74%)
4b = R_1 = H, R_2 = Br, R_3 = H (76%)
4c = R_1 = H, R_2 = Br, R_3 = OMe (57%)

6a = R_3 = H, R_5 = 6-[C_6H_4-3-$N(CH_3)_2$] (63%)
6b = R_3 = H, R_5 = 6-[C_6H_4-4-$CH_2(O)CH_3$] (72%)
6c = R_3 = OMe, R_5 = 7-[C_6H_4-3-$N(CH_3)_2$] (71%)
6d = R_3 = H, R_5 = 7-[C_6H_4-4-$CH_2(O)CH_3$] (72%)
6e = R_3 = H, R_5 = 7-[C_6H_4-3-$N(CH_3)_2$] (74%)
6f = R_3 = OMe, R_5 = 7-[C_6H_4-4-$CH_2(O)CH_3$] (69%)

Scheme 2. Synthesis of **6a-f**. Reagents and reaction condition: (i) **1a,b**, benzaldehyde **2a,b** (1.05 equiv.), 50% aq. NaOH (4 equiv.), MeOH, room temperature, 24 hours; (ii) **3a-c**, 8% aq. NaOH (3.1 equiv.), 30% H_2O_2 (14.1 equiv.), EtOH, room temperature, 2 hours; (iii) **4a-c**, **5a,b** (2 equiv.), KF (3 equiv.), $Pd(OAc)_2$ (5 mol%), XPhos (10 mol%), toluene/*t*-BuOH (6:1), argon atmosphere, 100 °C, 4 hours. The yields refer to pure isolated products.

5.2.2. Biological Activity

5.2.2.1. ABTS Radical Cation Scavenging Assay

The radical scavenging activity of the compounds of interest against ABTS radical cation was evaluated by ABTS assay. The regeneration of the ABTS from the radical cation causes a change in absorbance, which can be measured at 737 nm by spectrophotometer; the greater the change in the absorbance, the higher the scavenging potency of the tested compound. The calculated half-maximal scavenging rate (IC_{50}) of the compounds can be seen on Figure 18. The IC_{50} values were calculated for each compound from the mean (SD) inhibition percentage at 120 min in the concentration range of 10–200 μM. Compound **6c** was proven to be the most potent scavenger of the ABTS radical cation by having the lowest IC_{50} value followed by **6e** and **6a** respectively.

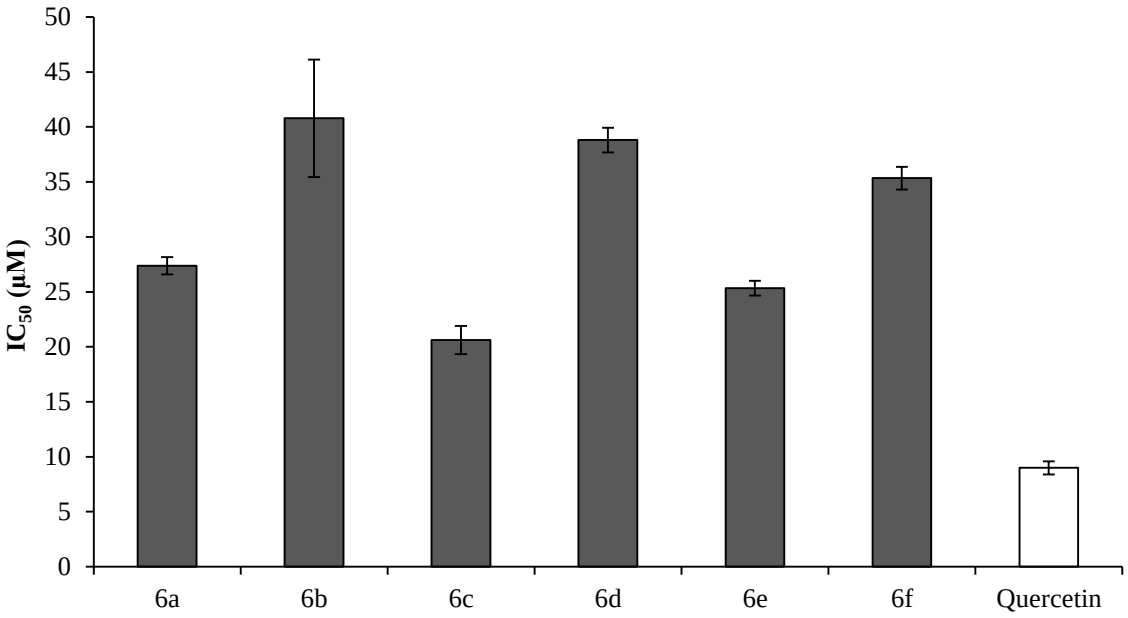

Figure 18. Mean (SD) IC_{50} values of $ABTS^{\bullet+}$ scavenging activity of the tested flavonol derivatives and quercetin standard given in μM. The inhibition percentage was determined at 120 min in the concentration range of 10–200 μM. The experiments were carried out in duplicate and repeated three times.

5.2.2.2. DPPH Radical Scavenging Assay

The solution of the stable DPPH radical is deep violet. As the antioxidant scavenges the radical, the decolorization can be detected at 515 nm by a spectrophotometer. Figure 19 represents the mean (SD) IC_{50} values for each investigated compound calculated from the inhibition percentage obtained at 90 min in the concentration range of 10–200 μM. Compound **6c** had the lowest IC_{50} value, followed by **6a**, **6d** and **6b** respectively.

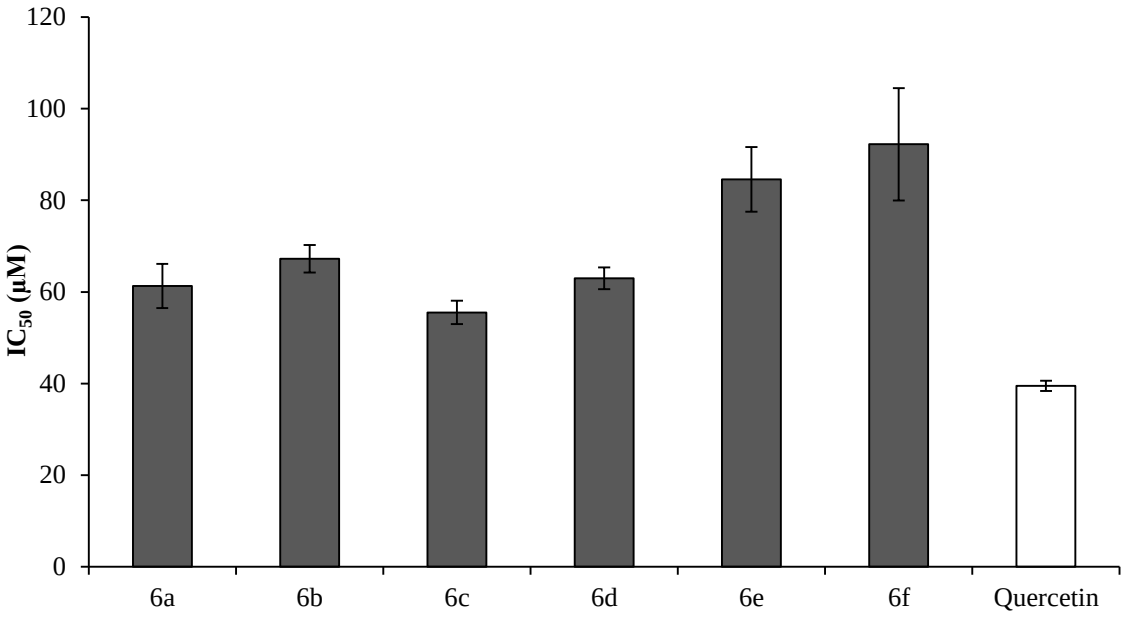

Figure 19. The mean (SD) IC_{50} DPPH scavenging rate was determined at 90 min in the concentration range of 10–200 μM for all investigated flavonol derivatives and quercetin standard. The measurements were run in duplicate and repeated three times.

5.2.2.3. Oxygen-Radical Absorption Capacity Assay

The oxygen radical absorbance capacity of flavonols was measured with ORAC assay at 2 and 10 μM concentrations and expressed as mean (SD) net area under the curve. The results are shown on Figure 20; at both flavonol concentrations compound **6e** had the highest ORAC value, followed by **6a** and **6b** respectively. The capacity of compound **6a** and **6e** are comparable to the capacity of quercetin at 10 μM concentrations, while surprisingly **6c** had only the fourth highest ORAC value.

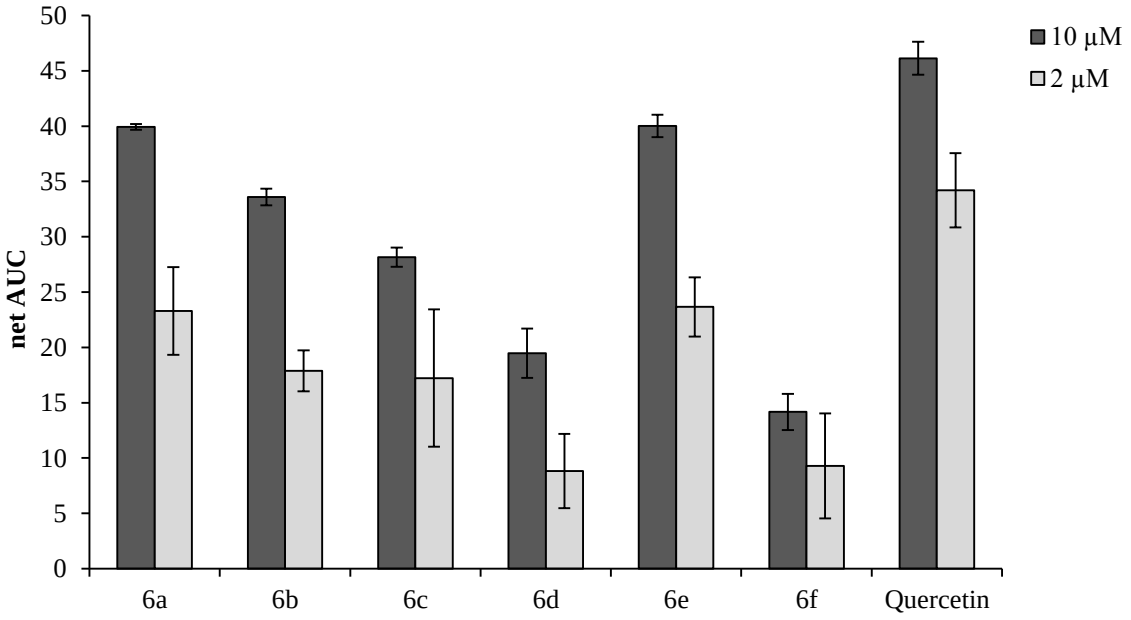

Figure 20. The ORAC values of the compounds of interest expressed in mean (SD) net AUC. The reaction was initiated by the rapid addition of 2,2'-azobis(2-amidinopropane) dihydrochloride solution into the mixture of the tested compounds and fluorescein. The fluorescence was monitored at 485 nm excitation and 520 nm emission wavelength for 2 hours in every 2 min. Each measurement was performed in duplicate and repeated three times. The net AUC was calculated by subtracting the blank AUC from sample AUC.

5.2.2.4. Ferric Reducing Antioxidant Power Assay

The ability of the compounds of interest to reduce Fe^{3+} to Fe^{2+} was measured directly by FRAP assay using $FeSO_4$ as standard. The results are represented on Figure 21; the results are given in mean (SD) μM ferrous equivalents. Compounds **6c** showed the highest FRAP activity at all the tested concentrations followed by **6a** and **6e** respectively, although the FRAP values of the investigated flavonol derivatives are significantly lower compared to the quercetin.

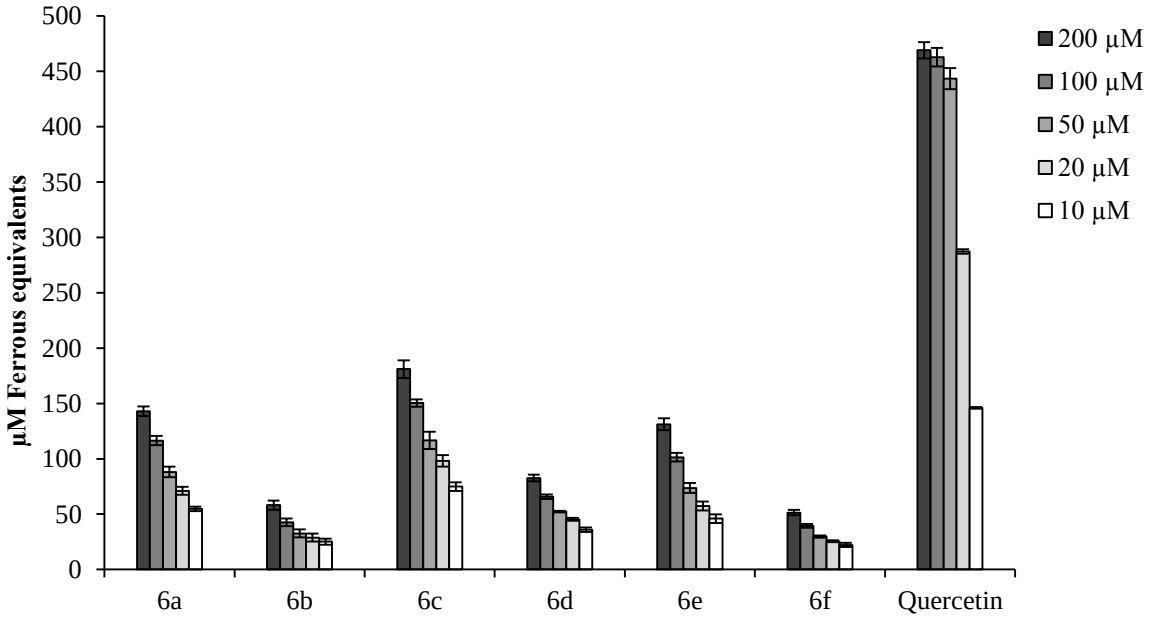

Figure 21. FRAP values of the investigated compounds. The FRAP working solution was prepared freshly from acetate buffer, TPTZ and $FeCl_3$ and was incubated at 37 °C for 15 min before use. Following the addition of the FRAP reagent to the solution of the tested compounds and the quercetin standard, the plate was incubated for 30 min. The change in absorbance was measured at 593 nm. The FRAP values were calculated using iron(II) sulfate heptahydrate calibration standard solutions and they are expressed as mean (SD) μM Ferrous equivalents. The experiments were run in duplicates and repeated three times.

5.2.2.5. Cytotoxic Activity

The results of the MTT assay using H9c2 cells are represented on the Figure 22. Compounds **6a**, **6c** and **6e** did not show cytotoxic activity. However, compounds **6b**, **6d** and **6f** had negative effect on the viability of cardiomyoblastoma cells.

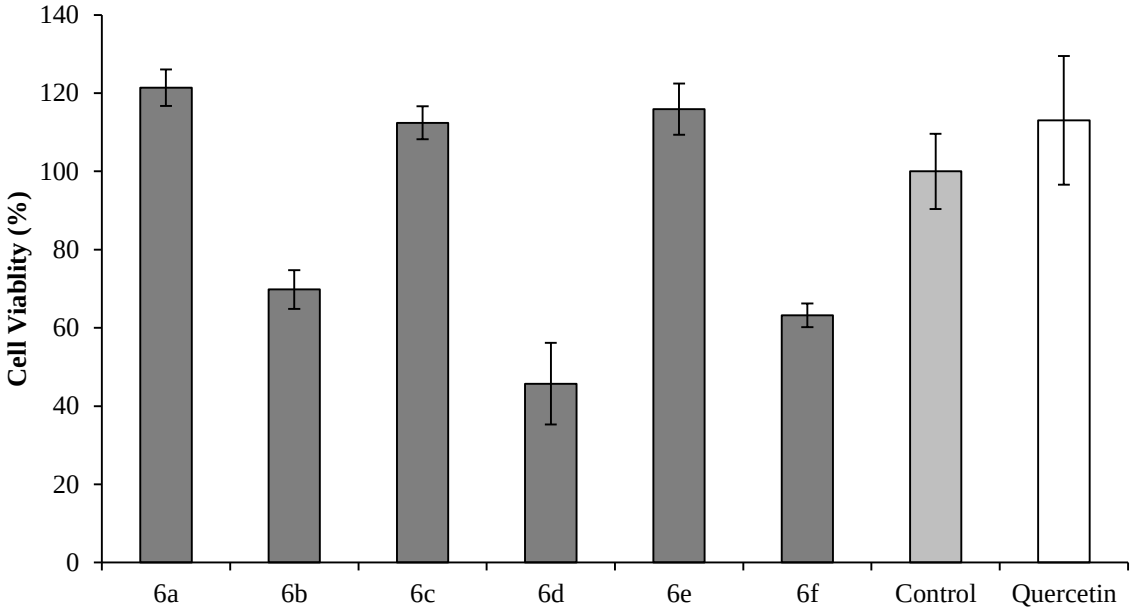

Figure 22. The effect of the tested compounds and the quercetin standard in 20 μM concentrations on the viability of H9c2 cells was evaluated by MTT assay. The cardiomyoblastoma cells were treated for 12 hours and following the addition of the MTT solution, the plates were incubated for 4 hours. The absorbance was measured at 540 and 630 nm. The results are expressed as mean (SD) cell viability percentage. The measurements were carried out in triplicate and repeated two times.

5.2.3. Oxidative Transformation

Compound **6c** exhibited very good antioxidant potency and it had positive effect on H9c2 cell viability, this molecule was selected for further studies in which its possible oxidative transformation pathways were investigated.

5.2.3.1. Chemical Fenton System

The chemical Fenton system was used to investigate the oxidative transformation of compound **6c**. Based on the spectral data (Figure 23) obtained with electrospray ionization mass spectrometry, we were able to detect and identify two oxidation products as potential metabolites. The **6c+O** (*m/z* 434.2) is a product of aromatic hydroxylation, while the most abundant metabolite **6cO-CH$_3$** (*m/z* 404.1) was formed though *O*-demethylation.

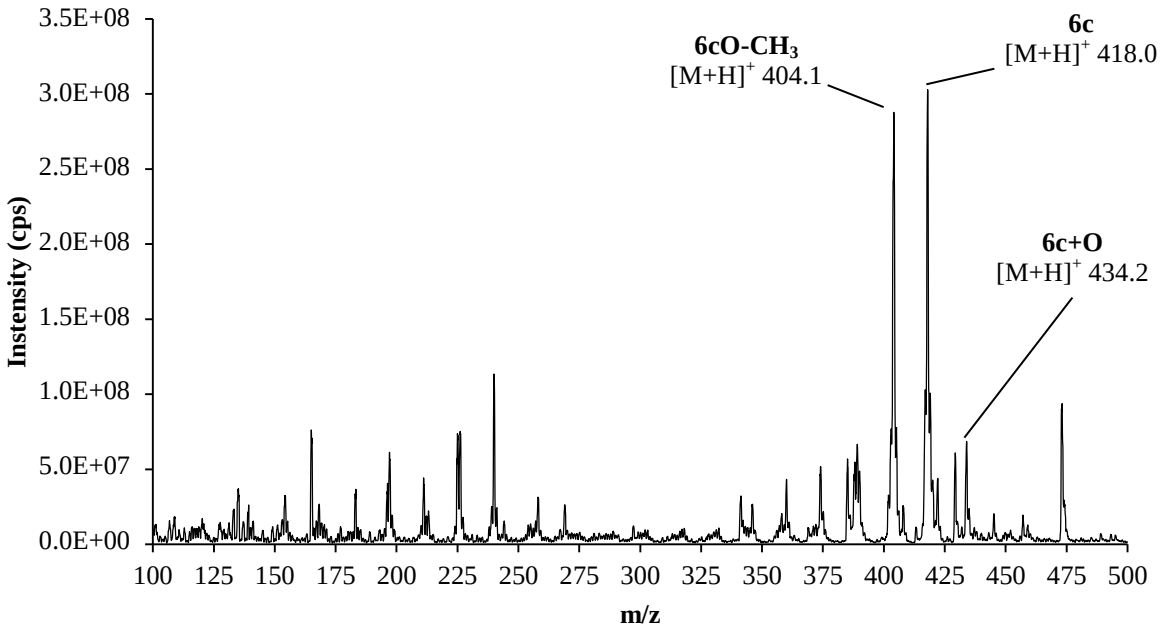

Figure 23. Chemical Fenton system was used to mimic the oxidative transformation of compound **6c**. The reaction mixtures were analysed by an electrospray ionization mass spectrometer. The structures of potential metabolites (**6c+O** and **6cO-CH$_3$**) were determined based on the obtained mass spectra.

5.2.3.2. The Possible Routes of the Oxidative Transformation of Compound ***6c***

Scheme 3 depicts the possible route of the oxidative transformation of compound **6c** based on the observed oxidation and the generated metabolites. The structural determination of metabolites **6c+O** and **6cO-CH$_3$** was performed using MS/MS data obtained with the method of product ion scan; the Retro-Diels-Alder reaction is also a characteristic fragmentation of flavonols. This reaction splits the flavonol in half indicated with red on the scheme, and thus helping to identify the location of the aromatic hydroxylation and *O*-demethylation; in this case, metabolite fragment II has higher (aromatic hydroxylation) or lower (*O*-demethylation) *m/z*, than fragment II of the compound **6c**. This change in the *m/z* of fragment B confirms that the place of the oxidative transformation is the B ring. However, due to the limitations of the used technique, the exact location remains unknown.

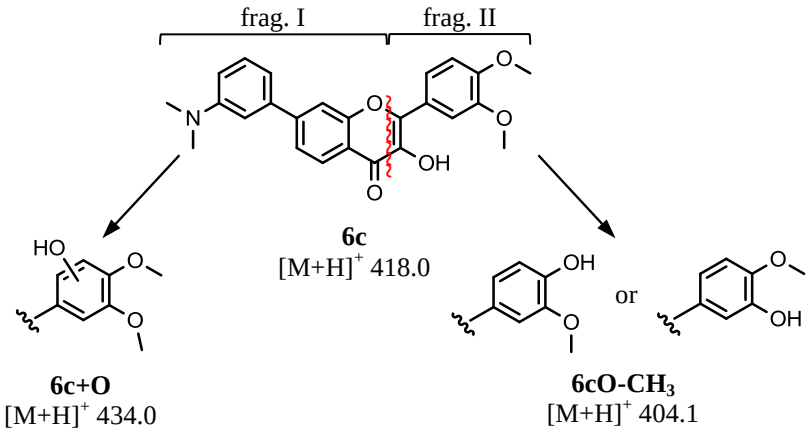

Scheme 3. The structure of compound **6c** and its potential metabolites. The red line indicates bond dissociation during the Retro-Diels-Alder reaction, which results in fragment I and II. This reaction helps to determine the location of the observed aromatic hydroxylation and *O*-demethylation. The oxidative transformation happens on the B ring and gives the metabolites **6c+O** and **6cO-CH$_3$**. The exact position of the hydroxyl group on B ring is unknown as the position of the O-demethylation.

6. DISCUSSION

The cardiovascular diseases caused 31% of the total deaths globally in 2015 [71]. The increased prevalence of the risk factors in the low-risk countries will result in the rise of cardiovascular disease related deaths. In the cardiovascular system under normal physiological conditions the reactive oxygen species function as signalling molecules to maintain the redox homeostasis [29], and their concentration is controlled by enzymatic and non-enzymatic endogenous antioxidant systems [72]. However, when these systems cannot maintain this balanced state, the excessive ROS formation contributes to the initiation and/or progression of many CVDs [73, 74]. The exogenous antioxidants, such as polyphenols, carotenoids, vitamin E, and vitamin C are necessary for the defence system in order to maintain this delicate equilibrium and their main source is the diet [75, 76]. The cytoprotective effect of these molecules is well known, but they can also exhibit prooxidant activities causing "antioxidative stress" depending on the conditions and the dose [77, 78]. The aim of the future exogenous antioxidants is to prevent the overproduction of the ROS without disrupting the redox homeostasis.

6.1. INTERPRETATION OF STUDY I RESULTS

Antioxidant activity cannot be determined based on a single assay or test; the ORAC assay is considered one of the most suitable methods for measuring antioxidant activity because it uses biologically relevant free radicals [79], while neither ABTS nor any similar radical can be found in biological system [80], however none of the tests has achieved general acceptance. Therefore, numerous assays and unified interpretation of their results are necessary to evaluate antioxidant activity adequately. Although, these tests should give consistent results despite of their different reaction mechanisms, it is rarely the case.

The results of the three different assays for compound **865** in Study I are consistent; it was revealed that compound **865**, an *N*,*N*-dimethylamino group containing simple-structured flavonoid has the highest antioxidant activity among the tested nine molecules; **865** demonstrated significantly higher ABTS radical cation scavenging and FRAP activity and it has better oxygen radical absorption capacity. However, the other compounds also showed significantly greater ORAC value than the coumarin standard. Surprisingly, compound **865** has only one of the most significant structural features to be an effective radical scavenger; the conjugation between the 2,3-double bond with a oxo function at position 4, but the other features are not present: OH-functions in positions 3 and 5 [81] and catechol (*o*-dihydroxy) system in the B-ring [82]. The difference in the results obtained by these three methods presumably is caused by their different mechanism; the ABTS and FRAP assays are SET-based, while the ORAC assay is based on HAT mechanism. The FRAP is the only method, which measures the direct antioxidant potency, whereas the other assays measure the antioxidant activity by the inhibition of a free radical [83].

The MTT assay is a first-approach method for measuring cell viability, although it measures the mitochondrial metabolic rate which can be affected by chemical treatments or different conditions, and thus providing results that are not necessarily connected directly to cytotoxicity [84]. However, in this case there are no factors affecting the outcome of the measurement and the results are consistent; the viability of the treated cells in case of compounds **865**, **876**, **893**, **987/3**, **876**, and **1019/2** increased compared to the untreated control. Similar results can be observed when the cells were treated with H_2O_2 besides the flavonoid-derivatives; they showed cytoprotective activity by preventing the H_2O_2-induced cell death of the cardiomyocytes. The antioxidant activity and the lack of cytotoxicity have made the compound **865** a prominent candidate for further *in vivo* testing.

Nevertheless, prior to any *in vivo* experiments, metabolic peculiarities and possible toxicity must be elucidated as early as possible in order to spare time and costs by rapidly identify robust candidates and prevent compound failures [85, 86]. The oxidative metabolism of compound **865** was investigated using three different biomimetic systems; to gather information about the behaviour of the molecule in an oxidative environment, it was oxidized first by chemical Fenton system and the data collection was performed off-line by ESI-MS/MS technique. The Fenton reaction is a biomimetic system used to model phase I metabolic reactions, such as *N*-dealkylation, *N*-oxidation, *O*-dealkylation, *S*-oxidation, dehydrogenation, and different hydroxylation reactions [50]. The chemical Fenton system was able to detect the following potential metabolites of the compound **865**; the *N*-dealkylation yielded the **865-CH$_3$** secondary amine with the highest intensity, and a second *N*-dealkylation afforded **865-2CH$_3$** primary amine. The aromatic hydroxylation of the B ring resulted in the metabolite **865+O**. However, the Fenton system is able to mimic dehydrogenation, the product of this reaction was not detected, probably due to its low concentration being under the limit of detection of the used method.

The synthetic metalloporphine system can mimic *N*-dealkylation, *N*-oxidation, *S*-oxidation, hydroxylation, epoxidation, and dehydrogenation reactions [57, 87, 88]. The off-line LC/MS analysis showed that three reactions of compound **865** were mimicked; the loss of two methyl group via *N*-dealkylation afforded **865-2CH$_3$** primary amine, the aromatic hydroxylation of the B ring yielded **865+O**, and the dehydrogenated derivative of the hydroxylated product **865+O-2H** was also detected. Product secondary amine **865-CH$_3$** was also observed, but it was also present in the control sample and further evidence have not verify its presence as metabolite it is considered as an impurity in this case.

The EC/LC/MS and EC/MS systems have been a useful tool to produce potential metabolites produced by aromatic hydroxylation, dehydrogenation, *S*-, *P*-oxidation, and *N*-dealkylation [50, 89, 90]. This method was used to generate the mass voltammogram, a graph of the mass spectra plotted against the varying applied potential, which helps to determine the most suitable electrochemical potential at which the highest oxidation conversion rate of the investigated compound can be achieved. For the compound **865**, this potential is 1500 mV. The EC/LC/MS method was able to produce the same potential metabolites as the two other model systems; **865-CH$_3$** secondary amine and the further oxidized **865-2CH$_3$** primary amine, the aromatic hydroxylated product **865+O** and its **865+O-2H** dehydrogenated derivative.

6.2. INTERPRETATION OF STUDY II RESULTS

The Study II was conducted to further investigate the possible effects of the *N*,*N*-dimethylamino group on the antioxidant and cytoprotective activity of flavonoid derivatives. Based on the results of Study I, new flavonol derivatives (**6a-f**) were designed and synthetized with phenyl-*N*,*N*-dimethylamino or methoxymethyl phenyl group connected to the A ring in position 6 or 7. These flavonols have the conjugated system between the 2,3-double bond and the oxo function in position 4, but the formation of catechol moiety on B ring have posed insuperable challenge; the synthesis of the demethylated derivatives requires such forceful conditions, which resulted in the decomposition of the molecules.

The antioxidant activity of the investigated molecules (**6a-f**) was evaluated based on one HAT-based and three SET-based assays. The ABTS IC_{50} value was calculated from the inhibition percentage at 120 min determined in the concentration range of 10–200 μM. As the ABTS abstracts an electron from the antioxidant, it is regenerated to its original form causing a change in the absorbance of the solution at 737 nm, which can be measured by a spectrophotometer. Compound **6c** had the lowest IC_{50} value, and therefore the highest ABTS radical scavenging activity, followed by **6e** and **6a**. These compounds bear with the phenyl-*N*,*N*-dimethylamino group on their A ring, and because the electronegativity difference their ability to donate an electron during the single electron-transfer to the ABTS radical cation is better than the methoxymethyl group containing derivatives (**6b**, **6d**, and **6f**).

The DPPH assay is based on similar principle as the ABTS assay; i.e., the solution of the stable DPPH radical is deep violet, which loses its colour as the DPPH is reduced by the antioxidant. This change can be detected at 515 nm. The DPPH IC_{50} values were calculated from the inhibition percentage at 90 min obtained in the concentration range of 10–200 μM. Compound **6c** exhibited the lowest DPPH IC_{50} value, followed by **6a**, **6d**, and **6b**. These derivatives (**6a**, **6b**, **6c**, and **6d**) have only two methoxy groups on the B ring, while the other compounds (**6e** and **6f**) have three. According to Kim B. T. et al., *ortho*- and *para*-substitution pattern of two hydroxyl groups on the B ring in chalcones have much higher antioxidant activity than the *meta*-substitution pattern. The *ortho*- and *para*-dihydroxylated benzene ring systems are much more efficient in delocalizing electrons than the meta- dihydroxylated ones, and thus resulting in more stable chalcone adduct formation during a reaction with free radicals [91]. Furthermore, the presence of three methoxy groups on B ring increases the steric hindrance causing a perturbed planarity leading to decreased ability of hydrogen abstraction, which would be easier in planar geometrical configuration, and hence these

compounds (**6e** and **6f**) have lower radical-scavenging ability [92]. The fact, that phenyl-*N*,*N*-dimethylamino group containing **6c** was the most active molecule in both ABTS and DPPH assay correlates well with the findings of Culhaoglu et al., in which among the investigated 3-hydroxyflavone derivatives, the 4'-*N*,*N*-dimethyl flavonol exhibited DPPH scavenging potency, comparable with a standard compound quercetin, and it had the highest ABTS cation radical scavenging potency [93]. Based on the results of radical scavenging assays in both Study I and Study II, the phenyl-*N*,*N*-dimethylamino-group could play a key part in the radical scavenger activity of the investigated flavonoid derivatives.

Among the investigated derivatives at all concentrations (10, 20, 50, 100 and 200 μM) compounds **6c**, **6a**, and **6e** exhibited the highest FRAP values, whilst compounds **6d**, **6f**, and **6b** had significantly lower ferric reducing antioxidant potential. However, the fact that each tested derivatives (**6a-f**) showed significantly lower FRAP value compared to the quercetin standard compound is not a surprise, as it is well-known that the methoxylation of flavonoids leads to decreased antioxidant activity compared to the unmethylated derivatives [94, 95]. Deng et al. reported that the methylated quercetin had a FRAP value 650-times lower than quercetin, but this drastic decrease was not observed in Study II, probably due to the presence of phenyl-*N*,*N*-dimethylamino group at ring A and the free OH group in position 3. The outcome of the FRAP assay also indicates the importance of the phenyl-*N*,*N*-dimethylamino group; all the tested compounds have the free OH group in position 3, however only those compounds had higher ferric reducing antioxidant potential, which have the phenyl-*N*,*N*-dimethylamino group (**6c**, **6e**, and **6a**).

Compounds **6e**, **6a**, and **6b** exhibited the highest oxygen radical absorption capacity, which was comparable to the capacity of the quercetin at a 10 μM concentration. Strikingly, the compound **6c** had only the fourth highest ORAC value at both concentrations. To test the cytotoxic effect of the flavonol derivatives, H9c2 cells were treated with 20 μM flavonol solutions for 12 h. These results are consistent with the findings of Deng et al.; in case of methylated polyphenols the change in the ORAC values was not as significant as in the FRAP results compared to the unmethylated derivatives [95].

The results of the MTT assay showed no cytotoxic activity in case of the phenyl-*N*,*N*-dimethylamino functional group containing molecules (**6a**, **6c** and **6e**); the cell viability percentages were comparable to the quercetin standard compound and untreated control as well. This correlates well with the report of Luo W. et al., in which they found that 4-dimethylamine flavonoid derivatives have protective effect against oxidative stress-induced cell death in PC12 neurons [96]. However, the compounds with methoxymethyl groups on A

ring (**6b**, **6d**, and **6f**) significantly decreased the cell viability. This negative effect of the treatment was the most significant in case of the compound **6d**; compared to the control the cell viability was decreased to 46%. These findings are consistent with that of other studies investigating the effect of the position and number of methoxy groups in flavonoid derivatives on antioxidant potency and cytotoxic activity [95, 97, 98]. Based on these results, depending on the number and position, the methoxy groups could have negative effect on cell viability, however the exact structure-activity relationship is yet to be discovered.

The possible oxidative transformation route and the formation of potential metabolites of compound **6c** were investigated due to its aforementioned antioxidant and non-cytotoxic characteristics. The chemical Fenton system was chosen as biomimetic model system of phase I metabolic reactions based on the structure of compound **6c**; this method has been proved useful in Study I to successfully produce metabolites of *N*-dealkylation and aromatic hydroxylation of the compound **865**, and it is also capable of *O*-dealkylation mimicry [49, 50]. The generated oxidative products of compound **6c** were detected and identified with ESI-MS and confirmed also by LC/ESI-MS analysis; based on the peak intensity the most abundant product were the *O*-demethylated **6cO-CH$_3$** derivative, and the atomatic hydroxylation on the B ring afforded the **6c+OH** potential metabolite. As in Study I, the place of these reactions was determined based on the retro Diels-Alder rearrangement fragmentation pattern characteristic to the 3-hydroxyflavone structure. Additional investigative methods, such as electrochemical oxidation and synthetic porphyrin systems could generate other metabolites; secondary **6cN-CH$_3$** and primary amine **6cN-2CH$_3$** after *N*-dealkylation. Although, the exact positions of these transformations cannot be determined due to the limitations of the analytical methods used.

7. SUMMARY

In Study I, nine flavonoids were tested for their possible antioxidant and cytotoxic activities. As the result of this investigation the significant antioxidant potency, cytoprotective activity, and the metabolic stability of 4-*N*,*N*-dimethylamino-flavon (compound **865**) (Figure 23) were observed.

Based on this outcome, six new flavonols were designed and synthetized for Study II, in which we investigated the effect of phenyl-*N*,*N*-dimethylamino group on the antioxidant activity. The *N*,*N*-dimethylamino group containing flavonol derivatives (**6a**, **6c** and **6e**) (Figure 24) showed increased activity during different antioxidant assays, and the also exhibited cytoprotective effect on H9c2 cardiomyoblast cells.

The results of both Study I and Study II suggest that the phenyl-*N*,*N*-dimethylamino group has a crucial role in the antioxidant potency and in the cytotoxicity of flavonoid derivatives. The oxidative stability of **865** and **6c** also makes them an ideal candidate for the investigation of oxidative stress related diseases in suitable animal models.

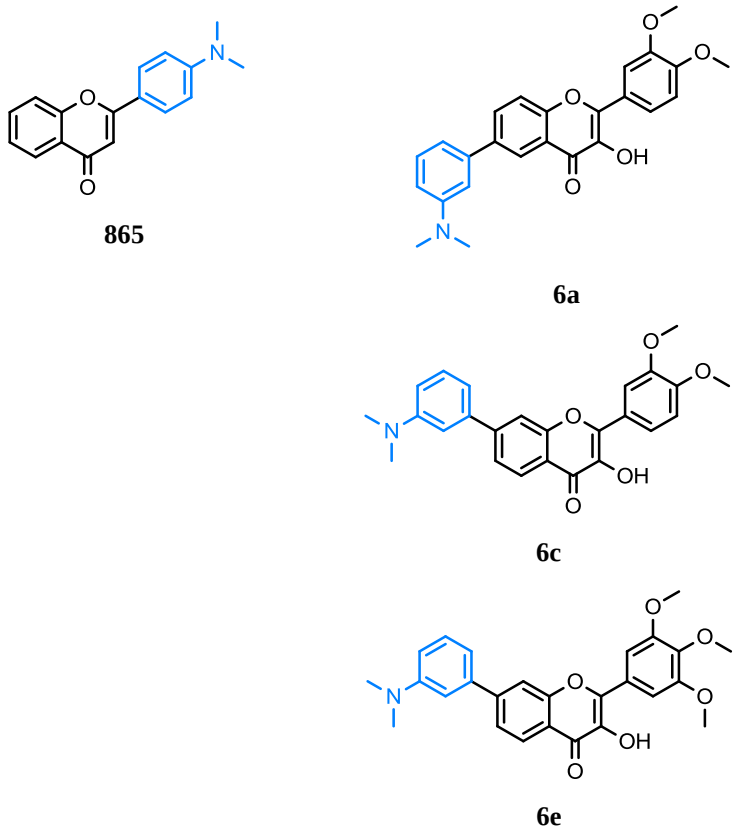

Figure 24. The structures of compounds **865**, **6a**, **6c** and **6e**, which demonstrated good antioxidant activity and increased H9c2 cell viability.

8. Összefoglalás

A kutatás első részében kilenc flavonoid származék antioxidáns hatását és citotoxicitását tanulmányoztuk. Eredményeinkből kiderült, hogy a 4-*N*,*N*-dimetilamino flavon (vegyület **865**) (24. ábra) jelentős antioxidáns és citoprotektív hatással rendelkezik, valamint metabolikusan stabil.

Ezen adatok alapján, hat új flavonol származékot terveztünk és állítottunk elő a kutatás második részében, amely során vizsgáltuk a fenil-*N*,*N*-dimetilamino-csoport hatását az antioxidáns aktivitásra. Az eredmények azt mutatták, hogy a fenil-*N*,*N*-dimetilamin-csoportot tartalmazó molekulák (**6a**, **6c** és **6e**) (25. ábra) antioxidáns aktivitása nagyobb, továbbá cardioprotektív hatással is rendelkeznek H9c2 sejtvonal esetében.

A kutatás első és második részének az összevont eredményei szerint a fenil-*N*,*N*-dimetilamino-csoportnak kulcsszerepe van a flavonoidok antioxidáns aktivitásában csoportnak kulcsszerepe van a flavonoidok antioxidáns aktivitásában és citotoxicitásában egyaránt. A oxidatív stabilitása ígéretes jelöltekké teszi a **865** és **6c** molekulákat az oxidatív stresszel kapcsolatos betegségek vizsgálatában a megfelelő állatmodelleket alkalmazva.

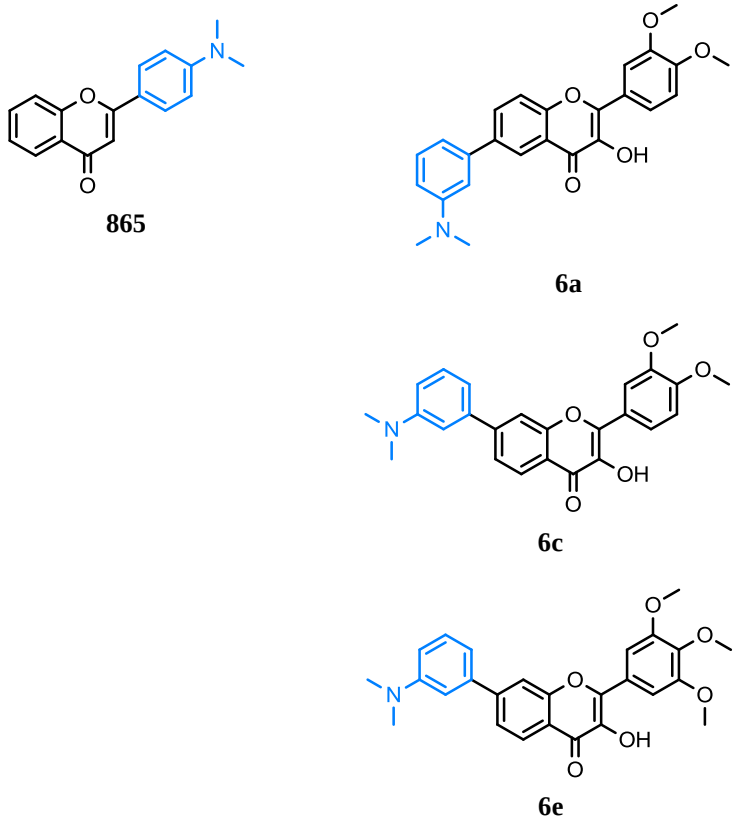

25. Ábra. A jó antioxidáns hatású és citoprotektív **865**, **6a**, **6c** és **6e** molekulák szerkezete.

9. REFERENCES

9.1. REFERENCES CITED IN THE THESIS

[1] M. Avkiran, M.S. Marber, Na(+)/H(+) exchange inhibitors for cardioprotective therapy: progress, problems and prospects, *J Am Coll Cardiol*, 2002. **39**: 747-753.

[2] D.N. Granger, Ischemia-reperfusion: mechanisms of microvascular dysfunction and the influence of risk factors for cardiovascular disease, *Microcirculation*, 1999. **6**: 167-178.

[3] R.J. Korthuis, D.N. Granger, M.I. Townsley, A.E. Taylor, The role of oxygen-derived free radicals in ischemia-induced increases in canine skeletal muscle vascular permeability, *Circ Res*, 1985. **57**: 599-609.

[4] H.M. Honda, P. Korge, J.N. Weiss, Mitochondria and ischemia/reperfusion injury, *Ann N Y Acad Sci*, 2005. **1047**: 248-258.

[5] A.P. Halestrap, S.J. Clarke, S.A. Javadov, Mitochondrial permeability transition pore opening during myocardial reperfusion--a target for cardioprotection, *Cardiovasc Res*, 2004. **61**: 372-385.

[6] H. Sies, Oxidative stress: from basic research to clinical application, *Am J Med*, 1991. **91**: 31S-38S.

[7] T.M. Paravicini, R.M. Touyz, Redox signaling in hypertension, *Cardiovasc Res*, 2006. **71**: 247-258.

[8] F. Bonomini, S. Tengattini, A. Fabiano, R. Bianchi, R. Rezzani, Atherosclerosis and oxidative stress, *Histol Histopathol*, 2008. **23**: 381-390.

[9] V. Schächinger, M. Zeiher Andreas, Quantitative Assessment of Coronary Vasoreactivity in Humans In Vivo, *Circulation*, 1995. **92**: 2087-2094.

[10] Y. Higashi, S. Sasaki, K. Nakagawa, H. Matsuura, T. Oshima, K. Chayama, Endothelial Function and Oxidative Stress in Renovascular Hypertension, *New England Journal of Medicine*, 2002. **346**: 1954-1962.

[11] T.M. Paravicini, R.M. Touyz, NADPH Oxidases, Reactive Oxygen Species, and Hypertension, *Clinical implications and therapeutic possibilities*, 2008. **31**: S170-S180.

[12] M.M. Elahi, B.M. Matata, Free radicals in blood: evolving concepts in the mechanism of ischemic heart disease, *Arch Biochem Biophys*, 2006. **450**: 78-88.

[13] A. Warnholtz, G. Nickenig, E. Schulz, R. Macharzina, J.H. Bräsen, M. Skatchkov, T. Heitzer, J.P. Stasch, K.K. Griendling, D.G. Harrison, M. Böhm, T. Meinertz, T. Münzel, Increased NADH-Oxidase-Mediated Superoxide Production in the Early Stages of Atherosclerosis, *Circulation*, 1999. **99**: 2027-2033.

[14] U. Landmesser, R. Merten, S. Spiekermann, K. Buttner, H. Drexler, B. Hornig, Vascular extracellular superoxide dismutase activity in patients with coronary artery disease: relation to endothelium-dependent vasodilation, *Circulation*, 2000. **101**: 2264-2270.

[15] M.J. Steinbeck, A.U. Khan, M.J. Karnovsky, Extracellular production of singlet oxygen by stimulated macrophages quantified using 9,10-diphenylanthracene and perylene in a polystyrene film, *J Biol Chem*, 1993. **268**: 15649-15654.

[16] H.J.H. Fenton, Oxidation of tartaric acid in presence of iron, *Journal of the Chemical Society*, 1894. **65**.

[17] S. Jang, J.A. Imlay, Micromolar intracellular hydrogen peroxide disrupts metabolism by damaging iron-sulfur enzymes, *J Biol Chem*, 2007. **282**: 929-937.

[18] C. Ceconi, A. Cargnoni, E. Pasini, E. Condorelli, S. Curello, R. Ferrari, Evaluation of phospholipid peroxidation as malondialdehyde during myocardial ischemia and reperfusion injury, *American Journal of Physiology-Heart and Circulatory Physiology*, 1991. **260**: H1057-H1061.

[19] D. Steinberg, S. Parthasarathy, T.E. Carew, J.C. Khoo, J.L. Witztum, Beyond cholesterol. Modifications of low-density lipoprotein that increase its atherogenicity, *N Engl J Med*, 1989. **320**: 915-924.
[20] V. Fuster, L. Badimon, J.J. Badimon, J.H. Chesebro, The pathogenesis of coronary artery disease and the acute coronary syndromes (1), *N Engl J Med*, 1992. **326**: 242-250.
[21] K.J. Moore, F.J. Sheedy, E.A. Fisher, Macrophages in atherosclerosis: a dynamic balance, *Nature Reviews Immunology*, 2013. **13**: 709.
[22] B. Halliwell, J.M.C. Gutteridge, Free radicals in biology and medicine, 2nd ed., Oxford University Press, Oxford, 1989.
[23] N.L. Oleinick, S.M. Chiu, N. Ramakrishnan, L.Y. Xue, The formation, identification, and significance of DNA-protein cross-links in mammalian cells, *Br J Cancer Suppl*, 1987. **8**: 135-140.
[24] S. Steenken, Structure, acid/base properties and transformation reactions of purine radicals, *Free Radic Res Commun*, 1989. **6**: 117-120.
[25] I. Bezprozvanny, M.P. Mattson, Neuronal calcium mishandling and the pathogenesis of Alzheimer's disease, *Trends in Neurosciences*, 2008. **31**: 454-463.
[26] A. Görlach, K. Bertram, S. Hudecova, O. Krizanova, Calcium and ROS: A mutual interplay, *Redox Biology*, 2015. **6**: 260-271.
[27] A.W. Harman, M.J. Maxwell, An Evaluation of the Role of Calcium in Cell Injury, *Annual Review of Pharmacology and Toxicology*, 1995. **35**: 129-144.
[28] I.A. Cotgreave, P. Moldeus, S. Orrenius, Host Biochemical Defense Mechanisms Against Prooxidants, *Annual Review of Pharmacology and Toxicology*, 1988. **28**: 189-212.
[29] W. Dröge, Free Radicals in the Physiological Control of Cell Function, *Physiological Reviews*, 2002. **82**: 47-95.
[30] R.S. Sohal, R. Weindruch, Oxidative Stress, Caloric Restriction, and Aging, *Science*, 1996. **273**: 59-63.
[31] I. Bogdan Allemann, L. Baumann, Antioxidants used in skin care formulations, *Skin Therapy Lett*, 2008. **13**: 5-9.
[32] B. Poljsak, D. Šuput, I. Milisav, Achieving the Balance between ROS and Antioxidants: When to Use the Synthetic Antioxidants, *Oxidative Medicine and Cellular Longevity*, 2013. **2013**: 11.
[33] R.L. Prior, X. Wu, K. Schaich, Standardized Methods for the Determination of Antioxidant Capacity and Phenolics in Foods and Dietary Supplements, *Journal of Agricultural and Food Chemistry*, 2005. **53**: 4290-4302.
[34] W. Brand-Williams, M.E. Cuvelier, C. Berset, Use of a free radical method to evaluate antioxidant activity, *LWT - Food Science and Technology*, 1995. **28**: 25-30.
[35] N.J. Miller, C. Rice-Evans, M.J. Davies, V. Gopinathan, A. Milner, A Novel Method for Measuring Antioxidant Capacity and its Application to Monitoring the Antioxidant Status in Premature Neonates, *Clinical Science*, 1993. **84**: 407-412.
[36] I.F. Benzie, J.J. Strain, The ferric reducing ability of plasma (FRAP) as a measure of "antioxidant power": the FRAP assay, *Anal Biochem*, 1996. **239**: 70-76.
[37] J. Nilsson, D. Pillai, G. Önning, C. Persson, Å. Nilsson, B. Åkesson, Comparison of the 2,2′-azinobis-3-ethylbenzotiazo-line-6-sulfonic acid (ABTS) and ferric reducing anti-oxidant power (FRAP) methods to asses the total antioxidant capacity in extracts of fruit and vegetables, *Molecular Nutrition & Food Research*, 2005. **49**: 239-246.
[38] X. Wu, R.L. Prior, Identification and characterization of anthocyanins by high-performance liquid chromatography-electrospray ionization-tandem mass spectrometry in common foods in the United States: vegetables, nuts, and grains, *J Agric Food Chem*, 2005. **53**: 3101-3113.

[39] P. Di Mascio, S. Kaiser, H. Sies, Lycopene as the most efficient biological carotenoid singlet oxygen quencher, *Archives of Biochemistry and Biophysics*, 1989. **274**: 532-538.
[40] O.I. Aruoma, Methodological considerations for characterizing potential antioxidant actions of bioactive components in plant foods, *Mutation Research/Fundamental and Molecular Mechanisms of Mutagenesis*, 2003. **523-524**: 9-20.
[41] K. Schlesier, M. Harwat, V. Böhm, R. Bitsch, Assessment of Antioxidant Activity by Using Different In Vitro Methods, *Free Radical Research*, 2002. **36**: 177-187.
[42] A. Karadag, B. Ozcelik, S. Saner, Review of Methods to Determine Antioxidant Capacities, 2009. **2**: 41-60.
[43] J.A. DiMasi, H.G. Grabowski, R.W. Hansen, Innovation in the pharmaceutical industry: New estimates of R&D costs, *J Health Econ*, 2016. **47**: 20-33.
[44] D.W. Nebert, D.R. Nelson, R. Feyereisen, Evolution of the cytochrome P450 genes, *Xenobiotica*, 1989. **19**: 1149-1160.
[45] A. Stier, Lipid structure and drug metabolizing enzymes, *Biochemical Pharmacology*, 1976. **25**: 109-113.
[46] D. Garfinkel, Studies on pig liver microsomes. I. Enzymic and pigment composition of different microsomal fractions, *Archives of Biochemistry and Biophysics*, 1958. **77**: 493-509.
[47] M. Klingenberg, Pigments of rat liver microsomes, *Archives of Biochemistry and Biophysics*, 1958. **75**: 376-386.
[48] F.J. Gonzalez, The molecular biology of cytochrome P450s, *Pharmacological Reviews*, 1988. **40**: 243-288.
[49] W. Lohmann, U. Karst, Biomimetic modeling of oxidative drug metabolism, *Analytical and Bioanalytical Chemistry*, 2008. **391**: 79-96.
[50] T. Johansson, L. Weidolf, U. Jurva, Mimicry of phase I drug metabolism--novel methods for metabolite characterization and synthesis, *Rapid Commun Mass Spectrom*, 2007. **21**: 2323-2331.
[51] E.F. Brandon, C.D. Raap, I. Meijerman, J.H. Beijnen, J.H. Schellens, An update on in vitro test methods in human hepatic drug biotransformation research: pros and cons, *Toxicol Appl Pharmacol*, 2003. **189**: 233-246.
[52] S. Goldstein, D. Meyerstein, G. Czapski, The Fenton reagents, *Free Radic Biol Med*, 1993. **15**: 435-445.
[53] S. Zbaida, R. Kariv, P. Fischer, D. Gilhar, Reactions of theophylline, theobromine and caffeine with Fenton's reagent--simulation of hepatic metabolism, *Xenobiotica*, 1987. **17**: 617-621.
[54] S. Zbaida, R. Kariv, P. Fischer, J. Silman-Greenspan, Z. Tashma, Reaction of cimetidine with Fenton reagent. A biomimetic model for the mixed-function oxidase drug metabolism, *Eur J Biochem*, 1986. **154**: 603-605.
[55] H. Masumoto, K. Takeuchi, S. Ohta, M. Hirobe, Application of chemical P450 model systems to studies on drug metabolism. I. Phencyclidine: a multi-functional model substrate, *Chem Pharm Bull (Tokyo)*, 1989. **37**: 1788-1794.
[56] U. Jurva, H.V. Wikstrom, A.P. Bruins, Electrochemically assisted Fenton reaction: reaction of hydroxyl radicals with xenobiotics followed by on-line analysis with high-performance liquid chromatography/tandem mass spectrometry, *Rapid Commun Mass Spectrom*, 2002. **16**: 1934-1940.
[57] J.T. Groves, R.C. Haushalter, M. Nakamura, T.E. Nemo, B.J. Evans, High-valent iron-porphyrin complexes related to peroxidase and cytochrome P-450, *Journal of the American Chemical Society*, 1981. **103**: 2884-2886.
[58] J.T. Groves, S. Krishnan, G.E. Avaria, T.E. Nemo, Studies of the Mechanism of Oxygen Activation and Transfer Catalyzed by Cytochrome P 450, in: Biomimetic Chemistry, AMERICAN CHEMICAL SOCIETY, 1980, pp. 277-289.

[59] C.K. Chang, F. Ebina, NIH shift in haemin–iodosylbenzene-mediated hydroxylations, *Journal of the Chemical Society, Chemical Communications*, 1981. 778-779.
[60] J. Bernadou, B. Meunier, Biomimetic Chemical Catalysts in the Oxidative Activation of Drugs, *Advanced Synthesis & Catalysis*, 2004. **346**: 171-184.
[61] M.C. Feiters, A.E. Rowan, R.J.M. Nolte, From simple to supramolecular cytochrome P450 mimics, *Chemical Society Reviews*, 2000. **29**: 375-384.
[62] M. Sono, M.P. Roach, E.D. Coulter, J.H. Dawson, Heme-Containing Oxygenases, *Chemical Reviews*, 1996. **96**: 2841-2888.
[63] T. Shono, T. Toda, N. Oshino, Preparation of N-dealkylated drug metabolites by electrochemical simulation of biotransformation, *Drug Metabolism and Disposition*, 1981. **9**: 481-482.
[64] G. Hambitzer, J. Heitbaum, Electrochemical thermospray mass spectrometry, *Analytical Chemistry*, 1986. **58**: 1067-1070.
[65] I.N. Acworth, Coulometric electrode array detectors for HPLC, Vsp, 1997.
[66] U. Jurva, H.V. Wikström, L. Weidolf, A.P. Bruins, Comparison between electrochemistry/mass spectrometry and cytochrome P450 catalyzed oxidation reactions, *Rapid Communications in Mass Spectrometry*, 2003. **17**: 800-810.
[67] A.N. Glazer, Phycoerythrin fluorescence-based assay for reactive oxygen species, *Methods Enzymol*, 1990. **186**: 161-168.
[68] S. Sugahara, Y. Ueda, K. Fukuhara, Y. Kamamuta, Y. Matsuda, T. Murata, Y. Kuroda, K. Kabata, M. Ono, K. Igoshi, S. Yasuda, Antioxidant Effects of Herbal Tea Leaves from Yacon (Smallanthus sonchifolius) on Multiple Free Radical and Reducing Power Assays, Especially on Different Superoxide Anion Radical Generation Systems, *J Food Sci*, 2015. **80**: C2420-2429.
[69] R. Re, N. Pellegrini, A. Proteggente, A. Pannala, M. Yang, C. Rice-Evans, Antioxidant activity applying an improved ABTS radical cation decolorization assay, *Free Radic Biol Med*, 1999. **26**: 1231-1237.
[70] G. Clarke, K.N. Ting, C. Wiart, J. Fry, High Correlation of 2,2-diphenyl-1-picrylhydrazyl (DPPH) Radical Scavenging, Ferric Reducing Activity Potential and Total Phenolics Content Indicates Redundancy in Use of All Three Assays to Screen for Antioxidant Activity of Extracts of Plants from the Malaysian Rainforest, *Antioxidants (Basel)*, 2013. **2**: 1-10.
[71] WHO, Cardiovascular diseases (CVDs) 2017. Available at: http://www.who.int/en/news-room/fact-sheets/detail/cardiovascular-diseases-(cvds) (accessed 03 September 2018). in.
[72] D.P. Jones, Redefining Oxidative Stress, *Antioxidants & Redox Signaling*, 2006. **8**: 1865-1879.
[73] G. Csányi, M. Yao, A.I. Rodríguez, I.A. Ghouleh, M. Sharifi-Sanjani, G. Frazziano, X. Huang, E.E. Kelley, J.S. Isenberg, P.J. Pagano, Thrombospondin-1 Regulates Blood Flow via CD47 Receptor-Mediated Activation of NADPH Oxidase 1, *Arteriosclerosis, Thrombosis, and Vascular Biology*, 2012. **32**: 2966-2973.
[74] R.M. Touyz, A.M. Briones, Reactive oxygen species and vascular biology: implications in human hypertension, *Hypertension Research*, 2010. **34**: 5.
[75] C.M. Andre, Y. Larondelle, D. Evers, Dietary Antioxidants and Oxidative Stress from a Human and Plant Perspective: A Review, *Current Nutrition & Food Science*, 2010. **6**: 2-12.
[76] D.V. Ratnam, D.D. Ankola, V. Bhardwaj, D.K. Sahana, M.N.V.R. Kumar, Role of antioxidants in prophylaxis and therapy: A pharmaceutical perspective, *Journal of Controlled Release*, 2006. **113**: 189-207.
[77] M.N. Alam, N.J. Bristi, M. Rafiquzzaman, Review on in vivo and in vitro methods evaluation of antioxidant activity, *Saudi Pharmaceutical Journal*, 2013. **21**: 143-152.

[78] W. Watjen, G. Michels, B. Steffan, P. Niering, Y. Chovolou, A. Kampkotter, Q.H. Tran-Thi, P. Proksch, R. Kahl, Low concentrations of flavonoids are protective in rat H4IIE cells whereas high concentrations cause DNA damage and apoptosis, *J Nutr*, 2005. **135**: 525-531.
[79] R.L. Prior, H. Hoang, L. Gu, X. Wu, M. Bacchiocca, L. Howard, M. Hampsch-Woodill, D. Huang, B. Ou, R. Jacob, Assays for Hydrophilic and Lipophilic Antioxidant Capacity (oxygen radical absorbance capacity (ORACFL)) of Plasma and Other Biological and Food Samples, *Journal of Agricultural and Food Chemistry*, 2003. **51**: 3273-3279.
[80] L.K. MacDonald-Wicks, L.G. Wood, M.L. Garg, Methodology for the determination of biological antioxidant capacity in vitro: a review, *Journal of the Science of Food and Agriculture*, 2006. **86**: 2046-2056.
[81] W. Bors, W. Heller, C. Michel, M. Saran, [36] Flavonoids as antioxidants: Determination of radical-scavenging efficiencies, in: Methods in Enzymology, Academic Press, 1990, pp. 343-355.
[82] S. Burda, W. Oleszek, Antioxidant and Antiradical Activities of Flavonoids, *Journal of Agricultural and Food Chemistry*, 2001. **49**: 2774-2779.
[83] B.L. Halvorsen, K. Holte, M.C. Myhrstad, I. Barikmo, E. Hvattum, S.F. Remberg, A.B. Wold, K. Haffner, H. Baugerod, L.F. Andersen, O. Moskaug, D.R. Jacobs, Jr., R. Blomhoff, A systematic screening of total antioxidants in dietary plants, *J Nutr*, 2002. **132**: 461-471.
[84] J.A. Plumb, R. Milroy, S.B. Kaye, Effects of the pH Dependence of 3-(4,5-Dimethylthiazol-2-yl)-2,5-diphenyltetrazolium Bromide-Formazan Absorption on Chemosensitivity Determined by a Novel Tetrazolium-based Assay, *Cancer Research*, 1989. **49**: 4435-4440.
[85] P.R. Chaturvedi, C.J. Decker, A. Odinecs, Prediction of pharmacokinetic properties using experimental approaches during early drug discovery, *Current Opinion in Chemical Biology*, 2001. **5**: 452-463.
[86] S.A. Roberts, High-throughput screening approaches for investigating drug metabolism and pharmacokinetics, *Xenobiotica*, 2001. **31**: 557-589.
[87] V. Balland, M.-F. Charlot, F. Banse, J.-J. Girerd, Tony A. Mattioli, E. Bill, J.-F. Bartoli, P. Battioni, D. Mansuy, Spectroscopic Characterization of an FeIV Intermediate Generated by Reaction of XO− (X = Cl, Br) with an FeII Complex Bearing a Pentadentate Non-Porphyrinic Ligand − Hydroxylation and Epoxidation Activity, *European Journal of Inorganic Chemistry*, 2004. **2004**: 301-308.
[88] Z. Gross, S. Nimri, A Pronounced Axial Ligand Effect on the Reactivity of Oxoiron(IV) Porphyrin Cation Radicals, *Inorganic Chemistry*, 1994. **33**: 1731-1732.
[89] U. Jurva, P. Bissel, E.M. Isin, K. Igarashi, S. Kuttab, N. Castagnoli, Model Electrochemical-Mass Spectrometric Studies of the Cytochrome P450-Catalyzed Oxidations of Cyclic Tertiary Allylamines, *Journal of the American Chemical Society*, 2005. **127**: 12368-12377.
[90] E. Nouri-Nigjeh, H.P. Permentier, R. Bischoff, A.P. Bruins, Lidocaine Oxidation by Electrogenerated Reactive Oxygen Species in the Light of Oxidative Drug Metabolism, *Analytical Chemistry*, 2010. **82**: 7625-7633.
[91] B.T. Kim, K.J. O, J.-C. Chun, K.-J. Hwang, Synthesis of Dihydroxylated Chalcone Derivatives with Diverse Substitution Patterns and Their Radical Scavenging Ability toward DPPH Free Radicals, *Bull Korean Chem Soc*, 2008. **29**: 6.
[92] K. Fukuhara, I. Nakanishi, H. Kansui, E. Sugiyama, M. Kimura, T. Shimada, S. Urano, K. Yamaguchi, N. Miyata, Enhanced Radical-Scavenging Activity of a Planar Catechin Analogue, *Journal of the American Chemical Society*, 2002. **124**: 5952-5953.
[93] B. Culhaoglu, A. Capan, M. Boga, M. Ozturk, T. Ozturk, G. Topcu, Antioxidant and Anticholinesterase Activities of Some Dialkylamino Substituted 3-Hydroxyflavone Derivatives, *Med Chem*, 2017. **13**: 254-259.

[94] G. Cao, E. Sofic, R.L. Prior, Antioxidant and prooxidant behavior of flavonoids: structure-activity relationships, *Free Radic Biol Med*, 1997. **22**: 749-760.
[95] D. Deng, J. Zhang, J.M. Cooney, M.A. Skinner, A. Adaim, D.J. Jensen, D.E. Stevenson, Methylated polyphenols are poor "chemical" antioxidants but can still effectively protect cells from hydrogen peroxide-induced cytotoxicity, *FEBS Letters*, 2006. **580**: 5247-5250.
[96] W. Luo, T. Wang, C. Hong, Y.C. Yang, Y. Chen, J. Cen, S.Q. Xie, C.J. Wang, Design, synthesis and evaluation of 4-dimethylamine flavonoid derivatives as potential multifunctional anti-Alzheimer agents, *Eur J Med Chem*, 2016. **122**: 17-26.
[97] J.M. Jeong, C.H. Choi, S.K. Kang, I.H. Lee, J.Y. Lee, H. Jung, Antioxidant and chemosensitizing effects of flavonoids with hydroxy and/or methoxy groups and structure-activity relationship, *J Pharm Pharm Sci*, 2007. **10**: 537-546.
[98] T. Walle, N. Ta, T. Kawamori, X. Wen, P.A. Tsuji, U.K. Walle, Cancer chemopreventive properties of orally bioavailable flavonoids--methylated versus unmethylated flavones, *Biochem Pharmacol*, 2007. **73**: 1288-1296.

UNIVERSITY AND NATIONAL LIBRAY
UNIVERSITY OF DEBRECEN
H-4002 Egyetem tér 1, Debrecen
Phone: +3652/410-443, email: publikaciok@lib.unideb.hu

Registry number: DEENK/375/2018.PL
Subject: PhD Publikációs Lista

Candidate: Péter Szabados-Fürjesi
Neptun ID: YZ19Y8
Doctoral School: Doctoral School of Pharmacy

List of publications related to the dissertation

1. **Szabados-Fürjesi, P.**, Pajtás, D., Barta, A., Csépányi, E., Kiss-Szikszai, A., Tósaki, Á., Bak, I.: Synthesis, in Vitro Biological Evaluation, and Oxidative Transformation of New Flavonol Derivatives: The Possible Role of the Phenyl-N,N-Dimethylamino Group.
Molecules. 23 (12), 1-15, 2018.
DOI: http://dx.doi.org/10.3390/molecules23123161
IF: 3.098 (2017)

2. Csépányi, E., **Szabados-Fürjesi, P.**, Kiss-Szikszai, A., Frensemeier, L. M., Karst, U., Lekli, I., Haines, D. D., Tósaki, Á., Bak, I.: Antioxidant Properties and Oxidative Transformation of Different Chromone Derivatives.
Molecules. 22 (4), 1-12, 2017.
DOI: http://dx.doi.org/10.3390/molecules22040588
IF: 3.098

UNIVERSITY AND NATIONAL LIBRAY
UNIVERSITY OF DEBRECEN
H-4002 Egyetem tér 1, Debrecen
Phone: +3652/410-443, email: publikaciok@lib.unideb.hu

List of other publications

3. Csépányi, E., Czompa, A., **Szabados-Fürjesi, P.**, Lekli, I., Balla, J., Balla, G., Tósaki, Á., Bak, I.: The Effects of Long-Term, Low- and High-Dose Beta-Carotene Treatment in Zucker Diabetic Fatty Rats: the Role of HO-1.
Int. J. Mol. Sci. 19 (4), 1132-, 2018.
DOI: http://dx.doi.org/10.3390/ijms19041132
IF: 3.687 (2017)

Total IF of journals (all publications): 9,883
Total IF of journals (publications related to the dissertation): 6,196

The Candidate's publication data submitted to the iDEa Tudóstér have been validated by DEENK on the basis of Web of Science, Scopus and Journal Citation Report (Impact Factor) databases.

18 December, 2018

DEBRECENI EGYETEM * Egyetemi és Nemzeti Könyvtár *

10. KEYWORDS

Cardiovascular diseases; oxidative stress; free radical; antioxidant; flavonoid; flavonol; cytotoxicity; drug metabolism; metabolite.

11. KULCSSZAVAK

Szív- és érrendszeri megbetegedések; oxidatív stressz; szabadgyök; antioxidáns; flavonoid; flavonol; citotoxicitás; gyógyszermetabolizmus; metabolit.

12. ACKNOWLEDGEMENTS

First and foremost, I would like to thank to my wife, Panka who supported this scientific and emotional endeavour from the very beginning in every possible way. Without her encouragement and love, I could not have achieved this. My parents, sister and my family, I thank them for their unconditional support.

I would like to thank to Professor Árpád Tósaki, head of department for providing all the necessary resources for my research.

I greatly appreciate the honesty, help and patience of my supervisor, István Bak; he has given me the freedom I needed to pursue my research, while providing support and guidance when it was necessary.

I am forever grateful for the cheery, funny and productive office-atmosphere created by Rita Zilinyi, who I became friends with.

I also would like to say thank you to my former and current colleagues for their help and support throughout my time at the department.

I take pride in acknowledging my gratitude to the work of Alexandra Elbakyan, the founder of Sci-Hub, because all barriers must be removed from the way of science.

Funding; the present research was supported by the GINOP-2.3.2-15-2016-00043 project and co-financed by the European Union and the European Regional Development Fund. The project was subsidized by the European Union and co-financed by the European Social Fund. The work of Péter Szabados-Fürjesi was supported by the EFOP-3.6.1-16-2016-00022 „Debrecen Venture Catapult Program”.

13. ANNEXES

Declaration of the own and collaborative experimental work in the present thesis:

Own work: sections 4.1.6., 4.1.7., 4.2.5., 4.2.6., 4.2.7., 4.2.8. and 4.2.10.;

Collaborative work: section 4.1.8.

13.1. ANNEX OF STUDY I

13.1.1. Structures of the Compounds of Study I

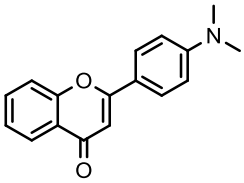

865

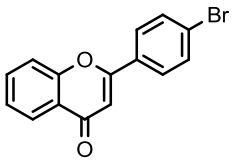

870

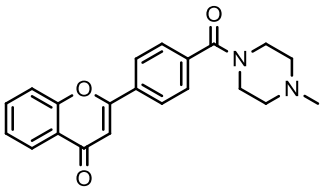

874

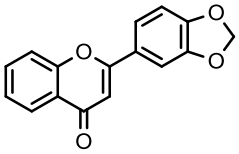

876

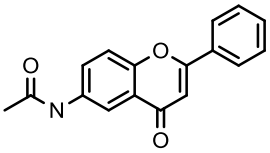

890

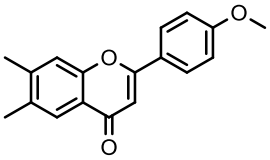

991

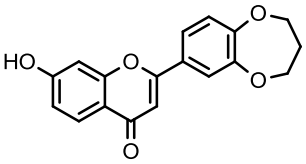

893

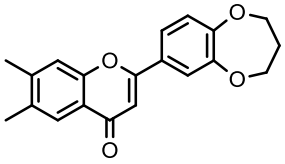

987/3

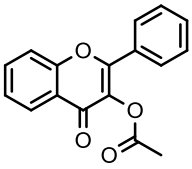

1019/2

13.2. ANNEX OF STUDY II

13.2.1. Structures of the Compounds of Study II

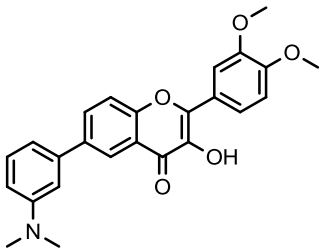

6a

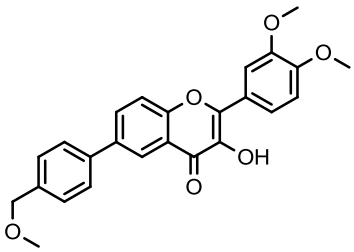

6b

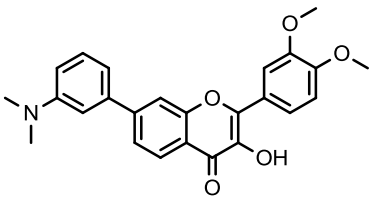

6c

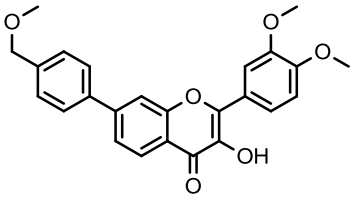

6d

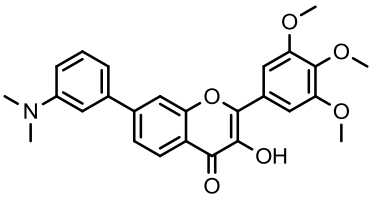

6e

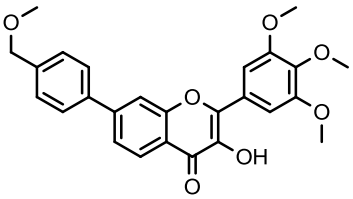

6f

13.2.2. ^{1}H-NMR and ^{13}H-NMR Spectra of **6a-f**

2-(3,4-Dimethoxyphenyl)-6-[3-(dimethylamino)phenyl]-3-hydroxy-4H-chromen-4-one (**6a**)

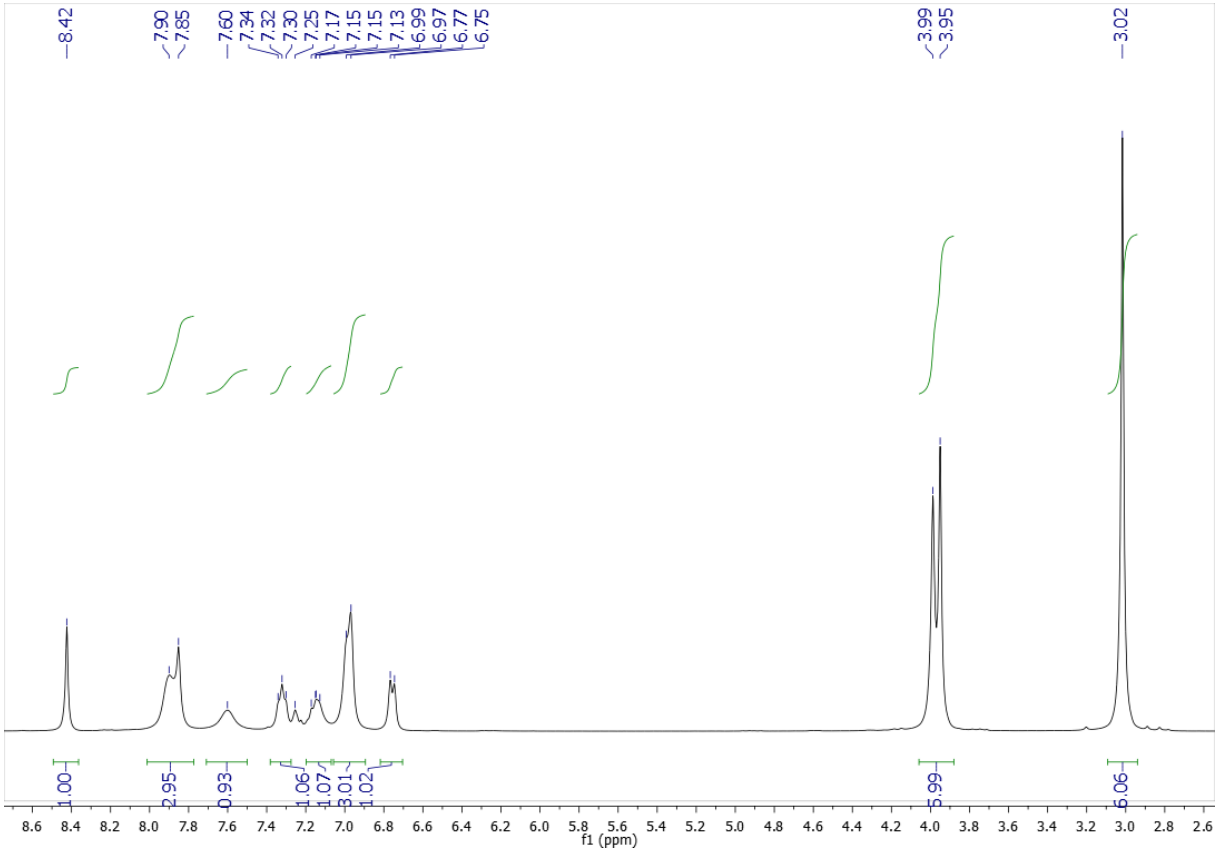

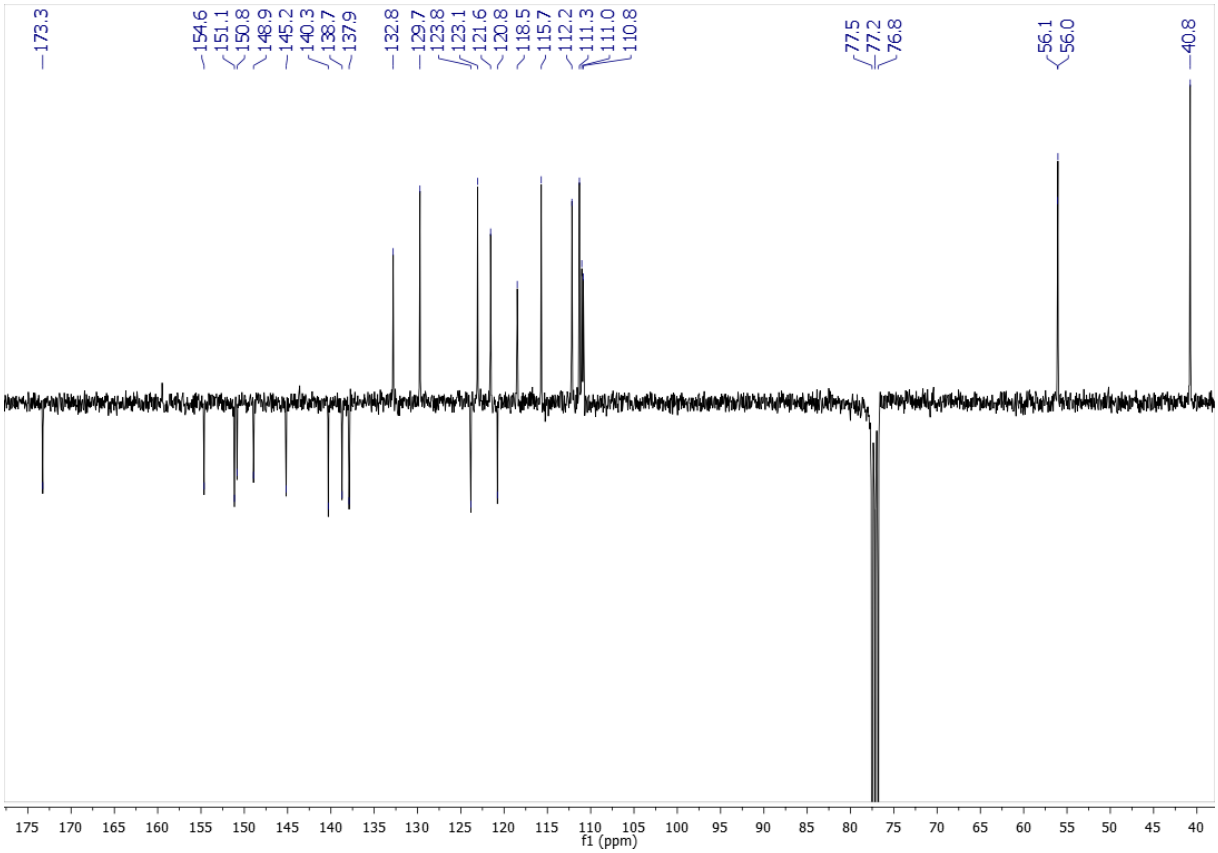

2-(3,4-Dimethoxyphenyl)-3-hydroxy-6-[4-(methoxymethyl)phenyl]-4H-chromen-4-one (**6b**)

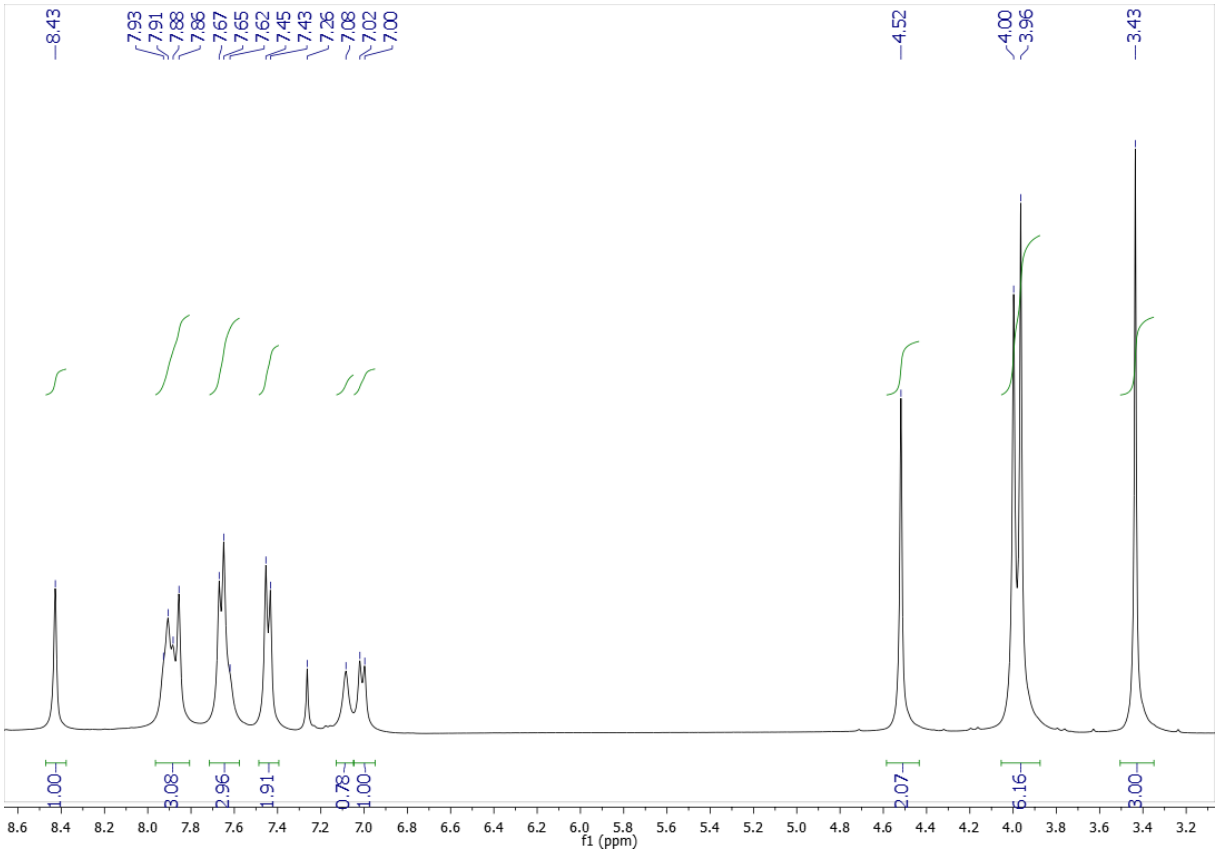

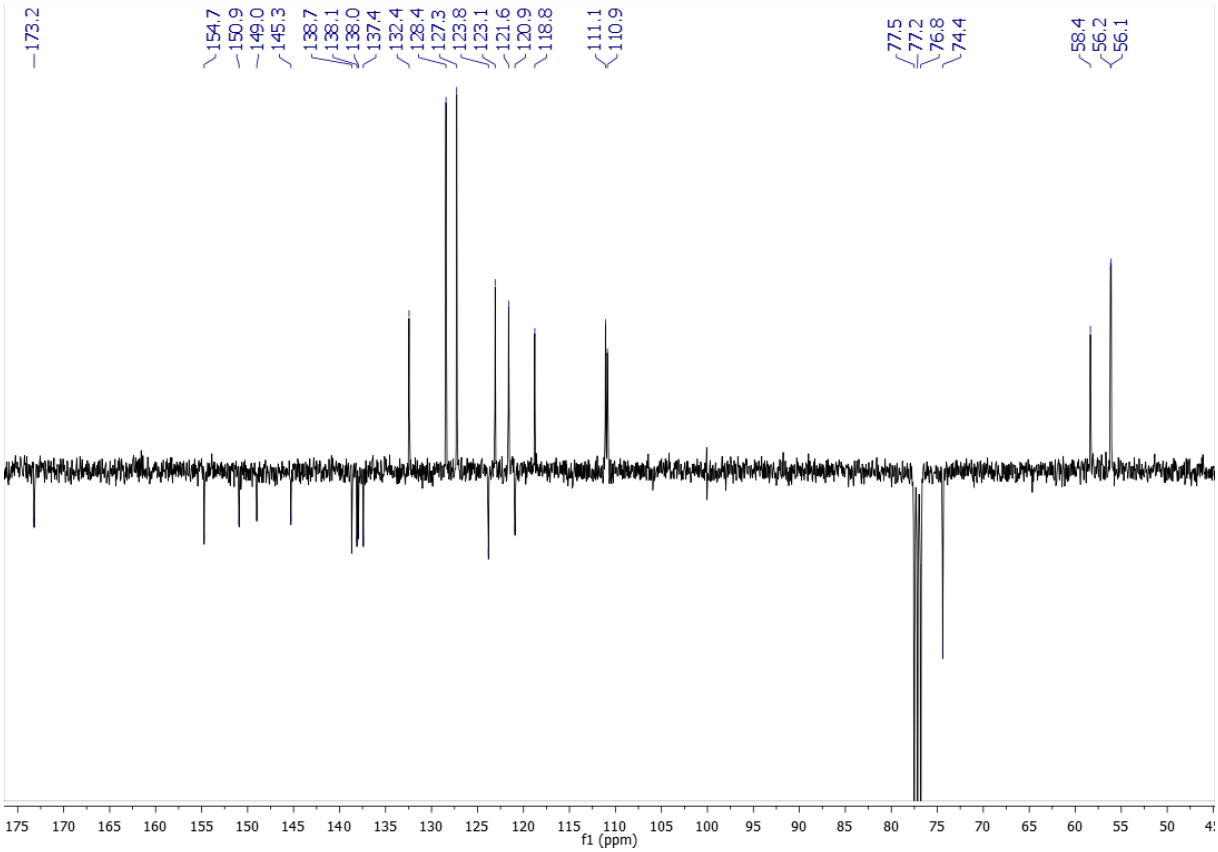

2-(3,4-Dimethoxyphenyl)-7-[3-(dimethylamino)phenyl]-3-hydroxy-4H-chromen-4-one (**6c**)

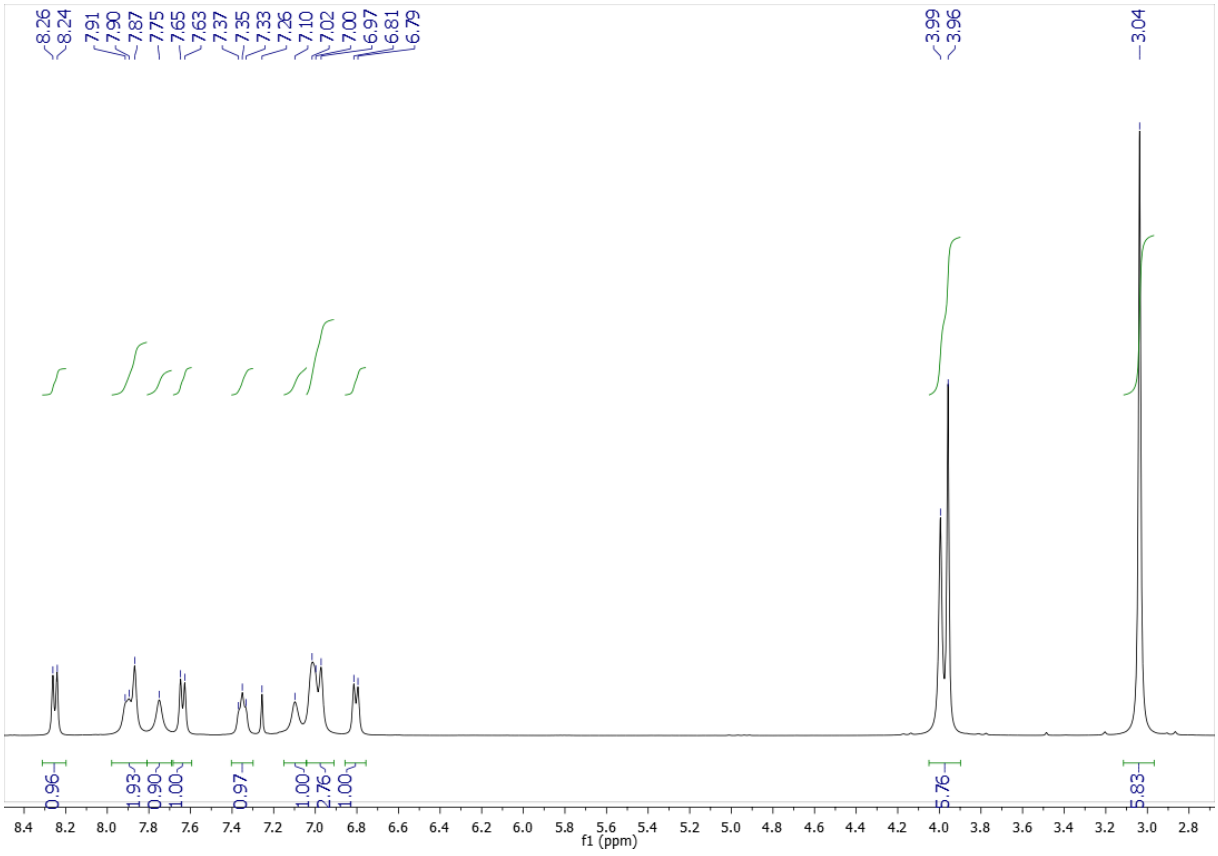

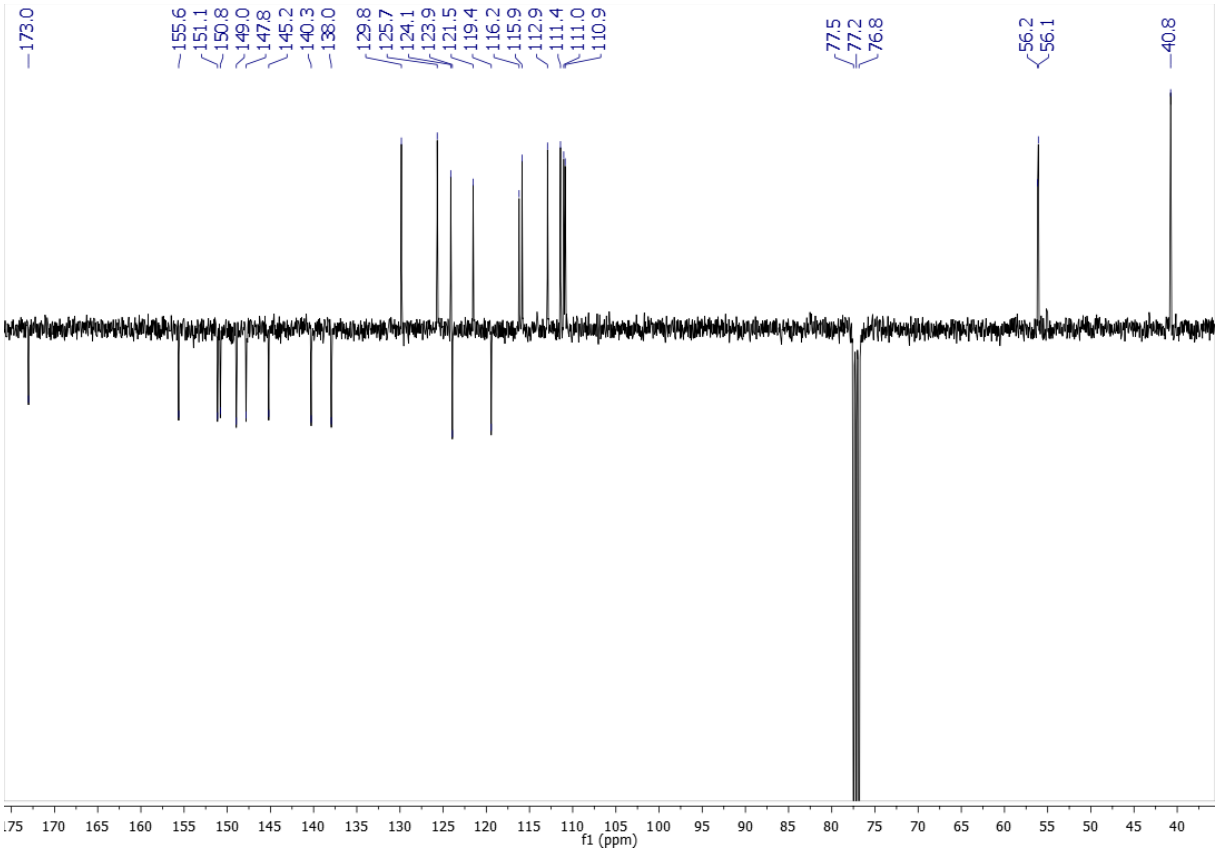

2-(3,4-Dimethoxyphenyl)-3-hydroxy-7-[4-(methoxymethyl)phenyl]-4H-chromen-4-one (**6d**)

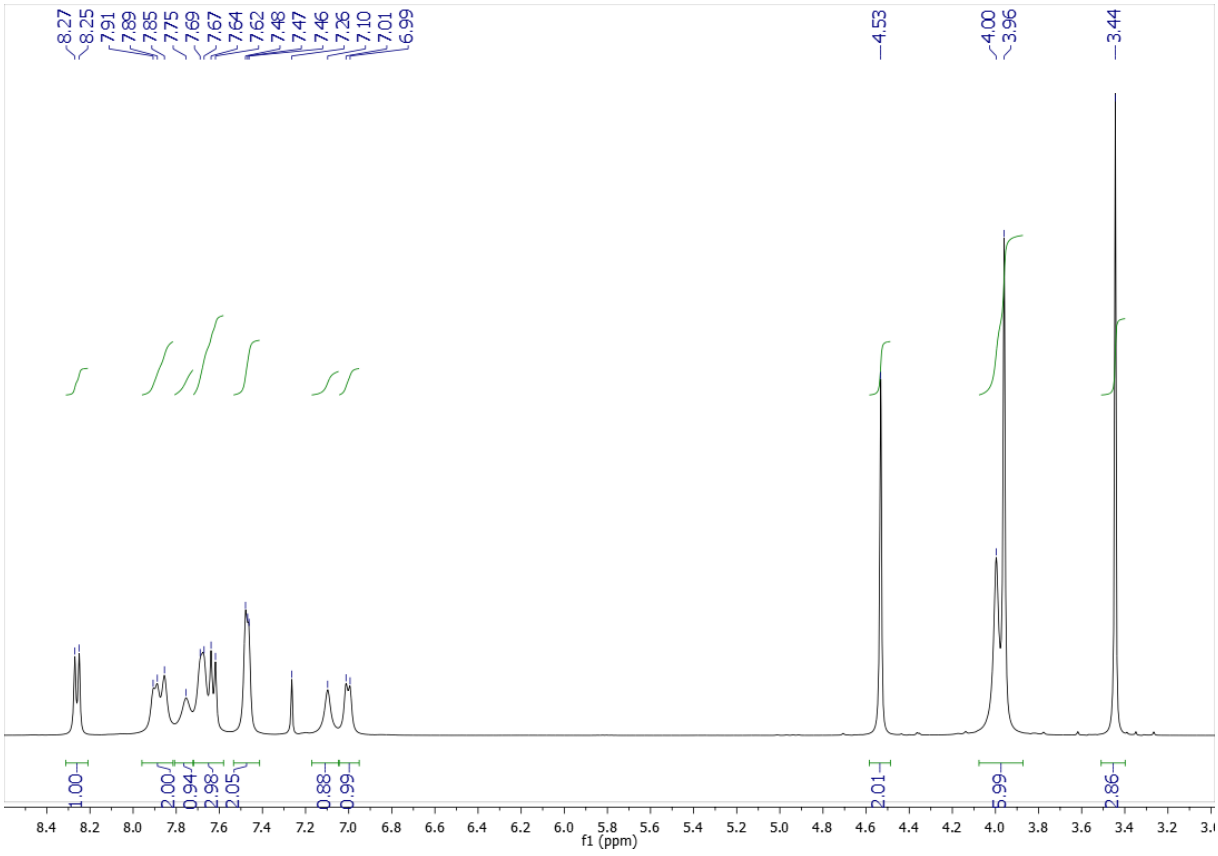

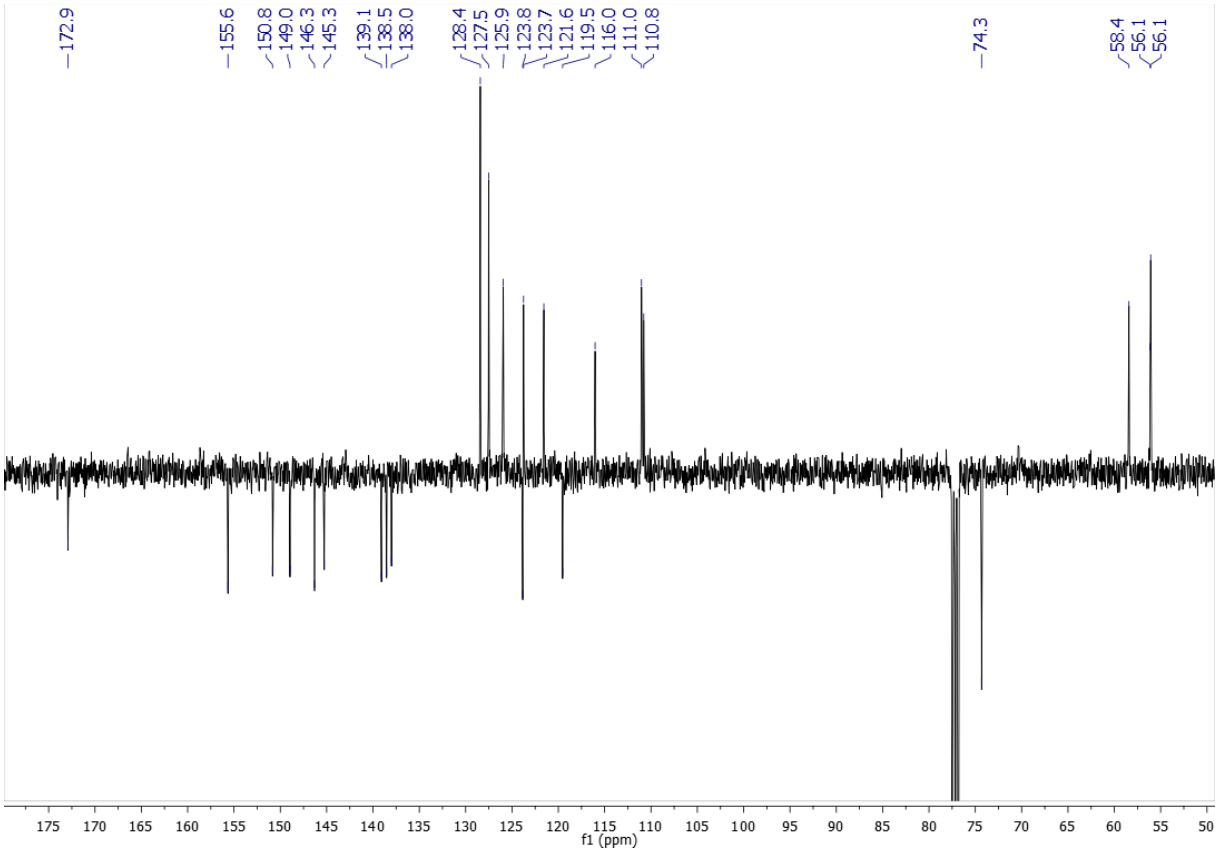

7-[3-(Dimethylamino)phenyl]-3-hydroxy-2-(3,4,5-trimethoxyphenyl)-4H-chromen-4-one (**6e**)

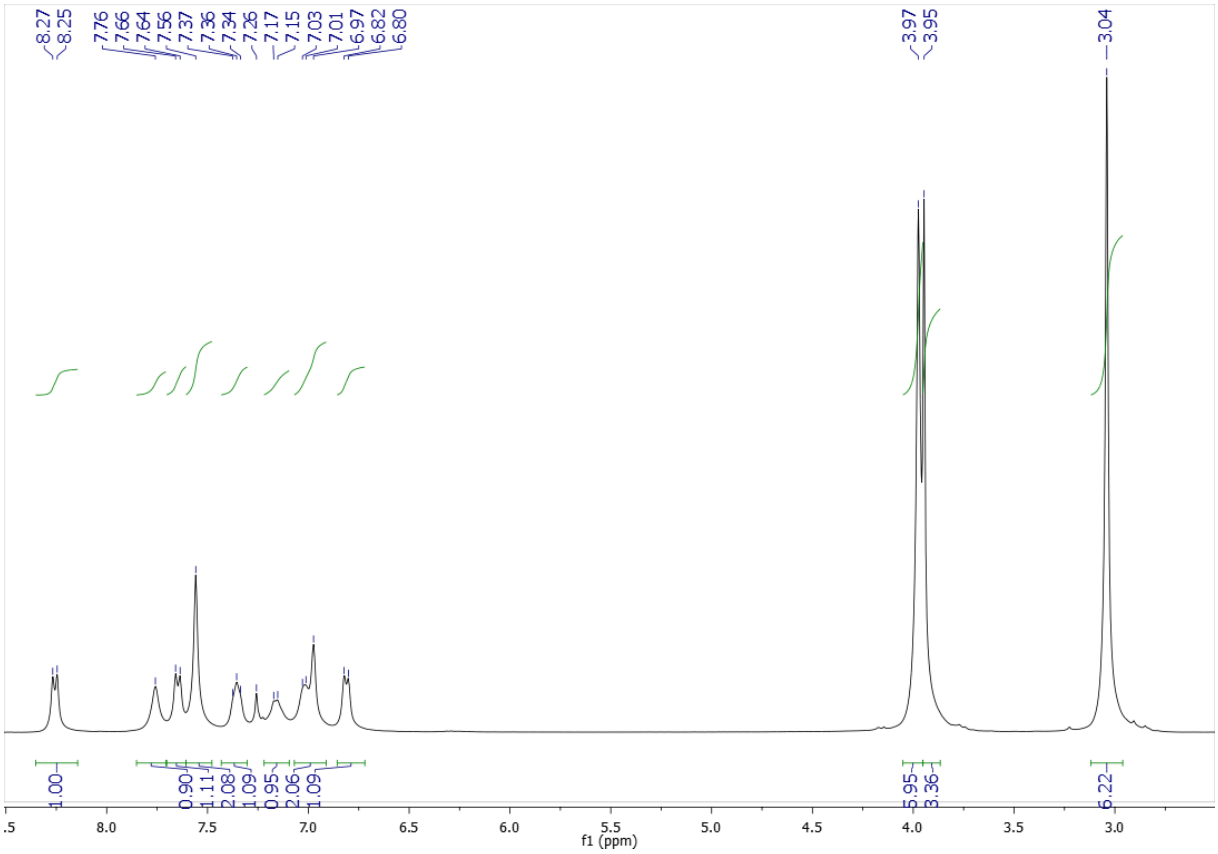

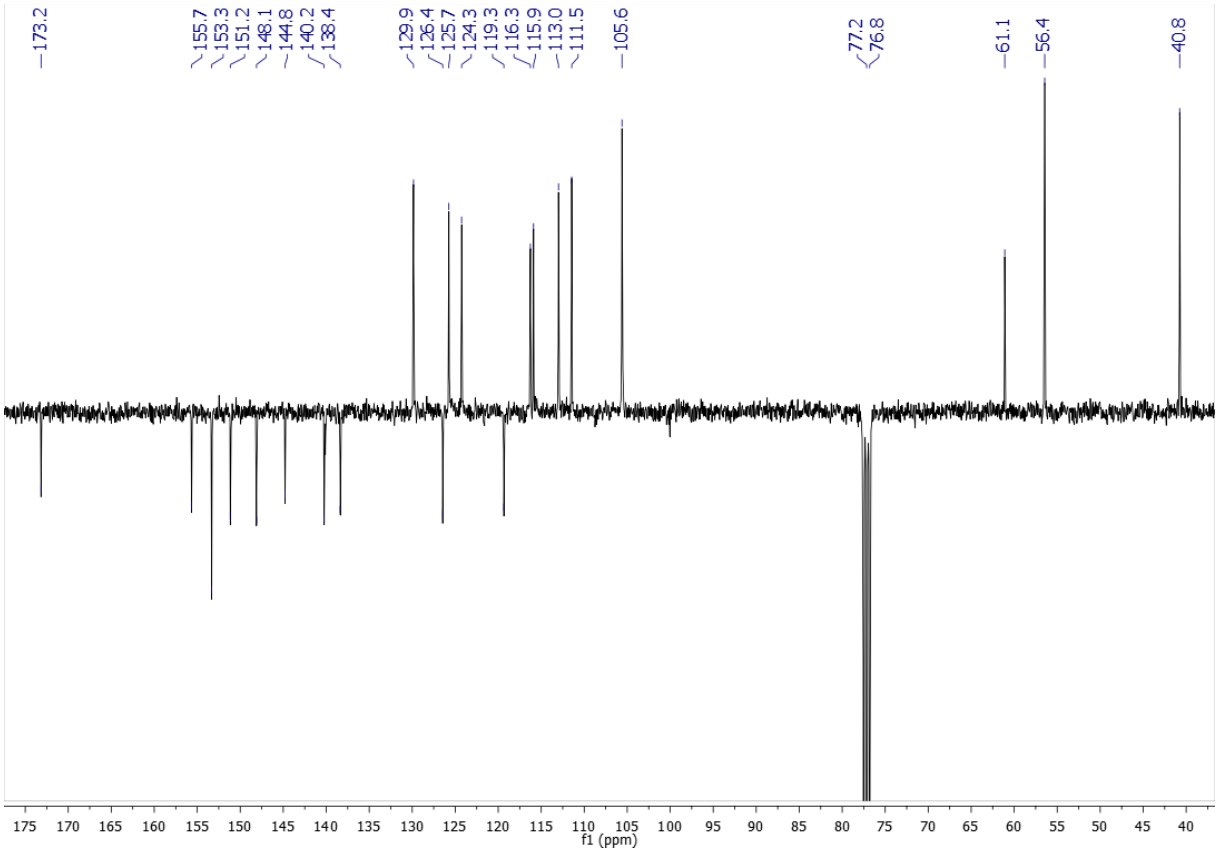

3-Hydroxy-7-[4-(methoxymethyl)phenyl]-2-(3,4,5-trimethoxyphenyl)-4H-chromen-4-one (**6f)**